PULSED TIME-OF-FLIGHT LASER RANGE FINDER TECHNIQUES FOR FAST, HIGH PRECISION MEASUREMENT APPLICATIONS

ARI KILPELÄ

Department of Electrical and
Information Engineering,
University of Oulu

OULU 2004

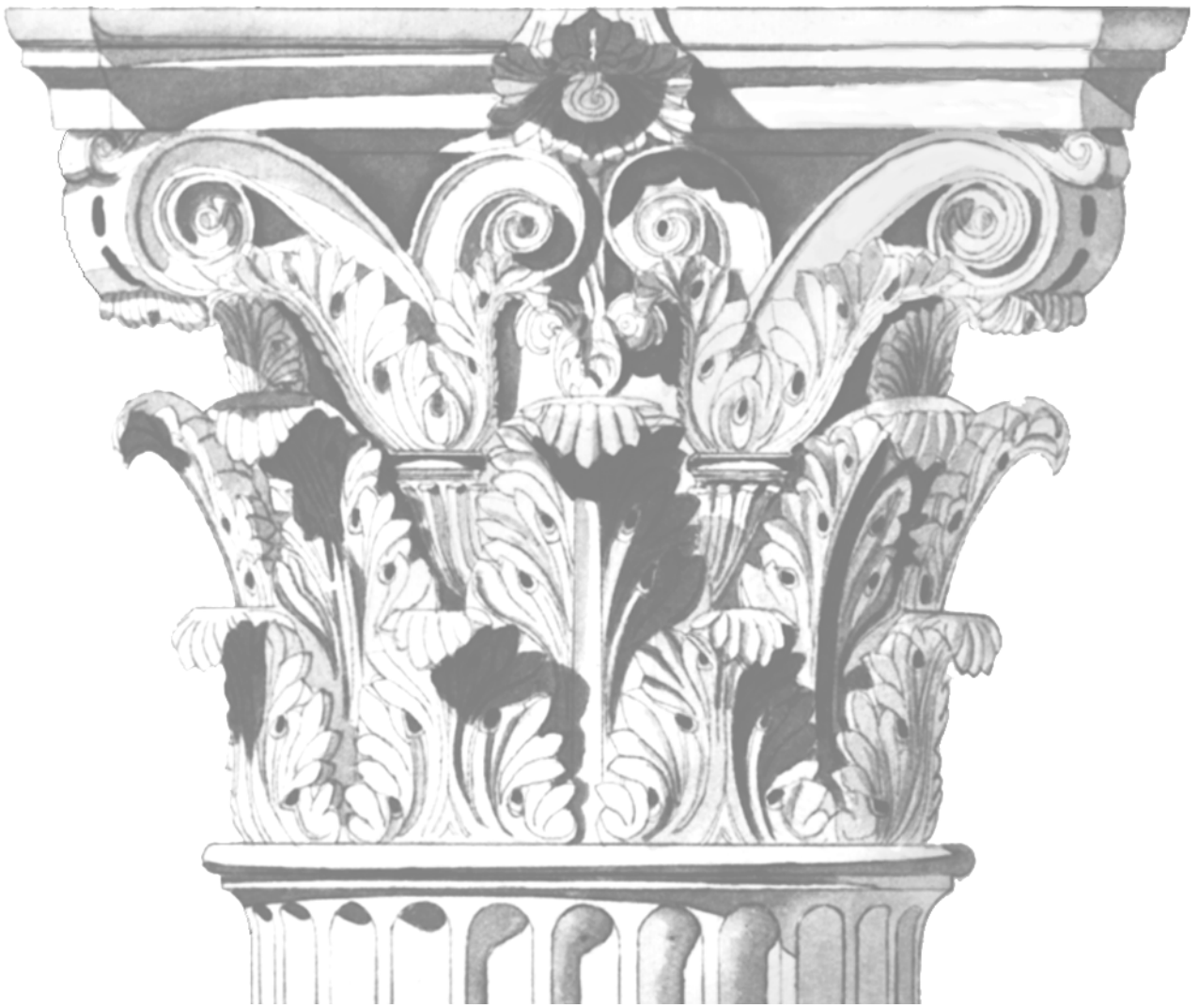

ARI KILPELÄ

PULSED TIME-OF-FLIGHT LASER RANGE FINDER TECHNIQUES FOR FAST, HIGH PRECISION MEASUREMENT APPLICATIONS

Academic Dissertation to be presented with the assent of the Faculty of Technology, University of Oulu, for public discussion in Raahensali (Auditorium L10), Linnanmaa, on January 30th, 2004, at 12 noon.

OULUN YLIOPISTO, OULU 2004

Reviewed by
Professor Erkki Ikonen
Professor Viktor Krozer

ISBN 951-42-7261-7 (nid.)
ISBN 951-42-7262-5 (PDF) http://herkules.oulu.fi/isbn9514272625/

ISSN 0355-3213 http://herkules.oulu.fi/issn03553213/

OULU UNIVERSITY PRESS
OULU 2004

Kilpelä, Ari, Pulsed time-of-flight laser range finder techniques for fast, high precision measurement applications
Department of Electrical and Information Engineering, University of Oulu, P.O.Box 4500, FIN-90014 University of Oulu, Finland
2004
Oulu, Finland

Abstract

This thesis describes the development of high bandwidth (~1 GHz) TOF (time-of-flight) laser range finder techniques for industrial measurement applications in the measurement range of zero to a few dozen metres to diffusely reflecting targets. The main goal has been to improve single-shot precision to mm-level in order to shorten the measurement result acquisition time.

A TOF laser range finder consists of a laser transmitter, one or two receivers and timing discriminators, and a time measuring unit. In order to improve single-shot precision the slew-rate of the measurement pulse should be increased, so the optical pulse of the laser transmitter should be narrower and more powerful and the bandwidth of the receiver should be higher without increasing the noise level too much.

In the transmitter usually avalanche transistors are used for generating the short (3–10 ns) and powerful (20–100 A) current pulses for the semiconductor laser. Several avalanche transistor types were compared and the optimization of the switching circuit was studied. It was shown that as high as 130 A current pulses are achievable using commercially available surface mount avalanche transistors.

The timing discriminator was noticed to give the minimum walk error, when high slew rate measurement pulses and a high bandwidth comparator were used. A walk error of less than +/- 1 mm in an input amplitude dynamic range higher than 1:10 can be achieved with a high bandwidth receiver channel. Adding an external offset voltage between the input nodes of the comparator additionally minimized the walk error.

A prototype ~1 GHz laser range finder constructed in the thesis consists of a laser pulser and two integrated ASIC receiver channels with silicon APDs (avalanche photodiodes), crossover timing discriminators and Gilbert cell attenuators. The laser pulser utilizes an internal Q-switching mode of a commercially available SH-laser and produces optical pulses with a pulse peak power and FWHM (full-width-at-half-maximum) of 44 W and 74 ps, respectively. Using single-axis optics and 1 m long multimode fibres between the optics and receivers a total accuracy of +/-2 mm in the measurement range of 0.5–34.5 m was measured. The single-shot precision (σ-value) was 14 ps–34 ps (2–5 mm) in the measurement range. The single-shot precision agrees well with the simulations and is better with a factor of about 3-5 as compared to earlier published pulsed TOF laser radars in comparable measuring conditions.

Keywords: internal Q-switching, laser pulsing, laser rangefinding, timing discrimination

Acknowledgements

The present thesis is based on research work carried out in the Electronics Laboratory of the Department of Electrical Engineering and Infotech Oulu during years 1992-2001.

I wish to express my sincere gratitude to my supervisor Professor Juha Kostamovaara for his guidance and encouragement. I also want to thank warmly Professor Risto Myllylä for introducing me to the challenging field of TOF laser range finders.

I express my appreciation to all co-workers in the Electronics Laboratory for the pleasant working atmosphere, especially all members of the laser range finder-team and my co-authors Dr. Kari Määttä, Dr. Sergei Vainshtein, Juha Ylitalo and Riku Pennala for their valuable collaboration and inspiring discussions.

The whole staff at the workshop of the Department of Electrical Engineering are acknowledged for their technical assistance in preparing the mechanical components.

I express my deep gratitude to my parents, Lalli and Irmeli Kilpelä, for the support they have given during all my life.

I owe my warmest thanks to my wife Sirpa and daughters Ellinoora and Helmi for their love and patience during these years.

This research was supported by the following foundations: Suomen Kulttuurirahaston Pohjois-Pohjanmaan Säätiö, Tauno Tönningin säätiö, Tekniikan edistämissäätiö and Seppo Säynäjäkankaan tiedesäätiö. Technology Reserarch Centre of Finland (TEKES) and Academy of Finland participated in financing the projects.

Oulu, 1. September 2003 Ari Kilpelä

List of terms, symbols and abbreviations

APD	avalanche photodiode
ASIC	application specific integration circuit
B	bandwidth
CCD	charge coupled device
CFD	constant fraction discriminator
CMOS	complementary metal oxide semiconductor
CW	continuous wave
D	thickness of active layer (in laser)
DLL	delay-locked-loop
EMI	electromagnetic interference
F(M)	excess noise factor of APD
FPGA	field-programmable-gate-array
FWHM	full-width-at-half-maximum
g	laser gain
GI	graded index
h	Planck constant ($6.626\ 068\ 76 \times 10^{-34}$ J s)
HCS	hard clad silica
I_n	density of noise current reduced to the input of a transimpedance amplifier
i_s	signal current
i_d	dark current
i_b	signal current produced by background light
J	current density
k	Bolzmann constant ($1.380\ 6503 \times 10^{-23}$ J/K)
LADAR	laser detection and ranging
LIDAR	light detection and ranging
M	multiplication factor of APD
MM	multimode
MSM	metal-semiconductor-metal
n	number of charge carriers
NA	numerical aperture
PSD	position sensitive detector

Q charge of electron (1.6×10^{-19} C)
t_r rise time (10 % - 90 % of full pulse amplitude)
t_f fall time (90 % - 10 % of full pulse amplitude)
RADAR radio detection and ranging
rms root-mean-square
S number of photons (in laser)
SR slew rate
SI step index
S / N signal-to-noise
TDC time-to-digital converter
TOF time-of-flight
$v_{n\text{-}amp}$ noise of electronics (amplifiers)
V_{out} voltage of the pulse in the timing point
Z gain of a transimpedance amplifier
α_e impact ionization coefficient for electrons
α_h impact ionization coefficient for holes
β the fraction of spontaneous emission, which takes part in laser oscillation
Δ_n refraction index difference
ε_r reflection coefficient of the target
τ_s spontaneous emission lifetime
τ_p average lifetime of a photon

Contents

List of original papers

I Kilpelä, A., Vainshtein S., Kostamovaara J., Myllylä R. (1992) Subnanosecond, high power laser pulses for time-of-flight laser distance meters. SPIE Proc., Industrial Applications of Optical Inspection, Metrology and Sensing, vol. 1821, pp. 365-374.

II Simin G., Vainshtein S., Kostamovaara J., Kilpelä A., Määttä K (1997) Isolated picosecond pulses obtained by spectral selection from gain-switched semiconductor lasers., Proceedings of the International Conference on Lasers '97, USA, pp. 71-77.

III Kilpelä A., Kostamovaara J. (1997) Laser pulser for a time-of-flight laser radar. Review of Scientific Instruments. Vol. 68, No. 6, pp. 2253 – 2258.

IV Kilpelä A., Ylitalo J., Määttä K., Kostamovaara J. (1998) Timing discriminator for pulsed time-of-flight laser rangefinding measurements, Review of Scientific Instruments, Vol. 69, No. 5, pp. 1978-1984.

V Kilpelä A., Kostamovaara J., Myllylä R., Karppinen A. A Liquid Crystal Optical Attenuator for a Time-of-Flight Laser Radar (1999), ODIMAP II, May 20-22, Pavia, Italy, pp. 339 – 344.

VI Pennala R, Kilpelä A. , Kostamovaara J. (2000) An Integrated Receiver Channel for Picosecond Range Laser Radar Pulses, Proc. 43nd Midwest Symp. On Circuits and Systems, Lansing MI, Aug. 8-11, pp.

VII Vainshtein S.N., Maslevtsov A. V., Kilpelä A.J., Kostamovaara J. (2000) A high-power picosecond near-infrared laser transmitter module, Review of Scientific Instruments, Vol. 71, Number 11, pp. 4039-4044.

VIII Kilpelä A., Pennala R., Kostamovaara J. (2001) Precise pulsed time-of-flight laser range finder for industrial distance measurements, Review of Scientific Instruments, Vol. 72, No. 4, pp. 2197 – 2202.

The research work described in this thesis was carried out during 1992-2001 in the Electronics Laboratory in the University of Oulu. The work was funded by the Finnish Technology Development Centre (TEKES) and the Academy of Finland. The original papers were published in four conferences and four journals. Papers I and II describe the Q-switching and gain switching phenomena in semiconductor lasers. The research described in Paper I was done by the author and in Paper II the author was assisting in the measurements. Paper II is written by G. Simin and S. Vainshtein, who have dealt with the

theoretical background of gain switching. The research described in Paper III, using a single avalanche transistor as a laser pulser, was done by the author, as well as the research described in Paper IV, in which J. Ylitalo and K. Määttä assisted in the measurements. Paper V deals with a liquid crystal attenuator used in a time-of-flight laser range finder. The measurements were carried out and the paper was written jointly by the author and A. Karppinen. The high bandwidth integrated receiver channel is presented with measuring results in Paper VI, which is written by R. Pennala and the author assisted in the photodiode section and in the measurements of the receiver. The theory on internal Q-switching of semiconductor lasers is presented in Paper VII, which is written by S. Vainshtein and the author assisted in the measurements. The whole structure of a high bandwidth TOF laser range finder utilizing short optical pulses is described in Paper VIII. The construction of the device as well as the measurements were done jointly by the author and R. Pennala.

1 Introduction

1.1 Goal and background of the work

The purpose of this work was to develop pulsed TOF (time-of-flight) laser range finder techniques with markedly improved single-shot precision compared to published systems. Especially the single-shot precision of ~10 ps was aimed at corresponding to 1-2 mm in distance. The most important difference to previous rangefinders has been to utilize clearly shorter laser pulses, a few tens of picoseconds, instead of 5-20 ns used typically in the existing laser radar systems /Määttä95, Riegl2002/. Also a new amplifier channel with ~1 GHz bandwidth has been developed for utilizing these narrow pulses. The main reasons for increasing the bandwidth and using narrower pulses have been to improve the precision and accuracy of the laser rangefinder and to increase the measurement speed. A direct consequence of better performance is that new applications for laser range finders can be found, for example, fast acquisition of 3D (three-dimensional) image data and analyzing the structure of materials. Also, if the measurement pulse is fast, simpler timing discriminator types, such as leading edge discriminator, suffice for good performance.

The pulsed TOF laser range finder is based on measuring the time difference between the laser pulses sent to and reflected back from the target. A common structure of the TOF laser range finder consists of a semiconductor laser, one or two receiver channels and timing discriminators and a time measuring unit. Optics and some kind of signal gain control method, either optical or electrical, are also needed. The receiver channel consists of a photodiode, PIN or APD, a transimpedance-type preamplifier and a postamplifier. Part of the laser output pulse is divided for the start-pulse in the optics. Both the laser and the photodiode can be connected to the optics using optical fibres, which makes the design of optics and mechanics easier. The use of fibres may also lead into some problems, measurement nonlinearity caused by the mode dispersion, for example.

The performance of the electronics must be good – change of one millimetre in the distance is equivalent to 6.7 ps change in time, if the measurement is carried out in air. Measuring short time intervals accurately and repeatedly makes wide bandwidth and low noise necessary in the electronics, because the precision of the instrument is directly related to the slew rate of the measurement pulse and inversely related to the noise level.

Other parameters describing the performance of the laser range finder are linearity, stability and walk error. The linearity of the whole device mainly depends on the linearity of the time interval measurement, which can be made good enough by utilizing quartz controlled digital counters. The stability is affected by many factors, for example changes in the temperature. The stability can be improved by controlling the temperature inside the laser range finder and by using the same path for both start- and stop-pulses. The walk error means changes in the distance measurement result as a function of amplitude of the measurement pulse and it is mainly caused by limited gain-bandwidth product of the comparator in the timing discriminator. The walk error can be decreased by using measurement pulses with a high slew rate. It means that laser pulses must be short and powerful and the receiver channel must have a sufficiently high enough bandwidth.

In many applications good linearity, precision and stability are needed, for example when measuring the 3D shape of objects with a scanning laser range finder. In some measurements a good precision is enough, for example when measuring short, repetitive movements. In most measurements good linearity is required, however. If the measurement result is nonlinear but repetitive, the linearity error can be decreased by calibrating. The calibration can be carried out by measuring a known distance of an optical fibre or a calibrated measurement track. Usually in all measurements good single-shot precision is important, because then the number of averaged pulses remains small and the total measurement time is short. A small walk error is also desirable, because eliminating the walk error afterwards from the results is cumbersome, especially in fast measurements, and necessitates to measure the pulse amplitudes at each point.

In the Electronics Laboratory of the University of Oulu several laser range finder devices have been developed for different kinds of applications. The starting point for the development work of laser range finders were positron lifetime measurements in the late 80s /Myllylä78/. Some examples of laser range finders developed have been flutter measurement of a paper track /Ahola86/, measurement of the shape of ship blocks /Manninen92, Kaisto93/, examining the wear of steel converters /Määttä93/, measurement of the shape of concrete elements /Mäkynen94/ and a fast scanning 3D laser range finder /Kilpelä89a/,/Moring89/. The milestones of the technical development have been digital time measurement using analog interpolators /Kostamovaara86/, digital time measurement realized in one printed circuit board /Rankinen91/, a receiver channel in one ASIC chip /Ruotsalainen94/ and the time measuring unit in one ASIC chip /Räisänen-Ruotsalainen97/.

There are several possibilities to improve the single-shot precision of the TOF laser range finder. The precision can be improved proportionally to the square root of change of any one of parameters like bandwidth of the laser range finder, the optical pulse power of the laser, repetition frequency or averaging time /Koskinen92/. Increasing the averaging time is most straightforward, but in a 3D shape measurement, for example, there is only limited time available for measuring the distance to one point in the target. Increasing the optical power or repetition frequency is restricted by the limitations of the laser and by the processing speed of the computer collecting the results. Using shorter optical pulses and increasing the measurement bandwidth improves single-shot precision (provided that the channel noise does not increase too much), which enables shorter measuring times, more accurate measurement results (due to smaller walk error) and better resolution of two sequential targets in an optical fibre.

In the TOF laser range finders published earlier and referred in chapter 2 the length of the laser pulse used and electrical bandwidth of the receiver have been 5-20 ns and 50-200 MHz, respectively. The main goal of this thesis is to study whether faster optical pulses and higher electrical bandwidth offer significant improvement to the performance of the laser range finder. The most important benefits expected are decreased walk error and improved single-shot precision. A laser range finder has been constructed to test the benefits of high bandwidth using a prototype transimpedance amplifier and a silicon APD (avalanche photodiode) having a GHz range bandwidth. A new type of laser transmitter has been used, which creates optical pulses with a length of some tens of picoseconds and power in the range of 100-200 W using commercially available SH semiconductor lasers.

1.2 Content of the work

This thesis consists of three main chapters: In chapter 2 some alternative distance measurement methods using light, ultrasonic sound or electromagnetic radiowaves are compared. The methods using modulated light, like modulated continuous wave (CW) and TOF, are discussed more accurately. Some laser range finder applications developed in the last three decades and new possible applications for fast pulse range finders are also presented in chapter 2. In chapter 3 the properties and typical sources of error of each block of a TOF laser range finder are presented. The properties of a laser transmitter, timing discriminator and photodiodes are discussed in more detail. Especially those sources of error are analyzed, which can be improved by using fast pulses. In chapter 4 the prototype high bandwidth laser range finder is presented with measurement results. In chapter 5 the most important results of the thesis are discussed..

2 Distance measurement methods and applications

The distance measurement techniques are needed for defining the position, dimensions or movement of the target. Possible applications are, for example, controlling dimensions or quality of goods in industry, measuring speed or acceleration, controlling a safety area, surveying, military applications or measuring distance to aeroplanes or satellites. The applications relating to 3D vision are object recognition, identification of the object orientation or calculating the number of objects. The applications of 3D vision often relate to guiding a robot in complicated tasks or navigation of a moving robot in working environment.

Active, nontouching distance measurement can be realized acoustically by ultrasonic sound, by RF (radio frequency) electromagnetic waves or optically with light. In all methods a signal is sent to the target and the distance is calculated based on the properties of the signal reflected back from the target. The properties of range finders using gigahertz range RF waves and optical methods have been compared in /Hovanessian88/. A common factor to both range finder types is that the angle resolution depends on wavelength. The divergence of the beam decreases, when the wavelength decreases. The optical methods are the best when a high resolution in horizontal and vertical dimensions is required. As the optical methods also enable the best resolution and accuracy in distance measurement, they are the most suitable methods in producing an accurate 3D image from the target, if the medium used (usually air) has not too much particles, like dust or smoke in it.

2.1 Acoustic and RF distance measurement methods

The distance meters utilizing sound waves use frequencies in the ultrasonic range from 20 kHz to some megahertz. The advantages of ultrasonic methods are relatively low frequencies, which are easy to handle with electronics, simple and cheap structure of the device as well as the capability to measure to metal-, mirror- and glass surfaces, which are difficult for optical meters. The main disadvantage is the large divergence of the beam (the width of the beam being some tens of degrees), slowness, multiple reflections and

large attenuation in long distances. The angle- and distance resolution can be improved by using several receivers or signal processing /Peremans93/. Speed can be increased by increasing the operating frequency. In measurement distances of a few centimetres also the measurement accuracy can be good, even 0.2 mm /Teshigawara89/. The ultrasound methods are most suitable in short distances (some tens of metres at the maximum) and for applications in which the measurement process is simple, for example, the collision alarms for cars and robots or for applications in which there is a large amount of dust or other particles in the air /Teshigawara89/. However, also ultrasonic 3D sensors have been developed /Watanabe92/.

The electromagnetic RF waves have been used since 1930s in traditional radars (radar = radio detection and ranging), which are used for measuring distances to all kinds of materials in boating, aviation and military- and space applications. The radars utilize frequencies from some tens of MHz to over 100 GHz. The most popular frequencies are microwaves in the range of 1-10 GHz. The resolution in measuring the angle or distance is usually worse than with optical methods. The angle divergence is tens to hundreds of mrad (from some degrees to tens of degrees) in microwaves (1-40 GHz) and 10-20 mrad (~1 deg.) in millimetre waves (over 40 GHz /Hovanssian88/). High pulse power (even some megawatts) and long measurement range, also in smog or dust, are achieved with RF radars. For example the police radars used for speed control are capable of achieving one kilometre working distance, but the divergence is relatively high, 200-300 mrad/Fisher92/. The millimetre wave RF radars are also suitable for shorter distances, like tens to hundreds of metres, because the distance measurement resolution achieved is reasonably good, for example +/- 15 cm when measured to 3D targets in the distance range of 0.5 to 15 m with a frequency of 94 GHz /Lange89/,/Boehmke98/.

2.2 Optical distance measurement methods

2.2.1 Classification of the methods

The optical distance meters are often called LADARs or LIDARs (LADAR = laser detection and ranging and LIDAR = light detection and ranging) or with the term laser range finder. The term laser radar includes both laser range finders and the devices measuring the absorption or scattering of light of the atmosphere. In this thesis the term laser range finder is used for laser distance meters.

The optical distance measurement methods can be divided in many ways, one of them being the classification to passive and active methods. The passive methods do not need their own light source, but they use the ambient light for gathering the distance information from the target. The active methods have a light source of their own for illuminating the target. The most important active methods are interferometric methods, geometric methods (triangulation) and time-of-flight /Bosch95/. Another classification divides the methods to image-based and direct methods. The direct methods give an unambiguous distance to some point in the target. In the image-based methods the

distance is calculated with some algorithm based on shades or relative positions of the different parts of the target, for example. The third classification type divides the methods to monocular and multiple view measurement methods /Jarvis83a,Moring89/.

The passive monocular methods are often based on calculating the shape from shading, texture, motion or focus /Optinav2002/ from an image created with a CCD or CMOS image sensor, for example. In these methods the typical problems are the small differences in the illumination (especially outdoors) or the reflectance of the target. The multiple view methods are also classified as triangulation methods or as stereo vision. The triangulation methods are the most common distance measurement methods, because they are simple and reliable in a demanding industrial environment /Besl88/. The idea in passive triangulation is to measure the angle formed between the points of two receivers (cameras) and a target. The larger the distance between the receivers, the better the sensitivity, but then there is also a greater possibility to have a "missing part" problem, which means that the target is partly shaded by some other object in the scene. The advantage of the passive methods is their simple structure and safety; there is no danger to the human eye. A one-dimensional CCD (or CMOS) photodiode matrix or a PSD (photosensitive detector) is enough as a sensor for passive triangulation. There are several variants of the stereo vision. For example, the target may be moving, in which case only one camera is enough. Most of them are, however, based on some kind of triangulation systems.

The active multiple view methods are based on stereo vision (triangulation) with active contrived lighting of the target, which makes it easier to calculate the distance. The contrived lighting is realized with a laser beam, which usually has the shape of a stripe, grid or some other pattern /Jarvis83a/. The advantage of using a laser is small divergence and small spot size, but high coherence may also bring unwanted interference patterns. The lighted spots may also be realized with a fibre grating /Ohya94/. Here fibre grating means that two layers (in a 90-degree angle to each other) of parallelled fibres are used as the optics for creating the net of spots. The accuracy for the measurement of one spot may reach even the precision of 50 µm in the distance of 3 metres /Besl88/.

The active direct monocular methods are interferometric methods and TOF methods. Also the shape-from-x methods, in which x means shading, texture, motion or focus, can be active, if the target is illuminated with a light stripe from a laser, for example. The interferometric methods include Moiré techniques, holographic interferometry and Fresnel diffraction. In the Moiré technique the target is illuminated with laser light through a grating and the image of the target is captured through another grating with a camera. The gratings create a diffraction pattern and the distance can be calculated by measuring the position of diffraction stripes. In holographic interferometry a hologram is created from the target and the hologram is used as a reference object. When the hologram and the original target are illuminated with a laser beam, their combination creates an interference pattern. The distance can be calculated from the distance between the lines in the pattern. The Fresnel diffraction is based on illuminating a grating with coherent light, whereupon the grating creates interference patterns in regular distances, which can be used for distance measurement. In general, the interferometers are very accurate, even in µm-class. The problem is that without reference distances it is impossible to measure distances unambiguously, and only the differences in distance can be measured. Using several wavelengths also absolute measurements can be carried out

/Bien81/. One application of interferometry is to measure the movements of earth's crust /Vali66/.

The monocular 3D vision sensors usually use scanning TOF laser range finders. The scanning is realized with mirrors which are turned by galvanometers (turning coil in a magnetic field) /Moring89/, stepping motors /Lewis77/ or acousto-optic crystals, in which a high frequency acoustic wave produces a series of different refraction coefficients inside a piezoelectric crystal. The turning angle can be measured, for example, with a capacitive sensor, if galvanometers are used. The TOF method may also have two optical axes, in which case one axis is for the transmitter and the other for the receiver, but because the optical axes are very close to one another, the method is classified as monocular.

In table 1 some optical distance measurement methods are presented according to the classification presented above in 8 classes in principle, but only 5 classes in practice.

Table 1. Optical distance measurement methods

	Passive, direct	Passive, image based	Active, direct	Active, image based
Monocular		shape-from-shading	interfero-metric	illuminated
		shape-from-texture	methods	shape-from-x
		shape-from-motion		
		shape-from-focus	TOF-methods	
Multiple view	passive triangula-tion		active triangulation	

The targets can also be classified as active or passive ones, mostly when the optical methods are used. The passive methods mean noncooperative targets, which may have very large variation of the reflection coefficient. The reflectance may also vary much as a function of the measurement angle, from a Lambertian surface (with equal brightness to all directions) to mirror-like reflective surfaces. The target will be active, when some reflector, such as a reflective tape or corner prism, is attached on it. The artificial reflectors reflect the incoming beam very effectively back to their source direction.

In the following chapters the TOF method is presented in more detail, also with the applications.

2.2.2 TOF method

Two of the main advantages of the TOF method are that the transmitter and receiver beams are coaxial and that the measurement accuracy does not depend on distance (which is not the case with triangulation, for example) /Strand85/. In TOF laser range finders either pulse, amplitude or frequency modulation is used. In the pulse modulation method the flying time of the pulse reflected from the target is measured /Goldstein67,Koechner68,Määttä93/. In the amplitude modulation method the phase difference between the sine modulated transmitted and reflected beams are measured. /Payne73,Zahid97/. In the frequency modulation (”chirp”) technique the signal frequency is swept across some limited range of frequencies. Using heterodyne techniques an

intermediate frequency is generated, the frequency of which depends on the distance of the target /Hulme81/. The most popular methods are the pulse and amplitude modulations. In /Koskinen92/ it has been shown with calculations that the pulse modulation method has better precision than the amplitude modulation method, when the average output powers are equal. The maximum unambiguously measured distance with the amplitude modulation method is only half of the wavelength. If longer distances are to be measured, several modulation frequencies must be used. With high modulation frequencies a high resolution can be achieved, but the measurement range is short. Also high accuracy can be achieved with long averaging times. For example, in /Smith80/ a commercial amplitude modulated laser range finder using three modulation frequencies has been presented. The accurary achieved was +/- 6 mm with an averaging time of 9 seconds and a distance of 1 km measured to an angle prism target. In short distances (0-7 m) and small output laser power (2 mW) an accuracy of 3 mm has been achieved with 10 us averaging time /Lamela96/ and in /Payne73/ an accuracy of +/- 0.08 mm in 60 m distance range has been achieved when using a retro-reflector as the target.

In the TOF method either direct or coherent detection methods can be used in the receiver. In direct detection the signal power from the detector is measured as a function of time. One advantage of coherent detection is the capability to measure not only distance, but speed as well, because also the phase information is preserved in the receiver and the speed can be calculated from the Doppler frequency /Halmos93/. The two alternative methods in coherent detection are heterodyne and homodyne methods. In the heterodyne method the signal arriving from the target is summed optically with the signal from the local oscillator. The local oscillator (LO) laser must be temporarily and locally coherent with the signal from the laser transmitter in order to reach the best S/N-ratio. The photodiode of the receiver operates as a low-pass filter and filters out the optical frequencies leaving the target information at a frequency, equal to the frequency difference (intermediate frequency) between the received signal and LO radiations. An electrical demodulator is needed to bring the signal frequency from the IF to the original baseband frequency. The distance of the target is calculated on the basis of the phase, amplitude or frequency of the IF (intermediate frequency) signal according to the modulation type chosen. A better sensitivity can be achieved with the coherent detection than with the direct detection, because the power of the local oscillator can be high. In this case the dominating noise source is the shot noise of the signal /Vaughan96/. The local oscillator beam can be realized, for example, with an acousto-optic modulator, which then defines the intermediate frequency /Duncan93/. In the homodyne method the beam of the laser is divided into two beams, one of which is the target beam and the other operates as a local oscillator. In this case the signal is transferred directly to the baseband, to the original signal frequency. Other possibilities for local oscillators are using a two-frequency laser, in which the difference of the frequencies of the output light is small enough for amplifiers, for example about 1 GHz /Araki94/, or modulating the current of the transmitter laser /Payne92/. In /Bosch96/ the operating principle of a laser range finder was based on using the laser also as a receiver and measuring the self-mixing effect in the laser. The precision achieved was 1.8 mm in a distance of 3 m.

Some commercially available laser range finders based on TOF method are presented in table 2. The operating principles are pulse and amplitude (sine wave) modulation. All range finders in table 2 utilize direct detection method. It can be seen that the sine wave

modulated range finders are slower, but accurate. The pulsed methods are used mainly in long distances and in applications which need short measuring time.

Table 2. Some examples of commercially available laser range finders utilizing semiconductor lasers.

Name	Modulation	Meas. range	Accuracy	Meas. time
LaserTech.Impulse 100LR	Pulse (900nm)	0-575m	3 cm @50 m, white target	0.3-0.7 s.
Riegl FG21-HA	Pulse (904 nm)	2-600 m	+/- 5 cm	0.1 – 1s.
Riegl LD90-3100VHS-FLP	Pulse	2-200 m (reflectance 80 %)	+/- 2.5 cm	0.5 ms
LaserOptronix LDM500 MIL	Pulse	0-999 m	+/- 1 m	-
Leica DISTO pro	Sine wave	0.3 – 100 m	+/- 3 mm	0.5 – 4 s.
LaserOptronix PH30	Sine wave	0-30 m	+/- 5 mm	-

2.2.3 Applications and required performance of the pulsed TOF laser range finder

Several applications of pulsed TOF laser range finders have been presented in /Riegl2001/. The applications have been classified to surveying, measurement of height, profiling, industrial applications and traffic safety. In these applications the distance varies in a large range, from zero to kilometres and the accuracy required varies from some centimetres to some tens of centimetres with passive targets. For example in surveying and in localizing the exact position of targets in buildings and in accurate robot work even millimetre level accuracy may be required. On the other hand, in warning systems and in long distances the accuracy required can be some centimetres, and in military applications even some metres. In real time control of robots and industrial processes and modelling of 3D targets also high measuring speed is needed, however in most applications speed is not critical, a measuring time of some seconds for one point is enough.

The first applications in the 1960s were measurements of height or surveying, often in long distances, especially in space to satellites or to the moon /Bender67,Poultney77/. In /Ammon70/ a laser range finder was used for measuring the position of an astronaut on the surface of the moon in distances of some hundreds of metres. The other coordinates were measured with a four-element position-sensitive detector. One of the first tests was also a laser range finder using a semiconductor laser and a light multiplying tube, which was used for measuring distances to passive targets in distances of some hundred metres to passive targets and even kilometres to active targets /Goldstein67/. A pulsed semiconductor laser and an avalanche photodiode have been used already in 1977 for measuring distances of 7 km /Salathe77/. In /Querzola79/ two wavelengths were used for

eliminating the errors caused by the atmosphere in some kilometres' range of distance. In shorter distances the applications of surveying are, for example, measuring the shape of walls and roofs of houses, which is necessary for defining the exact positions and dimensions of old buildings. Measuring of height is useful in defining the position of aeroplanes, missiles and parachutes.

One of the most popular laser range finder applications has been defining the profile of the target and identifying it, like a car passing under the range finder /Hansen69/. Also measuring the shape and volume of underground caves and tunnels or overground piles of materials is one of the profiling applications. The differences in height of earth ground have been measured from aeroplanes using semiconductor or Nd:YAG-lasers /Bufton89,Mamon78/. A kilowatt-power Nd:YLF laser working at 526 nm wavelength has been used for measuring the profile of the bottom of the North Sea in oil well areas /Klepsvik94/. In /Kaisto83/ a laser range finder was used for measuring the profiles of wood and metal surfaces in a distance range of 1.5 – 10 m and with an accuracy of +/- 3 cm and measuring time of 10 ms. In one sense also one type of profiling application was a paper flutter meter, which was able to distinguish a 20 μm back and forth movement at 5 Hz frequency /Ahola86/.

Some examples of industrial applications are positioning of ships and cranes, measuring the amount of stored liquids and solid materials, proximity switches, positioning of machine tools and measuring the tension of conveyor belts. One special application is to measure the level of molten steel /Araki96, Kompa84/. The accuracy achieved in the first reference was 1 mm at the distance of 1 m and in the latter +/- 3.5 mm in a distance range of 3 to 7 metres the measurement times being 200 ms and 20 ms, respectively. Other industrial applications are, for example, measuring the levels of liquids, like oil /Kostamovaara86/ and measurement of the wearing of the lining of a steel converter made of bricks /Määttä93/. The latter example was capable of an accuracy of +/- 10 mm in a distance range of 3 to 27 m and a single-shot precision of 10 mm, at best. One industrial application is also to measure the changes in the shapes of constructions by integrating an optical fibre inside the construction, which can be a glass-fibre container or a steel bar in a bridge, for example. It is possible to measure even local changes in the constructions, because the fibre contains Bragg grating reflectors positioned at even intervals /Lyöri97/.

Some military applications measure the distance to a flying aeroplane using a special type laser range finder /Steele76/ or a general purpose, binocular-shaped, laser range finder, which is capable of measuring up to 10 km distance with an accuracy of 10 metres /Guyer82/.

Safety applications of laser range finders are anticollision warning radars /Kawashima95,Sekine92/ and warning system for an approaching train /Tilleman96/. Laser range finders can also be used in traffic control and in safety control of automatically moving vehicles.

2.2.4 3D vision applications of pulsed TOF laser range finders

In 3D vision the TOF method gives several advantages compared to other optical methods /Lewis77/. The measurement result is unambiguous and accurate both in horizontal and vertical directions, because the measurement beam is narrow and there is no danger of the target being hidden behind some other object in the scene, like in triangulation. A further advantage of the laser beam is that it can be used, for example, to help direct a CCD or CMOS camera. The TOF method is also often faster than the methods based on analyzing the image created with a camera.

The 3D robot vision is used mostly in two different applications, in guiding robots and in industrial measurements. The robot appplications are connected to automated navigation, moving the leg of a walking robot, automated service vehicles, in manufacturing and inspection of the produced goods, car transportation and military and agricultural applications /Carmer96/. The industrial applications of 3D vision are for example picking of things, following a moving target, complicated assembly, tightening of screws, calibrating the position of a robot, and verification and localization of parts in assembling of printed circuit boards /Riggs85/.

The sensors producing 3D images can be divided according to the distance range to short range sensors (less than 10m) and long range sensors (distance range of some tens of metres). One of the first short range TOF-3D sensors was a sensor working at 10 kHz frequency and using a pulsed laser and a light multiplier tube, which was able to produce a 64 x 64 pixel picture in 4 seconds with an accuracy of 2.5 mm and measurement range of 4 m maximum /Jarvis83b/. A 3D sensor presented in /Moring89/ used a pulsed semiconductor laser and an avalanche photodiode and was capable of measuring a 128 x 128 pixel picture in 2.5 seconds at the distance of 4 metres with an accuracy of +/- 7 mm.

Long distance laser range finders have been used, for example, for guiding a walking robot on the surface of planet Mars /Krotkov94/. The device was a commercially available 3D sensor, which was capable of producing a 256 x 256 pixel picture in 0.5 seconds in 40 metres distance at the maximum and with a precision of 10-15 cm. Another device designed for robot guiding on planet surface was capable of measuring 100 points in a second to passive targets with an accuracy of 2 cm and up to a distance of 30 m /Lewis77/. The sensor presented in /Kaisto93/ was used for measuring distances to industrial metal blocks, like parts of a ship, in distances of 3 – 30 m and with an accuracy of 1 mm and a measurement time of 3 seconds to one point. A 3D sensor modification was manufactured from the same sensor and it searched and measured automatically the pieces of reflective tape attached to the target with an accuracy of +/- 0.3 mm in vertical and horizontal directions at distances of 15 metres maximum /Mäkynen94/.

2.2.5 Advantages of short pulses in TOF laser range finding

By using short laser pulses and wide bandwidth in TOF laser range finders almost all parameters are improved: the walk error decreases, single-shot precision improves and the possibility to distinguish two successive measurement pulses is also improved. All

these properties can be used in existing laser range finders, but they also enable some new applications to be achieved.

The most useful applications for fast and accurate laser range finding are the 3D sensors. Using short pulses improves the capability to measure unambiguously plenty of target points in a short time. If the distance measurement is accurate enough, even one single pulse may be enough for one measurement point, in case of which no averaging is needed. In this case acquiring a 128 x 128 picture takes 0.33 s with 50 kHz pulsing frequency, if the scanning mechanism is fast enough. Using shorter pulses is useful also in fibre strain measurements, because short pulses enable more accurate localization of the measurement point in complicated concrete-, steel or glass fibre structures, in which the fibres are embedded /Lyöri97/.

Some new applications for fast laser pulses are for example timing analysis measurements, in which the inner structure of materials like pulp /Karppinen95/ or paper /Plucinski99/ can be analyzed by measuring the widening and delay of the laser pulse going through the material. In the pulp measurement the size and distribution of the long fibres and small particles, which finally define the structure of the paper fabricated, are examined. In the paper measurements the actual problem is to measure directly from the just fabricated paper the features defining the printing quality, like porosity and roughness. The existing devices are based, for example, on measuring the permeability of the paper and using them needs laboratory conditions and they are not very reliable. In principle the same technique (optical tomography) can be also used for other materials, which do not attenuate near infrared light too much, such as investigating the properties of human tissue and internal organs in medicine.

3 Structure and error sources of a pulsed TOF laser range finder

3.1 Structure of a TOF laser range finder

The laser range finder presented in this thesis consists of a transmitter, one or two receiver channels and a time measuring unit (Fig. 1). The transmitter consists of the laser and a pulsing electronics. An IBM-compatible PC or a microcontroller card can be used for collecting the measurement results and controlling an optical attenuator, if it exists in the device and also to adjust the parameters, like APD gain, of the receiver channel. Each of the receiver channels consists of a photodiode, transimpedance type preamplifier, voltage type post-amplifier and a timing discriminator. In a two channel laser range finder the START- and STOP pulses each propagate in their own channels, in which case a PIN photodiode can be used in the START channel for lowering the cost and noise. In single channel range finder the START- and STOP pulses are connected optically to the same photodiode. The timing discriminator changes the analog measurement pulses to logic level pulses, which are fed to the time measuring unit. The most important property of the timing discriminator is to keep the timing event at the same point independent of the amplitude of the incoming pulse. The time measuring unit can be based on counting the clock pulses, like in TDC (time-to-digital converter) or on discharging a capacitor with constant current, like in TAC (time-to-amplitude converter). The TDC measures the time period using a quartz oscillator as a clock and the time between two sequential clock pulses more accurately using analog interpolators, TACs. The optics has either one or two axes and it is usually separated from the electronics, in the case of which optical fibres are used for guiding optical pulses between the optics and the transmitter/receiver.

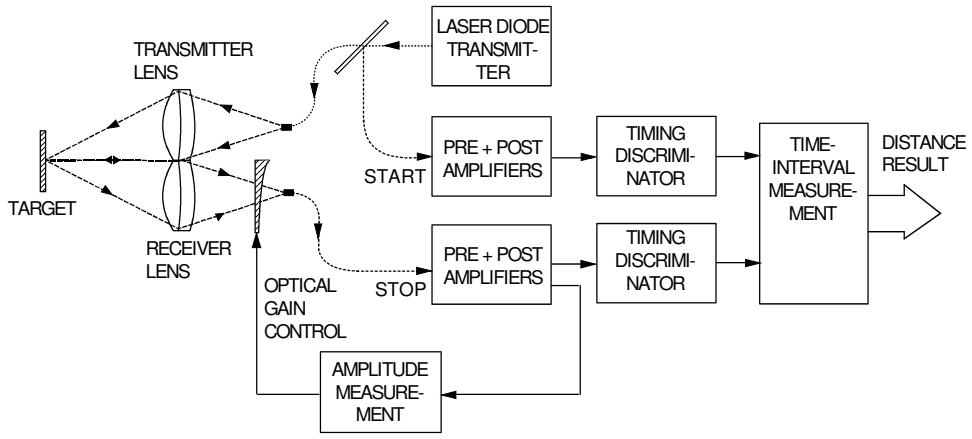

Fig. 1. The structure of a two-channel TOF laser range finderThe structure of a two-channel TOF laser range finder

3.2 Definitions of the performance parameters

The performance of the range finder is defined with several terms, such as resolution, precision, walk error, accuracy, linearity, stability and repeatability. In practice the values for terms stability, accuracy and linearity are expressed as nonstability, nonaccuracy and nonlinearity, even though the terms used are expressed without non-ending. These terms are based on definitions presented in /IEEE96/. Walk error, nonlinearity and nonstability are systematic errors. The terms precision and repeatability describe random errors. Systematic errors can be repeated in defined conditions and they can be compensated to some extent by calibrating. Random errors are not repeatable and they can not be removed by calibrating.

The term resolution means the smallest change in the distance that can be resolved. If the reading scale is digital, it means the smallest digit in the scale. In analog scale the resolution means the smallest change that can be resolved in the scale and is limited by some factor, such as optical clarity or width of the needle indicating the number. In the 3D range finder also the resolutions in vertical and horizontal axis are important and they can be limited by optical or mechanical factors.

The term single-shot precision describes the uncertainty limited by random errors in the measurement and it is defined with statistical variance (σ-value) of the distribution, when some constant distance is measured. The precision is calculated from a large enough group of measurement results. The single-shot precision σ_t depends on the slew rate of the incoming pulse and the sum of all squared noise sources:

$$\sigma_t^2 = \frac{\sigma_n^2}{(dV/dt)_{V=D}^2} \quad , \qquad (1)$$

where σ_n^2 is the sum of all squared noise voltage sources and $(dV/dt)_{V=D}$ is the slew rate of the input signal /Bertolini68/. Formula 1 is derived for a pulse, which crosses a constant level. The timing point should be chosen so that the ratio between noise and slew rate is at its smallest. If the single-shot measurements are repeated n times and the oscillators of the transmitter and the time measuring unit are not synchronous (the single-shot measurements are independent of each other), the precision of the averaged result is improved by a factor of $\sqrt{n}$ compared to the single-shot precision.

The repeatability includes all random errors, when a fixed distance is measured repeatedly in fixed conditions. The difference between repeatability and precision is that repeatability defines the repeatability of the whole measurement procedure whereas precision defines the differences between successive independent single-shot measurements.

The walk error means the error in the distance measurement result, which is created in the timing discriminator by the changes in the amplitude of the received measurement pulse, which in turn depends on distance, reflection coefficient and measurement angle. The walk error is an important factor in TOF laser range finders, because the changes in the power of the received pulses are large.

The term nonlinearity (or linearity) defines the deviation of the measurement results from a straight line, which is drawn in co-ordinate between the smallest and largest measured distances or from a straight line, which gives the smallest rms (root-mean-square) deviation for the individual measurement points.

The term stability defines the changes in the measurement results during some, usually long, time period. The stability may, however, worsen in the course of time, so it cannot be compensated by calibration.

The term accuracy means the largest total error in some defined measurement range and in a defined time period. Accuracy includes all errors, both statistical and nonstatistical, so accuracy can be improved by executing test measurements and calibrating the device in variable conditions, like temperature and humidity.

3.3 Error sources and factors limiting the performance

The measurement error is caused by noise, changes in the pulse shape and amplitude and changes in the delay of optical and electrical signals, for example. The operation of time measuring unit may also prove unstable during a long period of time and in varying temperatures. Noise creates statistical changes between successive results, but the changes in delays have an impact during long time periods in varying measurement distances and circumstances. If different error sources, which all create their own effect on the same error, are independent, the total rms (root-mean-square) error is calculated by summing the squares of the different error components together.

The noise in laser range finder consists of noise from amplifiers, dark current noise from the photodiode, shot (quantum) noise of background light, shot noise of the signal itself and the additional noise created by the instability of the multiplication process of the avalanche photodiode. Also electrical interference coming outside or from power supply may increase noise level of the amplifiers.

The changes in the level of the measurement signal are caused mainly by the changes in the reflection coefficient of the target, measurement distance or the temperature. The power of the signal reflected from the target may change, for example, in a range of 1:100 with passive targets (wood, paper, metal), when the distance varies in a range of 1-11 m /Kaisto83/. The reflection coefficient ε_r varies usually in a range of 0.1 to 1 with passive targets. If the optics is focused separately on each measurement distance, the level of the received signal varies according to the second power of the measurement distance. The changes in the temperature affect the power and wavelength of the laser and the gain of the APD. Also the changes in the wavelength may change the power received, for example if steep pass-band wavelength filters are used in front of the receiver or transmitter.

The pulse shape may change, for example, as a function of temperature, especially with high power SH-lasers, as shown in Paper I. Another possibility is that the amplifiers are nonlinear, especially in large amplitudes, and it leads to distortion in pulse shape. Some other electrical pulses may interfere with the measurement signals in the printed circuit board or inside the receiver integrated circuit, thus causing measurement errors. The interfering pulses may be, for example, logic pulses, pulses from the other receiver channel or disturbances from a switching power supply. The pulse shape may also change when it is reflected from a plane target, which is almost parallel with the measurement beam. The result is that the received pulse is wider than the transmitted pulse. If the measurement beam hits two different targets located at different distances, the received pulse may be constructed of two different pulses partly or totally separated from each other in time scale. The pulse shape may also change in optical fibres due to twisting or in multimode fibres due to mode dispersion.

The changes in the delay of the measurement signal path, either optical or electrical, affect directly the measured distance. In multimode (MM) fibres the mode dispersion causes widening and delay of the pulses and the delay of the fibre depends on temperature. Also the delay of the attenuators and (adjustable gain) amplifiers may vary, when attenuation, gain or temperature is changed. Using differential amplifiers and a single channel, the range finder structure may help to decrease the sensitivity to changes in the gain and temperature. In /Määttä90/ it has been measured that using a single channel structure the temperature sensitivity decreases in practice so much that the temperature sensitivity of the TDC is dominating. A third alternative for delay changes may be the changes in the pressure or temperature of air. Fourth, and in practice often the dominating source of delay error is the walk error in the timing discriminator.

Even if the time delay between the START- and STOP pulses were correct, the time measuring unit may create its own error. The changes in the bias voltages or currents in an analog time measuring unit may affect the result. In a digital time measuring unit the frequency of the oscillator may change as a function of time and temperature creating an additional error.

Using a pulsed TOF laser range finder faces some limitations, set by laws of physics or the semiconductor technology used. One of the limiting factors is the limited amplitude range of the measurement pulse. The smallest measurable signal amplitude is limited by the amount of noise present in the receiver amplifier channel. In order not to mix too many noise pulses with the measurement pulses, the peak amplitude of the signal should be at least 10 times larger than the rms-value of the noise, when the noise is assumed to have Gaussian distribution /Ziemer76/. In theory, even if smaller amplitudes than 7.1 times the rms-noise value are rejected, one pulse out of one million measurement pulses is a noise pulse. The absolute maximum voltage value received from the amplifiers is limited by the operating voltages of the amplifiers, which in turn is limited by the maximum operating voltage of the transistors. When commercially available amplifiers are used, the bandwidth is limited by the baud rates normally used in digital communication electronics. However, the baud rates and bandwidths have been increasing constantly. The width of the laser pulses is limited by the operating mode used in the laser /Vainshtein97/. One important limitation is also the wavelength of a sufficiently powerful laser, which is available. The wavelength and power may also be regulated by the safety class required. The safety class mainly depends on the wavelength of the laser, because long wavelengths (>1.4 μm) cannot be focused on the retina of a human eye - so with long wavelengths even several decades higher peak powers can be used than with less than 1 um wavelengths. However, currently the most powerful semiconductor lasers can be found in the wavelength range of 800-900 nm.

3.4 The transmitter

3.4.1 General structure

An amplitude modulated transmitter includes a laser and pulser electronics. The same structure is also used in this work. A pulsed semiconductor laser is the most common type in laser range finders, because it is small, relatively cheap, durable and it has good efficiency. The peak powers vary usually in the range of 5-100 W, and the current pulses needed vary from a few amperes to several tens of amperes. The required power is defined by the measurement distance, optical losses and the reflection coefficient of the target. The higher is the power needed, the larger are the dimensions of the laser. In the distance range from a few metres to several tens of metres both SH (single heterostructure), and DH (double heterostructure) type lasers can be used. The laser construction may include 1-3 laser chips piled on each other and the peak power level varies in a range from 2 to 30 W with one chip lasers and 5 to 150 W with several chip lasers /Laser2000/,/EG&G95/. The width, thickness and length of the active region of SH lasers vary in a range of 75 μm to 400 μm, 1 to 2 μm and 200 to 300 μm, respectively. The semiconductors used are GaAs, GaAlAs or InGaAs alloys and they operate over wavelength range of 850 to 910 nm. If the reflectivity of the target is high, like in measuring the fibre strain /Lyöri97/ or liquid level /Kostamovaara90/, also CW

(continuous wave) lasers with a small output power (1 mW – 50 mW), small size and long wavelength (1300 – 1550 nm, used primarily in fibre telecommunications) can be used in pulsed TOF laser range finders.

A basic laser type is a AlGaAs/GaAs single heterostructure SH-laser with GaAs active layer. Short pulse semiconductor lasers (pulse lengths varying from tens of picoseconds to hundreds of picoseconds) are used in fibre telecommunications, optical signal processing, LIDARs, as pumping lasers for nonlinear optical systems /White93/ and in time-resolved spectroscopy, which is used for analyzing biologically important reactions, for example /Dixon97/. The technological progress in semiconductor lasers follows quite strongly the needs of fibre telecommunications industry. The wavelengths 0.9 μm, 1.3 μm and especially 1.5 μm are favoured, because of attenuation minimas for glass fibres /Cheo89/. A common goal is high efficiency and low threshold current. The gain in the laser cavity can be increased by localizing the electrically and optically active region to as small a volume as possible and it can be achieved with heterostructure junctions. The charge carriers can be localized both with SH and DH structures (gain guiding) but optical radiation can be focused better (index guiding, i.e. diffraction losses are smaller) with DH structure. High power SH lasers have been commercially available up to the last years, but they are reducing in number as technologically old structures on the market. With multi-quantum well (MQW) lasers even higher gains and shorter pulses can be achieved than with DH lasers, because the density of the states is highly concentrated to the valence and conduction band edges, so the coherence is better and threshold currents are even smaller than with DH lasers /Sogawa91/.

The most straightforward way to generate optical pulses from a semiconductor laser is to modulate the current, which affects the gain and optical output power. Operating above the threshold current the optical output power increases linearly with the current in CW mode and with long pulses. However, the length of the optical laser pulse does not correlate linearly with the length of the current pulse, when short current pulses, i.e. about as long as the delay of the lasing, are used. The simplest circuit of the pulsing electronics includes a capacitor, which is discharged to the laser with a high power switch. The most common type of switch is an avalanche transistor. The optimum pulse length is defined by the bandwidth of the receiver. If the optical laser pulse is clearly shorter than the FWHMs calculated from the receiver bandwidth, the full gain of the receiver can not be reached. If the pulse is longer and the rise and fall times are slower, the precision will deteriorate. In practice the minimum length of the current pulse will be limited by the speed of the switch and the serial inductances of the high current loop in the circuit.

In special applications some other laser types may be more practical. If kW-class output powers or long wavelengths are needed, for example a PGT:Nd-laser /Arumov93/ or a CO_2-laser /Taylor78/ can be used. If an eyesafe laser is needed, the wavelength should be over 1.4 μm. For example with CO_2-lasers (λ=10.6 μm) a 2000 times higher power is allowed to reach the same safety class than with a Nd:YAG-laser (λ=1.06 μm) /Forrester81/. In long measurement distances the measurement errors resulting from temperature and pressure differences in the atmosphere can be compensated by using lasers with different wavelengths, like HeNe- and HeCd-lasers /Slater76, Querzola79/. The fibre lasers and microchip lasers are alternatives to semiconductor lasers in applications where short pulses with kilowatts of pulse power is needed. For example in /Morkel92/ a pulse power of 1 kW and pulse length of 2 ns have been reached with a

fibre laser at a wavelength and repetition frequency of 1.053 µm and 1 kHz, respectively. A Q-switched Nd:YVO_4 microchip laser is capable of producing a pulse with FWHM and peak power of 68 ps and 5.4 kW, respectively, at 160 kHz pulsing frequency and 1.064 µm wavelength /Braun97/. Both fibre lasers and microchip lasers are larger in size and their structure is more complicated than with the semiconductor lasers, because a pumping laser is needed.

3.4.2 Alternative ways for generating high speed laser pulses

Several ways exist for generating short laser pulses: gain switching, mode locking, Q-switching or modulating a CW laser with an external optical modulator. Mode locking techniques limit the usable operating frequency to some preferred ones. Q-switching, gain switching and optical modulators all allow to select the operating frequency from zero to the maximum usable frequency limited, for example, by excess heating of the laser.

A semiconductor laser can be operated in gain-switching mode by using high slew rate of the current pulse. The optical output typically includes a pulse train of short pulses with decaying amplitude. The FWHM of the pulses may be some tens of picoseconds and the peak power of the first pulse may be several tens of watts (Paper II). If the laser is operating in gain switching mode, the physical parameters of the laser and the amplitude and rise time of the current pulse all define the FWHM and amplitude of the optical output pulse.

In mode locking the principle is to lock all or a part of the longitudinal modes of the resonator to the same phase. In this way the pulse power can be increased by the number of the locked modes. The mode locking can be active or passive. An active mode locking means that the mean time between the modulating current pulses will be adjusted to the transit time of photons between the ends of the laser cavity or its multiple. In active mode locking the cavity of the laser is usually lengthened with an external lens and mirror, because otherwise the repetition frequency is too high, several gigahertz /Bowers89/. The passive mode locking is achieved by modulating the optical losses with a saturable absorber located between the laser medium and the other mirror. The saturable absorber is locked automatically to the frequency of longitudinal modes and current modulation is not needed /Koumans96/.

An active or passive Q-switch is one of the most common ways to achieve short laser pulses. The Q-switch is located inside the laser resonator and the quality (Q) factor of the laser cavity is changed by changing the optical losses. In the beginning the Q-switch is in off-state (Q-value is low) and the population inversion may reach a very high value. When the Q-switch is changed to on-state, the loop gain - which includes also the optical losses - increases rapidly and the result is a short, very powerful optical pulse. An active Q-switch is usually connected as an external optical switch between the active laser medium and the other mirror. The most common laser types used with Q-switches are fibre lasers, Nd:YAG-lasers and CO_2-lasers. The active, external Q-switches are for example electro-optical intensity modulators, which rotate the polarization angle of the

optical radiation. With several laser types, including semiconductor lasers, also a passive Q-switch can be used, which can be realized by adding a saturable absorber to the laser medium. The impurity ions brought to the medium have different energy gaps between the valence and conduction bands compared to the laser medium and they act as energy storages, which absorb energy in the beginning, but do not create laser action. When the energy storages are filled, the laser action starts and the energy storages create photons, which take part in the laser process. In the saturable absorbers the energy is stored and released in two ways: with intraband carrier-carrier scattering and thermalization, which last less than one picosecond and with trapping and recombination process between the bands, with which the duration of the process varies from picoseconds to nanoseconds /Keller96/. For example, a pulse power of 1.5 kW, pulse length of 4.6 ns and repetition frequency of 3.5 kHz have been achieved by using Cr-ions as a saturable absorber in a Nd:YAG-laser /Liu97/.

An alternative choice for electrical modulation is to modulate optically the output of a powerful enough CW-laser. Optical modulation can be realized with acousto-optical or electro-optical modulators, which can also be used as external Q-switches. With acousto-optical modulators a bandwidth of several hundreds of megahertz can be achieved /Isomet2001/ and with solid-state electro-optical modulators even 20 GHz frequencies are achieved. In acousto-optical modulators the refractive index of the crystal is modulated with ultrasonic acoustic waves resulting in an adjustable optical grating, which diffracts the laser light. The advantage of acousto-optical modulators is a large active area, whereas the disadvantage is high power consumption, even tens of watts. The electro-optical modulators, also known as Pockels cells, are the most used modulator types especially in optical telecommunications electronics in high frequencies /Jungerman90,Ramar2001/. In Pockels cells the electric field modulates directly the refractive index of the modulator material, and the changes in the refractive index modulate either the polarity or phase shift of the light. In the latter case (low-voltage lithium-niobate modulator) the light passing through two paths having different refractive indexes interfere with each other, causing amplitude modulation (Mach-Zender interferometer). The optically active area (diameter of several millimetres) and maximum optical power (from milliwatts to tens of milliwatts) of fast lithium niobate modulators are relatively small. With larger ($\varnothing$=10 mm) and slower (t_r=300 ps) Pockels cells, in which the active material is KDP (potassium dihydrogen phosphate), the maximum optical power may be even gigawatts with pulse lengths of some hundreds of picoseconds /Lasermetrics99/. They need a control voltage of several kilovolts. It is possible to separate a single pulse from a passively mode locked laser pulse train with a repetition frequency of 100 MHz with a Pockels cell, for example /Nampoothiri98/.

However, all external modulators increase the size, prize and complexity of the transmitter. The solid-state and gas lasers are usually expensive and cumbersome. The semiconductor laser is small, reliable and relatively cheap component. For these reasons the simplest and most tempting way to realize the laser transmitter is to use only a single pulsed semiconductor laser, which operates either in gain- or Q-switching mode.

3.4.3 Laser pulser electronics

The output power of a semiconductor laser is basically controllable with current. The on-state voltage of one chip is small, only several volts (if the inductances are neglected). In multichip lasers the chips are connected in series, the same current is flowing through all and typically the power/current (W/A) ratio of the pile of chips is clearly higher than with one-chip lasers. The pulse currents specified for the semiconductor lasers in the data sheets varies in the range from 6 to 60 A. The current pulses and output powers are usually specified for 100-200 ns pulse lengths. One manufacturer promises that the typical current values specified in the data sheets may be exceeded fourfold with the same operating life of the laser, if the length of the current pulse does not exceed 10 ns /EG&G95/. In this case even 100 A current pulses are needed, according to the data sheets. The duty factor of pulsed semiconductor lasers varies in the range of 0.04 to 0.1 % and limits the allowed operating frequency to the range of 40 kHz to 100 kHz, when 10 ns long current pulses are used.

The alternatives for switches are avalanche transistors, thyristors, mercury switches and MOSFETs. The avalanche transistors are most common when producing high currents (tens of amperes) and short (a few nanoseconds) pulses for semiconductor lasers. Also the mercury switches are fast (rise time tens of picoseconds), but their usage is limited by low maximum repetition frequency, for example in /Neuhold99/ only 100 Hz. Very fast, high current (t_r~600 ps, I~100 A), GaAs-thyristors have also been manufactured, but they are not available commercially /Vainshtein94/.

The MOSFETs are capable of switching current pulses of tens of amperes, but they are best suited for pulses of several tens of nanoseconds, because charging of the gate capacitances needs quite high slew rates of the current. One option is to charge the MOSFET gate capacitance with an avalanche transistor, which is capable of delivering high currents /Kilpelä89b,Baker90/. In the circuit presented in /Kilpelä89b/ the current amplitude switched by the MOSFET was adjustable in a range varying from 1 to 4.5 A by changing the operating voltage of the MOSFET in a range from 15 V to 75 V and keeping the FWHM of the pulse somewhat stable, at approximately 10 ns, with all current levels. The rise time was short, 1-1.5 ns. By using high voltage MOSFETs it was possible to switch even 800 V pulses to 50 Ω load with pulse widths of 30 - 40 ns with the circuit presented in /Baker90/.

The simplest laser pulser consists of a capacitor, an avalanche transistor, a laser and a few resistors. In the laser pulser presented in Fig. 2 also the serial inductances have been included in the wires, which conduct high slew rates of the current. The capacitor C2 is charged through the resistor R3 between the pulses and it is discharged rapidly with the avalanche transistor through the laser. The charging time of the capacitor can be shortened and the pulsing frequency increased by replacing the resistor R3 with an transistor switch. The additional components are R4, which enables the capacitor C2 to be charged and possibly also C3, which allows a slight increase of the peak current, when the value of C3 is chosen correctly. The transistor is triggered with a small current pulse to the base.

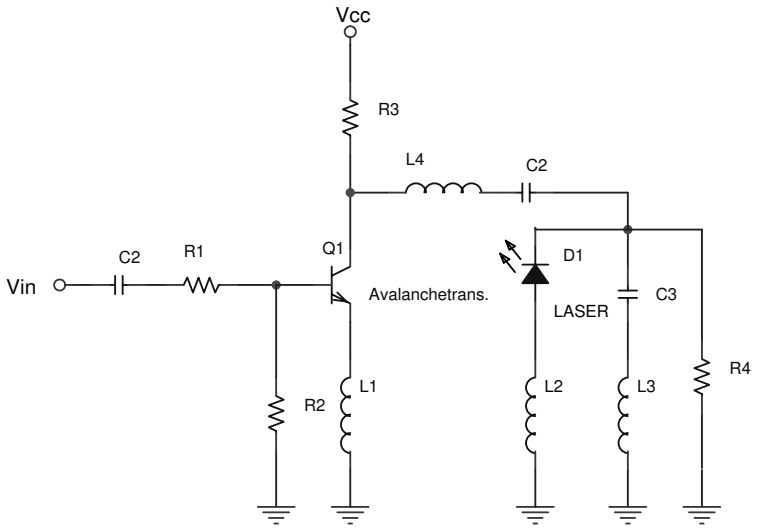

Fig. 2. A schematic diagram of a single transistor avalanche pulser.

Several types of commercial bipolar power transistors can be used as avalanche transistors, if the operating voltage is rises clearly above the normal operating voltage, typically to the level of 100-300 V. In Paper III a few normal bipolar power transistors were compared with a commercial avalanche transistor (ZTX415). The measurement is presented in Fig. 3. The maximum peak amplitudes of current pulses were measured with a 1 Ω resistive load and a 1nF capacitor. The FWHMs of the current pulses were in the range of 6-7 ns. The highest current pulse amplitude, 75 A, was achieved with the 2N5192-transistor with a rise time (10-90%) of 3.7 ns. The avalanche transistor ZTX415 gave a shorter rise time, 2.6 ns, but lower pulse amplitude, 55 A. It was also noticed that the switching delay of transistors of 2N5192 and ZTX415 depends strongly on trigger voltage, however the amplitudes of switched current pulses remained practically stable, when the trigger voltage amplitude was varied in the range of 0 to 5V (when measured to 50 Ω load). The rise and fall times of trigger pulses were 1 ns (to 50 Ω load).

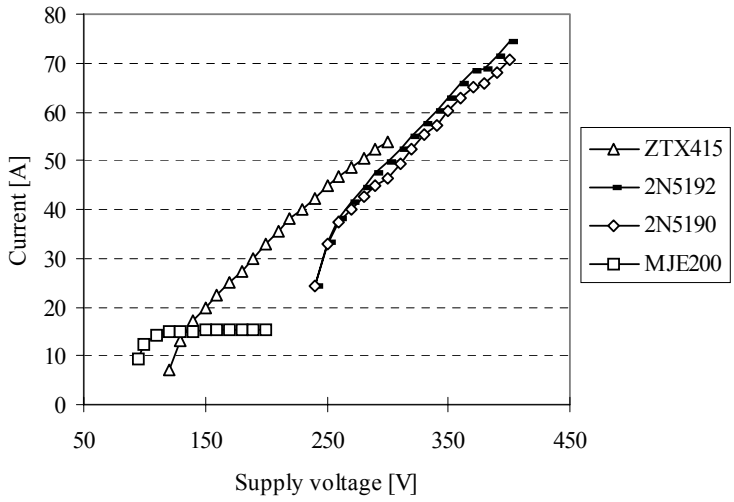

Fig. 3. The amplitudes of avalanche current pulses measured with three bipolar transistors and one commercial avalanche transistor. RL = 1 Ω, C2= 1 nF (Fig. 3, Paper III).

In the simplest model the operation of an avalanche transistor is based on a strong reverse bias in the collector-base junction. The high electric field creates high kinetic energy for the minority carriers and they create new electron-hole pairs with impact ionization, which results in the multiplication of the number of carriers by the multiplication factor M /Sah57, Poon72, Liou90/. During the switching transient the voltage between the collector and emitter jumps from the bias voltage BV_{CBA} to a voltage BV_{CEO}, and the maximum current can be evaluated with the formula 2 /Herden73/:

$$I = \frac{BV_{CBA} - BV_{CEO}}{R_L} \qquad (2)$$

The voltage BV_{CBA} is the bias voltage between the collector and base with some value of the base bias resistor R2 and the BV_{CEO} is the breakdown voltage between the collector and the emitter with open base. The smaller the value of the resistance of R2, the higher the value of BV_{CBA} (in Fig. 2 in Paper III the R2 is presented as R_b). The upper limit for BV_{CBA} is voltage BV_{CBO} (breakdown voltage between the collector and base with open emitter). The smaller the final on-state voltage BV_{CEO}, the higher the on-state current. The value for BV_{CEO} can be calculated with the formula presented in /Streetman80/:

$$BV_{CEO} = \frac{BV_{CBO}}{\sqrt[n]{\beta}} \ , \qquad (3)$$

where β is the ratio between collector and base currents and n ranges from 3 to 6 depending on the value of BV_{CBO} and the resistivity of the base. In practice the value of

BV_{CEO} depends not only on n and β, but also on the amplitude of the current pulse reaching the smallest value with medium size current values /Poon72/.

The life time of an avalanche transistor may be quite long, even if high voltages and currents are used. If the collector current during the avalanche breakdown rises too high, a secondary breakdown-effect may take place. During the secondary breakdown the collector-emitter voltage first decreases, which follows an increase in the collector current, while the collector-emitter voltage remains stable. The secondary breakdown may destroy the transistor permanently, because the temperature rises so high that the semiconductor material melts locally. A certain chip temperature, which depends on the power loss in the chip, is needed for the secondary breakdown /Unagami2002/.

The serial inductances in the path of the current pulse have a strong effect on the shape of the current pulse. If the inductances are very small, the current pulse switched to the laser has a very short rise time and slower, exponentially decaying trailing edge. In practice the inductances are so high that the leading edge slows down and the shape of the current pulse becomes almost symmetrically Gaussian. The shapes of current pulses measured with transistors ZTX415 and 2N5192 and 1 ohm load resistance are presented in Fig. 4. The effect of the inductance in the high current loop is seen as oscillation after the pulse. Another problem arising from the serial inductances is that a high voltage is created on them during the switching, which decreases the current pulse amplitude. The possibilities for decreasing the inductances are using as small cases as possible or even bare chips bonded directly to other components. In Paper VII pulses with peak amplitude of 130 A and rise time of 2.7 ns were achieved using surface mount transistor FMMT417, which allows higher operating voltage than with ZTX415 to be used. All inductances in the high current loop were minimized and the capacitor discharged was increased to 2.2 nF in the measurement presented in Fig. 2 in Paper VII.

The shape of the current pulse can also be changed by using a delay line as a discharged component instead of a capacitor. The impedance and length of the delay line have an impact on the amplitude and length of the current pulse, respectively. The most practical way is to use 50 or 75 Ω coaxial cables as the delay lines. In order to reach high currents, the cables must be parallelled or high operating voltages must be used. For example, in /Baker91/ a 40 A pulser (FWHM ~12 ns) has been constructed by connecting 11 transistors in series with an operating voltage of 2000 V. In the circuit developed the effective operating voltage was doubled with a Marx bank circuit. The delay lines were etched directly on the printed circuit board.

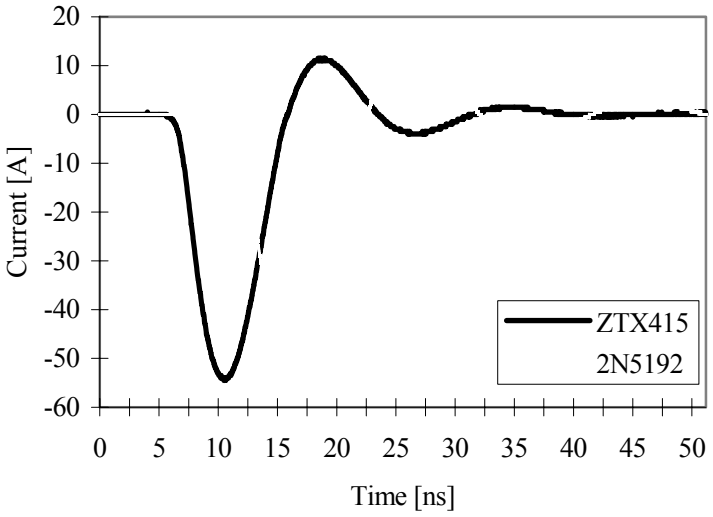

Fig. 4. Measured current pulses for transistors ZTX415 and 2N5192 (measured as voltage pulses across 1 Ω resistor).

Using the simplest avalanche transistor model the operation of an avalanche pulser can be analyzed with an SPICE simulator by replacing the avalanche transistor with an ideal switch, a serial resistor and inductor. A single transistor laser pulser circuit, which is equivalent with the circuit presented in Fig. 2, is presented in Paper III. An approximate value for the series resistor can be calculated by measuring the voltage BV_{CEO} during the switching transient and by subtracting the estimated voltage losses caused by the series inductances. The inductances in the circuit have been evaluated from the sizes of the components. The laser is replaced with a series connection of a diode, a resistor and an inductor. From the simulation results it can be noticed that the parallel capacitor C2 stores pulse energy and when the parallel capacitor (C3 in Fig. 2) has suitable capacitance, it releases its energy just on the top of the current pulse. In paper III it was measured that it was possible to increase the optical peak pulse power by 26 % (57 W -> 72 W) while the pulse was narrowed so that the pulse energy remained the same.

Higher currents and voltages can be reached by connecting several transistors in parallel or in series. With a series connection higher operating voltages are used and the inductances of the load are distributed over all stages in the series connection, which helps to decrease the rise time of the pulse. The main problem in using several transistors is that the switching delay depends on the ambient temperature and amplitude of the triggering pulse and it is also different for different individual transistors /Mizushima67, Paper III/. The differences can be eliminated by using transistors, which have equal BV_{CBO} -voltages in the same temperature. However, connecting the transistors in series usually shortens the transistor life time /Bostanjoglo87/. The lifetime may be lengthened by using liquid nitrogen cooling.

It has been noticed that by using a Marx bank generator the switching of several transistors can be synchronized. The Marx bank is a common circuit in producing fast pulses with very high voltages (kilovolts) and large currents (hundreds, even thousands of amperes). The basic idea is to charge the capacitors in parallel and to discharge them is series, which multiplies the effective operating voltage by the number of the capacitors in series (if the extra inductive losses are ignored). The switches used may be bipolar transistors, MOSFETs or thyristors /Grimes92/. After the first transistor in a series connection in the Marx generator has been triggered, the supply voltage of next transistors is increased, which makes it possible to rapidly trigger the next transistor to avalanche state /Benzel85, Vainshtein97/. In /Vainshtein97/ a Marx bank circuit with three transistors in parallel and four stages in series is presented (shown also in Fig. 5). The operating voltage of the whole circuit was 300 V. Rapid high voltage pulse during switching allows the synchronization of the transistors connected in parallel. Another possibility is to connect many transistors in series and to parallel the stages connected in series, as presented in /Benzel85/.

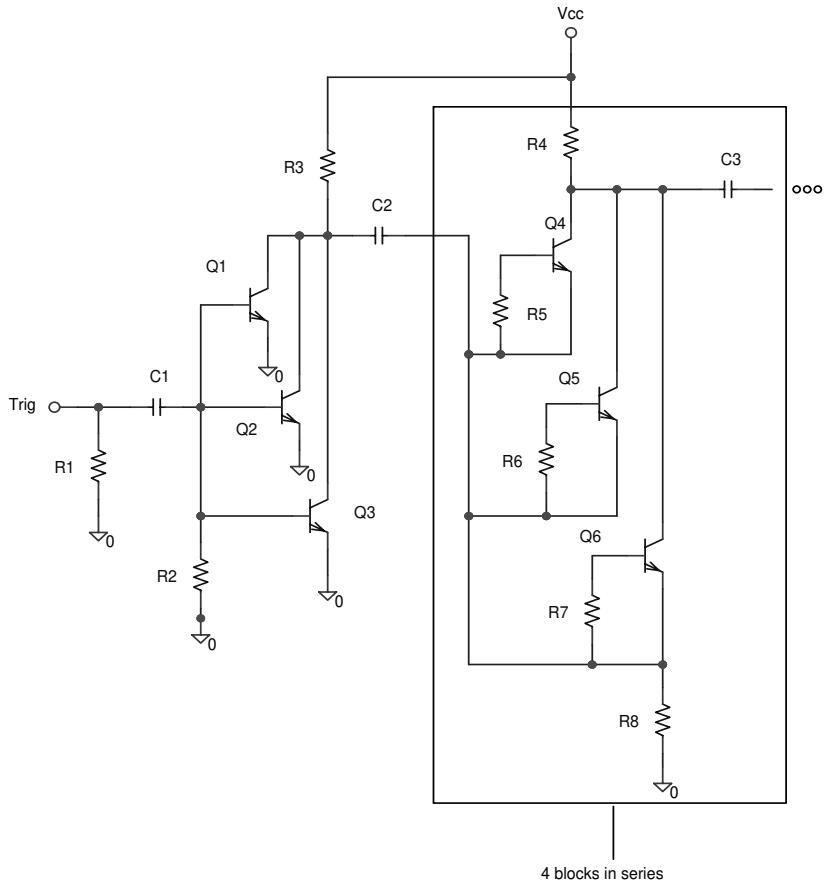

Fig. 5. A circuit example of a Marx bank generator /Vainshtein97/.

In references /Benzel85, Vainshtein97/ additional switching diodes were used for shortening the rise times of the pulses generated with the Marx bank circuits. In /Vainshtein97/ two diodes were used, first a Drift Step Recovery Diode (DSRD), which was connected in reverse polarity in parallel with the pulse created with the Marx bank pulser and secondly a SAS (silicon avalanche shaper) diode, which was connected in series, in reverse polarity with the load, as a closing switch. The current amplitude was 35 A and the rise time of the final pulse achieved 150 ps. The operation of a DSRD is based on a mechanism in which an electrical charge pumped to the diode is removed within a relatively short time (less than the carrier lifetime) with a delayed reverse voltage pulse /Grekhov83/, /Kardo-Sysoev95/, /Focia96/. The rise time of the current pulse to the load is shortened, because removing the charge from the diode consumes part of the charge in the leading edge of the pulse and it results in high slew rate voltage pulse to the load. In /Benzel85/ it was noticed that the DSRD-effect was achievable using normal commercially available high voltage diodes. Normal diodes operate in DSRD mode, if the forward current pulse is so short that the charge carriers diffuse only a short way to the low doped n-region of a p^+-n-n^+-diode. The operation of SAS-diodes is analyzed in references /Kardo-Sysoev95/ and in /Focia97/. The operation is very similar to that of TRAPATT (Trapped Plasma Avalanche Transit Time) –diodes. A very high slew rate and high current density is needed for the pulse arriving to the SAS-diode and it results in a very fast (rise time of some tens of picoseconds), slightly delayed breakdown. In the breakdown the electric field travels in the lightly doped n-region as an ionization wave, which may have much higher speed than the saturated velocity of electrons in a semiconductor.

The efficiency of laser pulsers is affected by the efficiency of the laser and the pulser electronics. The efficiency of semiconductor lasers is better than with other laser types, but clearly worse than that of LEDs. The efficiency of SH-lasers is only a few percent and that of DH-lasers is in the range of 8 to 20 percent. The efficiency of the pulser electronics is decreased by the fact that the capacitor discharged is normally charged through a resistive element (a resistance or a switch), making the element dissipate as much power as is charged to the capacitor. For example, the pulser presented in Paper VII consumes 23 W power with a pulsing frequency of 100 kHz, in theory, which means that it is clearly the most power consuming part in the laser range finder. The efficiency can be increased by charging the capacitor separately for each laser pulse with a transformer or an inductor instead of creating the high voltage first with a DC-DC converter and charging the capacitor with a switch or a resistance.

3.4.4 Picosecond pulse generation with a semiconductor laser

The operation of a current controlled semiconductor laser during the dynamic switching can be solved with rate equations. The rate equations are presented for example in /Boers75/,/Schöll84/ and in Papers I and II and they describe the amounts of electrons and photons in the active region during the current pulse. As shown in Paper I and in Eq. 4, the energy is brought to the laser as electrons (the first term on the right of the upper

equation) and the energy is removed as photons in stimulated emission (the last term on the right of the upper equation and the first term on the right of the lower equation) and in spontaneous emission (the second term on the right of the upper and equation and the last term on the right of the lower equation) and also as optical scattering and diffraction losses and the reflection losses in the mirrors (the second term on the right of the lower equation).:

$$\begin{aligned} \frac{dn}{dt} &= \frac{J}{ed} - \frac{n}{\tau_S} - gS \\ \frac{dS}{dt} &= gS - \frac{S}{\tau_p} + \frac{n}{\tau_S}\beta \end{aligned} \qquad (4)$$

The rate equations are nonlinear and they must be solved with numerical methods in high current amplitudes. The operation of all semiconductor lasers can be solved using rate equations and the laser parameters. The main differences in the rate equations between Papers I and II are that in Paper I the gain is simplified to be linearly related to n near the point of operation. In Paper II the equations include all laser modes and the fraction of spontaneous emission is assumed to be negligible in the photon output.

As an example the rate equations were solved for a single laser mode using equations given in Paper I and some laser parameters given in /Bhattacharya97/. The resulting optical pulse is shown in Fig. 6. In the calculations it has been assumed that current density J = 5000 A/cm^2, spontaneous emission life time τ_s = 3 ns, photon life time τ_p = 2 ps, fraction of spontaneous emission β = 5 x 10^{-5}, g = $2.5 \cdot 10^{-7}$ cm^3/s $\cdot$(n-n_{nom}), where n_{nom} is the injected carried density to make the cavity transparent (in this case $0.7 \cdot 10^{18}$cm^{-3}), and the modulating signal is a 500 MHz sine wave, which begins at time 0. It can be seen from the solution shown in Fig. 6 that the rise time of the optical pulse may be clearly shorter than the rise time of the current pulse. With high slew rates and amplitudes of the current, if the current exceeds the threshold current manifold, in principle any laser can be operated in the gain-switching mode. Then the pulse starts with a relaxation oscillation and the typical FWHM of the pulses during the oscillation is some tens of picoseconds. If the current pulse is long, the following part of the optical pulse follows the shape of the current pulse. The equations for the pulse shown in Fig. 6 have been solved with a Mathcad program.

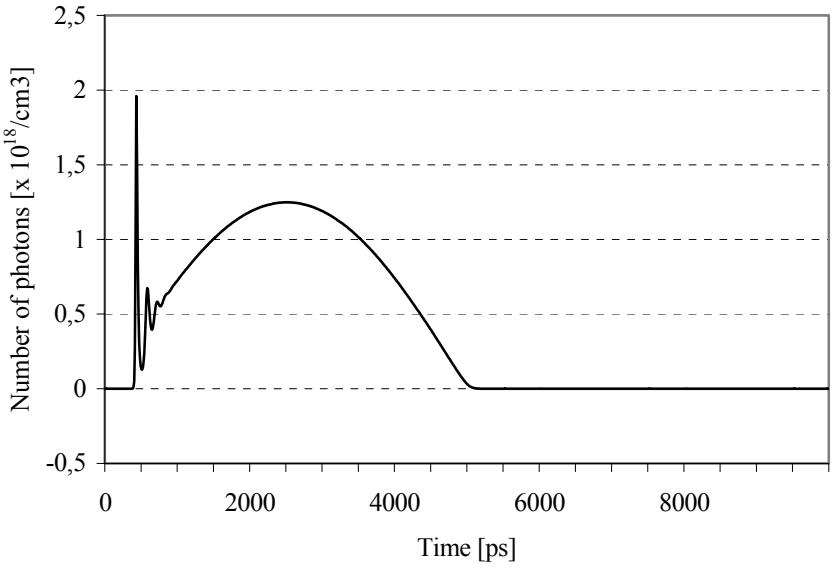

Fig. 6. The relaxation oscillation of photon density in gain-switching mode.

The amplitude of the first optical pulse in the relaxation oscillation depends mainly on the amplitude of the current pulse and the laser parameters like the lifetime of carriers and the fraction of spontaneous emission. If the rise time of the current pulse is shorter than the delay of lasing, it does not have a very significant effect on the amplitude and width of the optical pulses /Schöll84/. The frequency of the relaxation oscillation increases, when the life times of charge carriers or photons decrease, the amplitude of the current pulse increases or the length of the cavity decreases. The oscillation frequency also increases sligthly during the oscillation process, because the number of charge carriers is decreasing in the cavity after the first light pulse has been formed. The frequency of the relaxation oscillation determines the highest usable current modulation frequency and the oscillation creates peaking in the frequency response near the relaxation oscillation frequency. If there is a need to modulate the laser with a sine wave, the laser should be biased above the threshold current in order to linearize the frequency response at high frequencies. The bandwidth of a gain-switched semiconductor laser can also be increased by injecting cw-power with a pumping laser to the laser cavity /Anandarajah2000/. Even as short as 4 ps pulses have been achieved from a small power gain-switched VCSEL (vertical cavity surface emitting laser) by optimizing critical parameters like length of the cavity and reflection coefficients of the mirrors /Melcer91/.

As shown in Paper II, gain-switched single optical pulses with a FWHM of 25 ps and a pulse power of 20 W have been achieved using transient mode spectral filtering, a high power DH-laser (CVD-193, Laser Diode Labs.) with a threshold current of 1.3 A and using current pulses with a rise time of 300 ps and amplitude of 20 A. The measured gain-switched pulse power was approximately 50 % of the output power specified for the

laser at that current level. It was also noticed that if the slew rate of the current pulse were high enough, the wavelength of the first pulse in the relaxation oscillation was different from the following ones and it could be separated in time scale by wavelength filtering. Then the laser spectrum widens and the maximum of the gain moves to higher energies, i.e. lower wavelengths. When the first pulse has used the energy storage, the charge carriers move to lower energy levels and the photons in the following pulses have longer wavelengths. It was also noticed in the simulations of Paper II that the rise time of the current pulse has an optimum value (300 ps in this case) and shortening it did not increase the peak power of the first optical pulse. Another (theoretical) possibility to eliminate the succeeding optical pulses is to abort the current pulse at the right time. This requires, however, very accurate timing and high slew rate of the current pulse trailing edge. For example, in /Garside83/ it has been calculated using rate equations that with small power gain-switched GaAs-lasers the first optical pulse widens from 50 ps to 100 ps and the amplitude falls down to one hundredth part, if the current pulse starts to decay 100 ps too early. A common problem with high power lasers is that a very high slew rate of the current pulse is needed, which is not achievable with avalanche transistors, and that sharpening diodes are needed, which makes the circuit complicated.

Another alternative for producing fast optical pulses with semiconductor lasers is passive Q-switching. Usually higher pulse powers can be achieved with Q-switching and the slew rate of the current pulse needs not to be as high as in the gain-switching mode. In semiconductor lasers the Q-switching can be realized internally, for example, with a saturable absorber or by integrating a modulator inside the laser, which makes it possible to modulate the absorption with optical pulses from a fast pulsed laser. Using the last method an optical peak power of 6 W and FWHM of 21 ps were achieved using a 300 µm wide semiconductor laser /Thedrez93/. In /Portnoi97/ the saturable absorber was made by bombarding the cavity with high energy ions (N^+, O^+ or Ar^+) near the mirrors. A peak power of 380 W and FWHM of 40 ps were achieved by using a laser, which has a normal peak power of 5 W and wavelength of 900 nm (LD-62, Laser Diode Inc.). An additional advantage was that the far field distribution of the optical radiation could be modified by local ion bombardment. In /White93/ a peak power of 40 W, FWHM of 2 ps and repetition frequency of 117 MHz were achieved with a one chip 800 nm laser, in which an internal saturable absorber was used. Inside the laser cavity two bias methods were used: besides normal forward current biasing a reverse voltage was used for biasing the saturable absorber region in the middle of the cavity. However, it is possible that the ion bombardment used with the saturable absorber shortens the lifetime of the laser /Delfyett92/.

Also without ion bombardment optical pulses with a peak power of 200 W and FWHM in the range of 30 to 65 ps were achieved using a commercial SH-laser (LD-65, Laser Diode Labs), which is presented in Papers I and VII. A suitable temperature, a few tens of degrees Celsius above room temperature depending on the laser item, is needed for starting the Q-switching operation. The laser can be heated either with external heating (used in Paper I) or with a continuous bias current (used in Paper VII and in the pulser presented in Paper VIII). A short, powerful Q-switched pulse is followed by a slower, low-power part, which can be removed by wavelength filtering. In Paper I narrow (50 – 200 ps) Q-switched pulses with nominal peak power (10-20 W) were achieved by pulsing the LD-65 laser with current pulses having peak amplitude, FWHM and rise time

of 40 A, 8.2 ns and 3 ns, respectively. The laser pulses measured with a reference photodiode and oscilloscope having a bandwidth of 570 MHz are presented in Fig. 7. When the temperature of the laser is increased, the amplitudes of the optical pulses increase and the FWHM decreases having a typical value of some tens of picoseconds. When the temperature is increased further, the amplitude decreases, while FWHM remains stable.

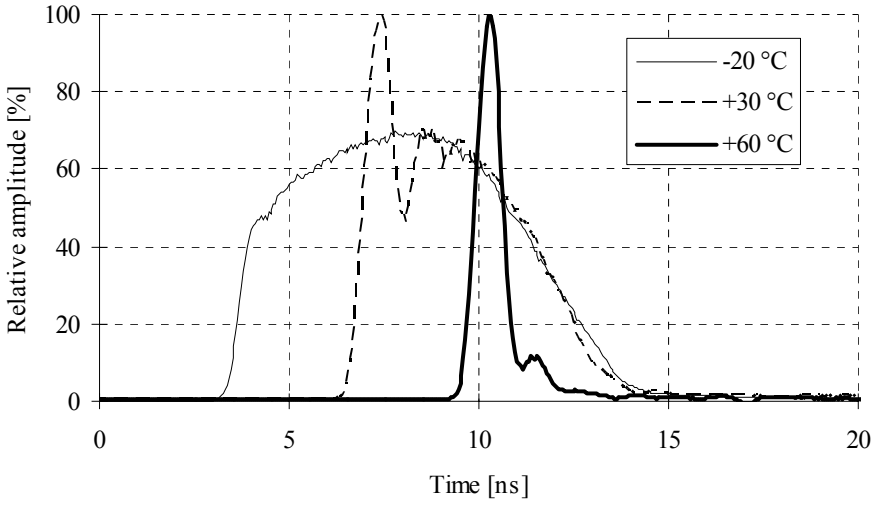

Fig. 7. Optical pulses from LD-65- laser in 3 temperatures. Q.switching is present in the last one. The pulse amplitudes are not comparable to each other (Paper I, Fig. 11).

Several theories have been proposed for the theory of internal Q-switching without a saturable absorber /Ripper74, Nunes77, Paper VII/. In all references either homojunction or SH-lasers have been used. Common findings were long delays on some temperatures between the current and optical pulses. The optical pulse (with a relatively small amplitude) may arrive even after the current pulse, if the current pulse has a suitable amplitude (not too high) and it is long enough. The delay depends on the individual laser item and also nonlinearly on the temperature so that when the temperature is increased, the delay and amplitude of the optical pulse may increase strongly in some narrow temperature range (from a few degrees to some tens of degrees). Then the operation is changed from a normal laser mode (with short relaxation oscillation in the leading edge) to a Q-switching mode.

In /Nunes77/ one possible theory was presented for an internal Q-switching mode. According to that the internal Q-switching is caused by the optical diffraction losses in the homojunction of the SH-laser. The number of carriers and the gain and temperature of the laser all modulate the refraction index difference Δ_n in the homojunction (the junction between n-GaAs and p-GaAs materials) of the SH-laser so that the diffraction losses increase, when the number of the charge carriers increase, and decrease, when the gain or

temperature increase. Because the diffraction losses depend strongly on the refraction index difference Δ_n above an upper limit δ_{cutoff} , lasing may start even after the current pulse has decayed, because the total losses may decay more rapidly than the laser gain, when the number of the carriers is decreasing and the gain may exceed losses for a short period (a few hundreds of picoseconds). This theory also explained long delays by the fact that the temperature of the cavity rises slowly in the leading edge of the current pulse and the lasing starts after the rise of temperature has sufficiently decreased the diffraction losses. According to /Nunes77/ internal Q-switching, in which the light pulse arrives after the current pulse has decayed, has not been noticed in DH-lasers.

However, the theories presented above have not adequately explained the very strong optical pulses that are present in the trailing edge of a (very powerful) current pulse. In Paper VII a new theory was presented. According to the new theory the localized band-tail states of a strongly doped SH-laser and the relatively thick cavity (2 μm) have a significant role in the Q-switching mode due to saturable absorption. The band-tails act as absorbers of charge carriers and they must be filled in the beginning of the current pulse. This phenomenon increases the delay of the light pulse. Another factor increasing the delay results from the fact that in the centre of the laser cavity the conductivity is small and the electric field is high compared to the sides of the cavity, which decreases the gain in the centre. Due to high electric field the high energy carriers are heated. When the current pulse decays, the charge carriers in the active region cool down and move from upper to lower energy levels, which results in transitions of free carriers (band-to-band or band-to-tail). When the losses in the centre of the cavity decrease strongly enough, the lasing starts rapidly everywhere in the cavity. In order to create a powerful Q-switched optical pulse a suitable temperature is needed, as well as a long enough current pulse (a few nanoseconds) and a short enough fall time for the current pulse, which is not longer than the recombination time of the charge carriers (less than 2 ns in this case).

3.4.5 Practical problems of semiconductor lasers

The temperature of a semiconductor laser has a strong influence on the laser properties, the wavelength spectrum and optical output power to name a few. The wavelength spectrum consists of single peaks, the wavelengths of which are defined by the longitudinal laser modes. The properties of the semiconductor and the temperature both have an impact on the internal gain of the laser, which defines the power of each longitudinal mode. The centre wavelength of the laser spectrum increases, when the temperature increases, because the bandgap decreases. In an ideal case the total wavelength spectrum should be as narrow as possible, so that chromatic dispersion (the different wavelengths propagate at different speeds) would not be present in the fibres. In practice it does not cause any problems, because the fibre lengths used in the laser range finders are short. If there are wavelength selective filters used in the optical path, changes in the wavelength spectrum may decrease the optical power. Also the optical output power of the laser decreases, when the temperature increases, because the threshold current increases. The changes in the power level must be taken into account in the

optical power budget, or the temperature of the laser must be stabilized. If internal Q-switching is used, temperature stabilizing is inevitable, as noted in Papers I and VII.

The near field distribution of a semiconductor laser may be nonhomogeneous due several reasons. The power-current –curve of a semiconductor laser may be nonlinear so that there are some local kinks. The reason for the kinks is that a wide cavity laser has many waveguides, which all have their own laser modes. Narrow cavities do not have this problem /Bhattacharya97/. It has been noticed that in DH-lasers with saturable absorbers the first pulse in the Q-switched pulse train has TEM_{00} –mode, but the succeeding pulses have a higher degree TEM mode distribution /Barrow93/. The explanation was that the relaxation time of the saturable absorber was shorter than the time elapsed for the increase of gain in the laser cavity. In this case the pulses following the first pulse come from the edges of the cavity, where the gain is larger than in the middle after the first pulse. In Paper I the near field distribution of a high power SH-laser, which operated in Q-switching mode, was measured. It was noticed that the near field distribution is nonhomogeneous - at some measuring angles the fast part in the leading edge of the pulse was totally missing. In multichip lasers there may also be variation in the pulse shape between different chips.

The laser noise consists of intensity noise and phase noise, both of which may be induced by shot noise, longitudinal mode-hopping noise, mode partition noise and noise from optical feedback (for example from reflections from external components) /Jang93/. The spontaneous emission causes intensity- and phase noise and affects the wavelength spectrum of the single modes inside a laser. If the laser is operated high enough above the threshold current, the effect of spontaneous emission is very small and the amplitude response can be calculated using the small signal equations based on rate equations /Bhattacharya97/. Quantum noise is the ultimate lower limit for the laser noise and it is created by the quantum character of photons and electrons; the electrons transferring from the conduction band to the valence band are not in the same phase with the photons /Yariv97/. The effect of quantum noise can be analyzed by adding the noise terms to the rate equations which results in Langevin rate equations /Czylwik89/. In /Czylwik90/ the intensity noise of a small power gain switched semiconductor laser was measured and when the results were analyzed with the calculations it was noticed that during the gain switched pulse the quantum noise is clearly higher than during the stationary, continuous lasing. According to that analysis the intensity noise can be interpreted mainly as timing jitter between the current pulse and the current switched light pulse train. It was also noticed that very little time jitter exists between gain switched optical pulses. In /Jang93/ noise from small power AlGaAs-laser was measured to be in low frequencies higher than the quantum noise of the laser and the thermal noise from the laser serial resistor together. The extra noise was interpreted to originate from the impurities creating extra traps in the active region. In TOF laser range finders the noise analysis using only signal shot noise and noise from electronics have given quite accurate results, so extra laser noise has not been a significant factor in the noise analysis thus far. Some explanations may be that the START and STOP pulses both originate from the same optical pulse. In an optimal case also the timing point is the same in the START and STOP pulses.

3.5 The receiver

3.5.1 Required properties and alternatives for receivers

The receiver includes a photodiode and an amplifier, which includes a preamplifier and a postamplifier. In some applications also photomultiplier tubes have been used as a photo receiver, but because the photomultiplier tube is expensive and large in size, photodiodes are much more common. Also some kind of attenuator, electrical or optical, is normally used, because the dynamic range of amplifiers is limited.

The preamplifier types used with the photodiode are a transimpedance amplifier and a high impedance amplifier. A transimpedance amplifier includes a basic amplifier, either a voltage amplifier or a current amplifier /Wilson96/ and feedback, which defines the transimpedance of the amplifier. Negative feedback keeps the effective input impedance small, enabling a high bandwidth. The feedback resistor defines mainly the value of transimpedance, the value of which is a compromise between bandwidth and noise. The drawback of the transimpedance amplifier is that it may be sensitive to oscillations at the high values of a feedback resistor and photodiode capacitance. The high-impedance amplifier includes a resistor of relatively high value for transferring the photodiode current to voltage and a voltage amplifier /Yano90/. The drawback of a high-impedance amplifier is the need for equalizing, because the high resistance combined with the photodiode capacitance limit the upper frequency limit of the passband to a relatively low value. The dynamic range of input power may also be limited, because the low frequencies are amplified more than high frequencies in the input resistor of the amplifier. The value of equalizing depends on the value of input capacitance, which may vary according to the temperature, bias voltage of the photodiode and the individual photodiode item. The high-impedance amplifier has in practice better sensitivity (lower noise) than the transimpedance amplifier, because the value of the feedback resistor in the transimpedance amplifier is lower than the value of the input resistor in the high-impedance amplifier, thus creating higher thermal noise. The transimpedance amplifier is a more common type in high frequency photo receivers due to its high dynamic range of the input power.

The amplifier channel should be linear in the dynamic input power range used. Normally the photodiode does not limit the dynamic range, because the linear range of a silicon photodiode is high, in the order of $1{:}10^7$ /Tamari97/ or even $1{:}10^{10}$ /Schmitz2000/. The wide dynamic range of the photodiode is important, if an electrical attenuator is used, like in /Palojärvi97/. The lower limit of the dynamic range is limited by noise and the upper limit is limited by the largest output current of the diode and by the highest usable output voltage amplitude of the amplifier. In the lower limit the dominating noise source is the electrical noise of the amplifiers. Typically the highest peak currents from the silicon photodiode are in the range of a few tens of milliamperes. The highest output amplitude from the amplifier is limited by the operating voltage and it is typically in the range of 1-2 V.

In order to achieve the best possible single-shot precision, noise should be minimized and the measurement pulse should not be slowed in the receiver (chapter 3.2, equation 1).

In practice it means that the frequency response of the amplifier should be equal to the frequency spectrum of the signal itself (matched filter). The impulse response of the whole amplifier channel, without the comparator in the timing discriminator, should be the derivative of the impulse response of the matched filter /Rehak83, Ruotsalainen99/. Derivating (with passive components) is done after the amplifier /Rehak83/.

The pulse used in the design of the matched filter should be the pulse sent to the target according to the radar theory /Wehner87/. However, the photodiodes may significantly widen the measurement pulse in GHz-frequencies and the capacitance of the photodiode also increases the high frequency noise in the amplifier, which makes it difficult to use strictly the matched filter-theory in the design of a receiver channel. The goal is to minimize the ratio between the noise and slew rate of a signal, which can also be tested by simulation.

3.5.2 Properties of photodiodes

The choices for photodiodes are PIN, avalanche and MSM (metal-semiconductor-metal) photodiodes. The properties required from a photodiode are the same as the requirements of the whole amplifier: as good response (A/W) as possible in the wavelength used (usually 850-900nm), good linearity, high enough bandwidth and small noise. The properties are defined by the type (MSM, PIN, APD), material (silicon, GaAs), doping and size of the photodiode. The best response can be reached with the avalanche photodiode (50-200 times higher than with PIN photodiodes), but avalanche multiplication produces extra noise and necessitates high supply voltage (typically 50-200 V). The PIN photodiodes manufactured from silicon have about equal bandwidth as the silicon APDs ($f_{-3\ dB} \approx$1-2 GHz at its highest), but with silicon MSMs over 100 GHz frequencies can be measured at a wavelength of 400 nm /Liu93/.

The response is defined by the width of the bandgap, absorption coefficient of the semiconductor material at the used wavelength and the structure of the photodiode. With MSM photodiodes the response is usually lower than with PIN photodiodes, because the metal finger structure hides part of the active area. Silicon suits well for 900 nm, because the sensitivity is at the maximum just on that wavelength. PIN and MSM photodiodes are manufactured either from silicon or GaAs for wavelengths under 1 μm. However, silicon is the only kind of material available for APDs in the wavelength range of 0.8 – 1 μm, because GaAs-APDs are slow. The speed of an APD is defined by impact ionization coefficients α_e and α_h of electrons and holes, respectively. The coefficient α_e should be clearly larger or smaller than α_h in order to achieve fast response. If the ratio $k_r = \alpha_e / \alpha_h$ is close to one, both electrons and holes take part into the multiplication process and the charge carriers move back and forth between the anode and cathode, resulting in a long response time. If $k_r = \infty$, the response time is equal to the transit time of one electron across the depletion region. For silicon α_e is normally 30-50 times larger than α_h, but for GaAs $\alpha_e \approx \alpha_h$.

The active area of the photodiode is reasonable to adjust equal or slightly larger than the active area of the laser in order to maximize power and to minimize background

noise. The photodiode area should be minimized for minimizing the capacitance. Excess capacitance may decrease stability and increase the noise of the amplifier in high frequencies. The capacitances of suitable-size photodiodes (diameter 100-500 μm) of PIN and avalanche photodiodes are in the range of 1.5 – 2 pF. The equal-size MSM diodes have capacitances in the range of 0.15-1.6 pF, so they are often better choices than PIN photodiodes for low capacitance/high frequency applications. The capacitance of PIN and avalanche photodiodes can be slightly decreased by increasing the bias voltage.

The upper frequency limit of the bandwidth is defined by three factors: diffuse time of the photons to the depletion region, the transit time of the photons across the active (depletion) region with saturated velocity and the RC-time constant formed by the load resistance and photodiode capacitance. The active region is with PIN and avalanche photodiodes about equal to the depletion region, which is about equal to the I-(intrinsinc) layer. A compromise is needed in dimensioning the I-layer, because widening it increases the responsitivity, but it increases also the transit time, which slows the diode response. In APDs also the multiplication time affects the bandwidth. With small multiplication factor values the RC-product dominates and the bandwidth stays about equal, when multiplication factor M is increased, but with large values of M the gain-bandwidth – product (GBW) is constant /Senior92/. The transit time of charge carriers across the active region should be equal to the RC time constant defined by the load resistance and photodiode capacitance in order to maximize the bandwidth of the APD /Riesz93/. In MSM-diodes the width of the active region is the distance between the metal fingers, which defines mainly the bandwidth of the MSM-diode. However, the charge carriers diffusing deeply under the metal fingers slow down the pulse response. In silicon the absorption coefficient is low in long wavelengths (in silicon 1/e penetration depth is 12.7 μm @ 830 nm and in GaAs 0.25μm @ 800 nm), which creates a slow tail to the impulse response, if the input signal includes long wavelengths. For this reason the silicon-MSM-diodes suit best for short wavelengths. The upper frequency limit of silicon-MSMs may be increased for example by placing an insulating SiO_2 layer under the active thin silicon layer in order to minimize the slowing effect of deeply penetrating photons /Honkanen99/.

The impulse response of an APD can be approximated as a Gaussian pulse, if the multiplication factor M is large, in the range of 100 to 1000, the dark current is small, nanoamperes, and the background radiation is small /Davidson88/. With a true Gaussian pulse and 1 GHz bandwidth the FWHM of the optical pulse is 314 ps. In /Bhattacharya97/ a formula $f_{3dB} = 1/(2 \cdot FWHM)$ is presented for a fast photodiode based on impulse response measurements, which results in 500 ps FWHM for a 1 GHz bandwidth. The difference compared to true Gaussian pulse width is due to partly RC-limited bandwidth of the photodiode, which gives an exponential pulse tail.

The noise current of photodiodes consists of dark current noise, background signal current noise, signal current noise and thermal noise from load and bias resistances. Usually the noise current from bias resistance is clearly smaller than from load resistance, since the bias resistance is much larger in value. With good quality PIN photodiodes the dark current noise is small and the signal current noise together with noise from electronics dominate. In small signal levels the noise from electronics dominates all other noise sources. When the capacitance of the photodiode increases, the noise of the receiver increases /Smith&Personick79,Rogers91,Johns97/), especially at high frequencies. The

effect of input capacitance is similar in MOSFET- and BJT-amplifiers resulting in noise peaking. The total noise in a MSM-receiver is normally smaller than in a PIN receiver due to the smaller capacitance of MSM photodiode.

In avalanche photodiodes all squared current noise terms are multiplied with the factor $M^2 \cdot F(M)$. The APD also has a dark current noise term caused by the surface leakage current, which is not multiplied, but it is very small compared to other noise terms. The excess noise factor F(M) can be calculated with parameter k_r and multiplication factor M /Sze85/ and it increases strongly, when the bias voltage and multiplication factor are increased to high values:

$$F(M) = k_r M + (2 - \frac{1}{M})(1 - k_r) \tag{5}$$

For example in silicon the parameter k_r may have a value of 0.006 /Davidson88/, which gives the excess noise factor of F(M) = 2.58, when M = 100. A common value for M is in the range of 50 to 200. When the bias voltage is increased in an APD-receiver the S/N-ratio increases up to the point, where the APD excess noise is stronger than the electronics noise /Bhattacharya97/. The multiplication factor M also depends on temperature, so a bias voltage compensation (typ. 0.7 V/°C /RCA88/) or temperature stabilization is needed. Fluctuation of the APD bias voltage is also a possible source of noise.

One of the main advantages of MSM and PIN photodiodes is that they can be integrated on the same chip with the amplifier /Chang90,Cheng88/. The advantages of integrated construction are a more simple structure, cheaper price and decreasing of stray capacitances and inductances due to shorter bonding wires and smaller bonding pads, which also decreases noise. A practical problem may arise from the amplifier semiconductor material, which is not necessarily optimal for the photodiode. Silicon is generally preferred because of its low price and highly developed manufacturing technology. It is also possible, yet difficult in practice, to grow GaAs-photodiodes on a silicon substrate /Tewksbury93/. For example, the MSM-photodiode suits well for integrating in the same process with MOSFETS. It is common to integrate PIN photodiodes to a matrix form, but also fast APDs (t_r = 0.9 ns) have been integrated to a 8 x 8 matrix /Gramsch94/. PIN photodiodes and CMOS amplifiers manufactured from silicon have been integrated to the same chip to form a receiver with 1 Gb/s baudrate /Schow99/. A 40 Gb/s receiver has been manufactured using InGaAs PIN photodiodes and InP/InGaAs SHBTs (submicron heterojunction bipolar transistors) /Huber99/. An additional advantage of integrating multiple photodiodes and amplifiers on the same chip is that distances to multiple targets can be measured at the same time, which performs the same function as a low resolution scanning range finder. In /Palojärvi2001/ a four-channel pulsed laser range finder has been realized.

The best photodiode type for each application depends on the optical power, bandwidth and structure of the amplifier channel (integrated / not integrated). In /Ruotsalainen99/ it has been calculated that in a 100 MHz laser range finder amplifier channel a PIN photodiode is preferred, if the input power were a few microwatts or higher. The useful operating range with APD starts from a few tens of nanowatts input

power. In /Rogers91/ the sensitivities (S/N-ratios) of GaAs PIN and GaAs MSM photodiodes have been compared as a function of bandwidth. The result was that a MSM-diode is better for frequencies lower than 11 GHz, because it has a lower capacitance and better sensitivity, even though the finger structure decreases the response. Some typical properties of commercial MSM, PIN and avalanche photodiodes have been compared in table 2. Fig. 8 shows the calculated S/N-ratios and output amplitudes for the PIN and avalanche photodiodes numbers 3 and 6 shown in table 2, respectively. In the calculation it was assumed that the spectral density of noise current in the input, bandwidth, total transimpedance and multiplication factor M are 10 pA/√Hz, 1 GHz, 10 kΩ and 100, respectively. The capacitances are equal, so the effect of the capacitance on the amplifier noise level is equal in both photodiodes. It can be seen from the figure that for example in the APD-channel a S/N-ratio of 10 is reached with a power of 0.14 uW, which produces an output voltage peak amplitude of 66mV. In the PIN channel a S/N-ratio of 10 is reached with a input power of 7 uW, which produces an output voltage peak amplitude of 33 mV. In theory the S/N of the PIN channel approaches the S/N of the APD-channel with an input power of 1 mW, which produces an output voltage and S/N-ratio of 930 and 4.3 V in the PIN channel, respectively. However, the highest possible S/N-ratio in the APD-channel is only 630, if it is assumed that the maximum output voltage is 2 V. The same output voltage of 2 V gives an S/N-ratio of 500 in the PIN channel. So the APD seems to be a clearly better choice also in a high bandwidth receiver channel.

Table 3. The comparison table of MSM, PIN and avalanche photodiodes. The material of all diodes is silicon, except in ref. 1 it is GaAs. The refererences are: 1) /Krishnamurthy2000/, 2) /MacDonald99/, 3) Hamamatsu S5973-01, 4) EG&G C30971E, 5) Hamamatsu S2381, 6) Silicon Sensor SSO-AD-230i.

	MSM	PIN	APD
Responsivity	0.18 A/W (820 nm) [1]	0.47 A/W (830 nm) [3]	35 A/W (900 nm, M=100)[5]
	0.13 A/W (860 nm)[2]	0.5 A / W ((830 nm) [4]	35 A/W (900 nm, M=100)[6]
Material	GaAs[1]	Silicon[3]	Silicon[5]
	Silicon[2]	Silicon[4]	Silicon[6]
Capacitance	1.6 pF[1]	1.5 pF [3]	1.5 pF[5]
	0.15 pF[2]	1.6 pF[4]	1.5 pF[6]
Bandwidth	4 GHz[1]	1.5 GHz[3]	1 GHz[5]
	0.75 GHz[2]	0.85 GHz[4]	2 GHz[6]
Area	400 x 400 µm[1]	∅ 400 µm[3]	∅ 200 µm[5]
	100 x 100 µm[2]	∅ 500 µm[4]	∅ 230 µm[6]
Dark current	0.8 nA[1]	≤ 0.1 nA[3]	0.5 nA (M=100) [5]
		10 nA[4]	≤ 1.5 nA (M=100) [6]
Excess noise factor F(M)	-	-	3 (M=100) [5] 2.2 (M=100) [6]

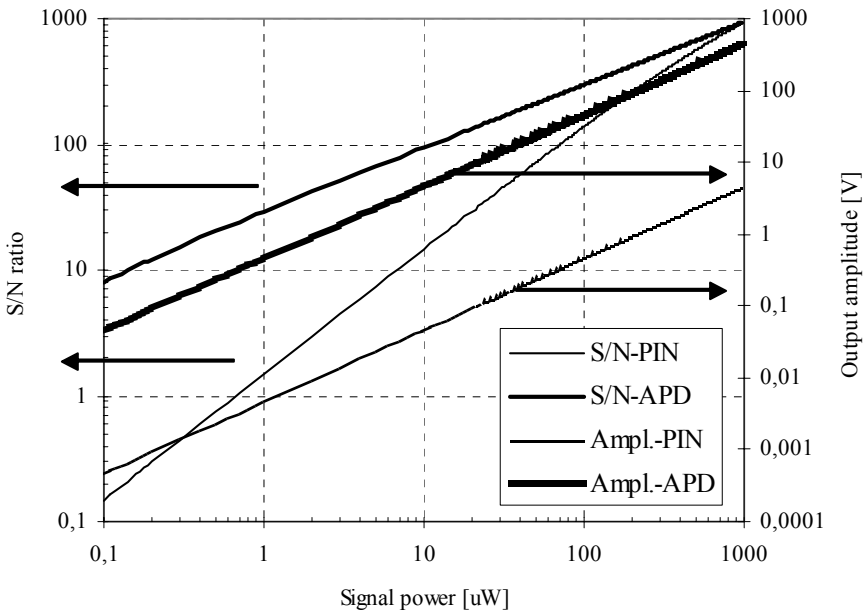

Fig. 8. Signal/noise-ratio and amplitude in the output of the amplifier as a function of optical input power for the PIN photodiode n:o 3 and APD n:o 6 in table 3.

3.5.3 Structure and properties of the transimpedance amplifier

A simple structure is recommended for the transimpedance amplifier, because the bandwidth should be wide and the delay should be small in order to have enough phase margin. Usually one voltage amplifier stage and one current buffer are enough /Ruotsalainen99/. However, the low number of stages limits the open loop gain, which limits the value of maximum transimpedance /Muoi84/. The choices for input stages are common emitter-, common collector- or common base circuits. The common emitter (or common gate) is the most usual, in which the Miller effect of the collector-base capacitance can be reduced using a cascade transistor. If the Miller-capacitance of the input transistor defines the dominating pole, the capacitance of the photodiode may vary in a wide range without significantly affecting the bandwidth of the amplifier /Meyer86/. With the common base- (or common gate) stage Miller-effect can also be minimized, but another bias voltage supply is needed /Ruotsalainen99/. The drain resistor in the common gate stage creates a high noise current reduced to the input, because there is no current gain, but its effect can be compensated by selecting a high value for the drain resistor /Vanisri92/. The advantage of a common base stage is small input resistance, which reduces the importance of input capacitance and also a current feedback can be used,

which increases the bandwidth /Vanisri95/. The disadvantage of common collector stage is small gain, which necessitates low noise in the following stage.

The transimpedance amplifier is the most common amplifier type in fibre optic telecommunication. The digital optical telecommunication standards define the baud rates and bandwidths of the amplifiers. The most common baud rates are defined by SONET (Synchronous Optical NETwork), OC (Optical Carrier) standards OC-12, OC-48 and OC-192 with baud rates of 622 Mb/s, 2.5 Gb/s and 10 Gb/s, respectively. Especially amplifiers meeting the first two standards are available from several manufacturers (table 3).

Table 4. Examples of commercial transimpedance amplifiers. 1) /Meyer94/, 2) Sony CXA1684M, 3) Anadigics ATA 30013, 4) /Neuhäuser95/

	1	2	3	4
Bandwidth (-3 dB)	130 MHz	630 MHz	2 GHz	7.5 GHz
Speed class		Sonet OC-12	Sonet OC-48	Sonet OC-192
Material	Silicon	Silicon	GaAs	Silicon
Transresistance	98 kΩ	3.9 kΩ	1.8 kΩ	45 kΩ
Noise reduced to input	1.5 pA/√Hz	4 pA/√Hz	5 pA/√Hz (<1 GHz) 10pA/√Hz (>1 GHz)	10 pA/√Hz (<7.5 GHz)
Specified input capacitance	1 pF	0.5 pF	< 0.5 pF	0.1 pF
Power consumption	100 mW	50 mW	500 mW	1000 mW

The noise of a BJT transimpedance amplifier consists mainly of three sources: the thermal noise of the feedback resistor and thermal noise of the base spreading resistor and shot noise of the collector current in the transistor of the first stage. Increasing the feedback resistor decreases both the bandwidth of the amplifier and the current noise reduced to the input. In high bandwidth MOSFET-amplifiers the noise consists mainly of thermal noises of the feedback resistor and thermal noise of the FET-channel, because the typically high 1/f-noise in MOSFETs is not significant in high frequencies. Typically the MOSFET amplifiers have smaller noise below 100 MHz frequencies / Kasper88,Ruotsalainen99/.

The input capacitance creates noise peaking in high frequencies. The series resonance of stray capacitance and inductance of bonding wires (0.7-0.8 nH/mm for 25 μm wires /Kester90/) also creates signal peaking in high frequencies, which may lead into stability problems with large-size PIN and avalanche photodiodes. Usually commercial amplifiers are matched to low capacitances of clearly less than 1 pF. The noise bandwidth is usually higher than the signal bandwidth, if peaking due to capacitance is present. Some calculated capacitances and inductances of the bonding pads and wires are shown in Fig. 9. The values are calculated for a circuit, in which the photodiode chip is glued on a ceramic hybrid substrate and the wires are bonded directly to the input of the amplifier chip. The resistors and capacitors are surface mount versions and the wires have been bonded directly onto them, when possible. Also a chip resistor creates serial inductance and the photodiode bottom plate creates stray capacitance. The result of inductive peaking at 2.3 GHz frequency can clearly be seen in Fig. 10, which shows the bandwidth of the receiver simulated with PSPICE. Simplified models of the APD and amplifier were

used in the simulation. The photodiode was modelled as a current source with 100 GΩ parallel resistance, 1.5 pF parallel capacitance and –3 dB upper corner frequency of 1 GHz. The amplifier was a voltage amplifier having a single high-frequency pole at 2.5 GHz and input resistance of 14 Ω.

The peaking effect may also be used intentionally for increasing the signal bandwidth /Morikuni92,Kim2001/. Gain can be increased using a serial inductor and parallel capacitor (photodiode and stray capacitances) between the transimpedance amplifier and photodiode. Using different kind of 2-ports formed by inductors and capacitors the gain-bandwidth product may be increased significantly in a limited bandwidth range, but the disadvantage is the complicated structure of such kind of circuits /Goyal95/. Also stability problems may arise.

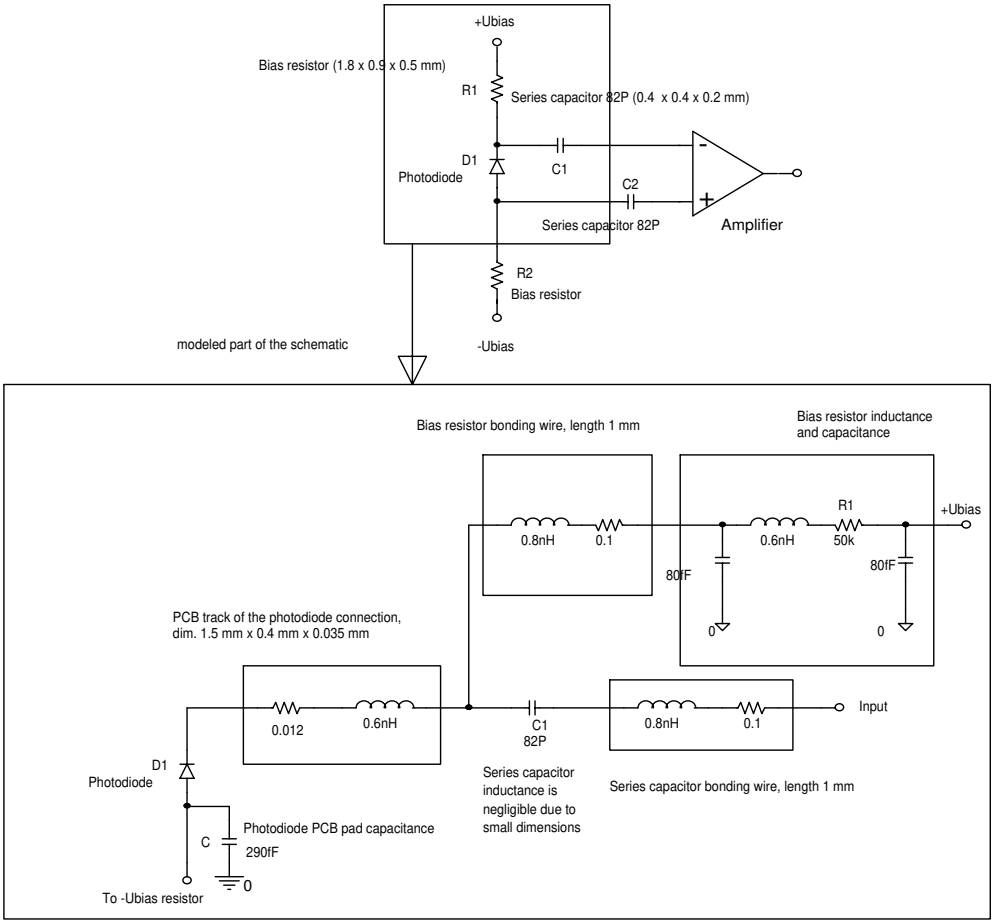

Fig. 9. The stray inductances and capacitances of the photodiode with its bias circuit.

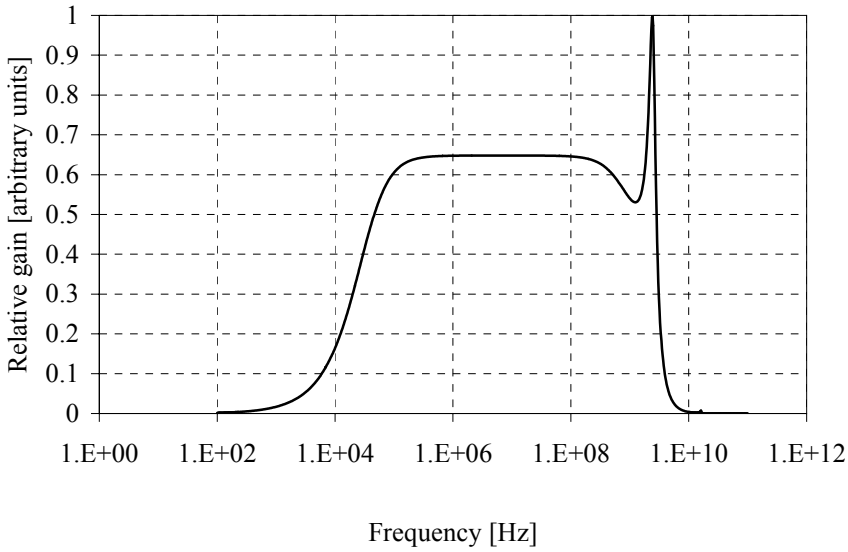

Fig. 10. Peaking in high signal frequencies created by series inductors and capacitors in the input of the transimpedance amplifier.

The amplifier can be either differential- or single-ended. The differential structure improves noise tolerance and common mode rejection ratio (CMRR), but the disadvantage is that two bias voltages are typically needed. In the differential structure the noise of the input transistors may increase, but the parasitic capacitances to the ground in the input are cut to half, which reduces noise. Then the total effect to the noise may be small compared to the single-ended structure /Ruotsalainen94/. The most common structure is a differential output stage /Ota92/, but also totally differential structures have been used /Chang92,Ruotsalainen94/.

3.5.4 Electrical attenuators

The purpose of the attenuator is to limit too large variation in the received signal power, mainly for two reasons: to keep the signal power in the linear range of the amplifier and to keep the signal power in the optimal range for walk error of the timing discriminator. The attenuator should be as linear and the noise should be as low as possible and its delay should not depend on the attenuation value. The required speed of the attenuator depends on how fast the changes in the power level are in the incoming signal. The speed requirements are ultimate in the 3D-sensor, when a surface with large changes in the reflection coefficient is scanned. Usually an electrical attenuator is faster than an optical one. The electrical attenuator is also smaller and suits better for integrating in the same

monolithic circuit or printed circuit board with the amplifier. There are several choices for implementing the electrical attenuator: a PIN diode attenuator, resistor network with switches, Gilbert cell or adjustment of the APD bias voltage. The optimal placement for the attenuator is after the amplifiers, if noise is to be minimized, but if the linearity of the amplifiers were to be maximized, the attenuator should be placed before the amplifiers in the signal chain.

The PIN diode is used commonly as an adjustable attenuator and switch in RF-frequencies. When the PIN diode is used as an attenuator, it is biased by a dc current, which is used for changing the number of charge carriers in the intrinsic (I-) region and thus the RF-resistance. A PIN diode may be connected in series or in parallel with the signal or in a T-shaped circuit, in which the input and output impedances remains constant, when the attenuation is changed. If the RF-signal modulates significantly the number of charge carriers, distortion is created. In the laser range finders the disadvantage of PIN diode attenuators is that the capacitance of the PIN diode attenuators change, when the attenuation is changed, which affects the delay of the attenuator. If the attenuation constant is one to a few tens, the delay variation may be tens, even hundreds of picoseconds /Caverly87/, /Määttä95/.

There are two modifications from the Gilbert cell /Gilbert68/, a multiplier cell and a attenuator cell. The multiplier cell has been used for example as a detector in the RF-receiver /Yamawaki97/ and the attenuator cell has been used between the photodiode and the preamplifier in a laser range finder /Palojärvi97/. The attenuation in the Gilbert cell is performed by changing the proportions of the currents flowing through two differential pairs. The practical difference between the multiplier- and attenuator cells is that in the multiplier cell there are two extra bias current generators. The distance measurement error caused by the Gilbert cell attenuator has proved to be small, for example +/- 6 ps in an amplitude range of 1:15 /Palojärvi97/. In this case the attenuator was integrated in the same chip with the preamplifier and when the attenuation was at the minimum, the attenuator operated as a common base amplifier stage. An additional advantage of the Gilbert cell is that it buffers the large capacitance of the photodiode, thus improving the stability and decreasing the noise peaking in high frequencies.

A resistor network with switches is a straightforward and simple way to implement an adjustable attenuator, in which, however, the delay changes as a function of attenuation due to changes in the total capacitance produced by the resistors and switches. For example in a R-2R-resistor network implemented in /Ruotsalainen97/ a distance error of +/- 75 ps was achieved in an attenuation range of 1:52. The advantages of the resistor network are good linearity and wide bandwidth.

One of the easiest ways to realize an electrical attenuator is to change the bias voltage of the APD. It can be assumed with many types of APDs that the multiplication factor M depends nonlinearly on the bias voltage in the same way as in avalanche transistors:

$$M = \frac{1}{1-\left(V / V_{br}\right)^{r}}, \tag{6}$$

where M = the multiplication factor of APD, V = bias voltage, V_{br} = breakdown voltage and r = coefficient depending on the material /Dragoman99/. For example, in the silicon APD number 6 in table 2 the coefficient r is 0.33 and the bias voltage should be decreased by 4.5 V in order to decrease the multiplication factor from 100 to 50 at a 150 V bias voltage. However, the bandwidth of the APD depends on the bias voltage, because in large values of M the time needed for multiplication changes and also the capacitance of the diode depends on bias voltage, even strongly on small bias voltages. In practice it has been noticed that the useful adjustment range of the bias voltage corresponds to 1:2 – 1:3 in the attenuation, while the delay error stays in the range of 10-20 ps and increases rapidly outside this attenuation range /Koskinen89/.

One possibility to decrease the error caused by the electrical attenuator is to use a single channel laser range finder, in which the START and STOP-pulses propagate in the same channel and the delay error caused by the attenuator has the same effect on both pulses and is cancelled out. However, changing the attenuator level will, of course, also affect the START pulse causing walk error, but if the amplitude of the START pulse can be adjusted to the middle of the range of optimal amplitude for walk error, the method is useful in a limited amplitude range. The walk error caused by the changes in the START pulse amplitude in an optimal amplitude range is clearly smaller than the error caused by the changes in the STOP pulse in low amplitude levels. This method was used in /Kilpelä90/, in which the error caused by a PIN attenuator in a two-channel implementation was several hundreds of picoseconds, but by changing the structure to one-channel type the total accuracy could be improved to a range of +/- 14 ps in an amplitude range of 1:24. In that application the PIN diode attenuator was connected between the negative input of a fast operational amplifier (used in noninverted configuration) and the ground.

3.6 The timing discriminator and time measuring unit

3.6.1 Operating principle of a timing discriminator

The purpose of the timing discriminator is to change the analog timing pulses to logic ones, which have accurately defined positions in the time scale at some point of the analog timing pulse. Another task for the timing discriminator is to separate the timing pulses from the noise pulses. The timing discriminators are used commonly not only in laser range finders, but also in nuclear physics (particle radiation measurements) for generating accurate timing pulses from the pulses with a changing shape and amplitude.

The pulse shape in the laser range finders usually remains stable and only the amplitude changes as a function of distance and reflectivity of the target. The pulse shape may also change if, for example, the angle of the target surface changes almost in parallel with the measurement beam, thus making the beam reflect back from a long part of the target. One possibility for changes in the pulse shape may be that the measurement beam hits two targets located at different distances at the same time. In this case the most logical result is that the measurement result is some intermediate distance of the targets. The shape of the pulse may also change due to the nonlinearity of the amplifier or attenuator.

The performance parameters of the timing discriminator are walk error, drift and precision. The walk error, which is usually the most important error type created by the timing discriminator, means that the measurement result changes, when the averaged amplitude or shapes of the incoming pulses change. If the walk error of the timing discriminator were small enough and the dynamic range of the input pulse amplitude were not larger than the linear range of the amplifiers, an adjustable electrical or optical attenuator is not needed. A timing discriminator is also often faster than the attenuators, because it accommodates itself to two sequential pulses. The drift in the timing discriminator may be present, for example, if the offset voltage in the timing comparator changes due to aging or temperature variations. The single-shot precision of the laser range finder is defined by the slew rate of the measurement pulses and total noise. Being located at the end of the amplifier channel chain the timing discriminator has only a minor impact on the slew rate, and its contribution to the total noise is minimal. The bandwidth of the timing discriminator comparator is high, because no feedback is needed and thus no stability problems arise.

The timing discriminators are divided to two main groups: constant fraction discriminators (CFD) and leading edge discriminators. In the leading edge discriminators (the topmost curve in Fig. 11) the timing point is created at the moment, when the incoming pulse crosses a constant level. The walk error is high in the leading edge discriminator, because the timing moment depends on the rise time and amplitude of the incoming pulse. When the slew rate of the incoming pulses increases, the walk error decreases. In the traditional CFD (second from the top in Fig. 11) the input pulse is divided to two pulses, one of which is attenuated and the other is delayed. The timing point is the moment, when the delayed pulse crosses the top of the nondelayed pulse. If another of the pulses is inverted, the sum of the pulses crosses zero level at the timing point, which can easily be detected with a comparator. Optimal attenuation and delay are chosen so that the walk error is minimized /Gedcke68/. The timing moment in the traditional CFD does not depend on the amplitude of the pulse. In a special case of the traditional CFD called ARC (amplitude-risetime-compensated) timing discriminator, the delay of the delayed pulse is shorter than shown in Fig. 11 and timing takes place on the leading edge of the input pulse and the timing moment does not depend on the amplitude or the rise time of the input pulse. One variation of a CFD is a leading-trailing edge CFD, in which the pulse is divided to two identical pulses, one of which is delayed and the timing point is formed at the crossing point of the leading edge of the delayed pulse and the trailing edge of the nondelayed pulse (Fig. 11, the curves third from the top) /Kostamovaara86/. In the leading-trailing- edge timing the timing moment is stable also in the case of a tilted object, in which the leading and trailing edges of the pulse are

slowed symmetrically. If the amplitudes of the input pulses change in a wide range and the amplifiers saturate, the walk error of a CFD may increase to very high values. In this case a leading edge discriminator may give better results.

A third alternative for the timing discriminator is a crossover timing discriminator (in Fig. 11 second from the bottom), in which the incoming pulse is highpass-filtered and the timing moment is formed at the crossing point of zero voltage level. The timing point does not depend on the amplitude of the incoming pulse. In differential crossover timing the timing point is the crossing point of two high-pass filtered differential incoming pulses (Fig. 11, pulses at the bottom) /Ruotsalainen99/. Crossover timing does not, however, compensate the walk error due to the changes in the rise and fall times. The advantage of crossover timing is that it does not need delay cables and thus suits well for integration in ASICs.

The most practical way to detect the crossing of two pulses is to use a fast comparator, since in that case there is no need to sum the pulses to each other, rather they can be directed to the different input nodes of the comparator. Another possibility for detecting the timing point is to use a tunnel diode, but it leads to a more complicated circuit than with the comparator /Leskovar76/.

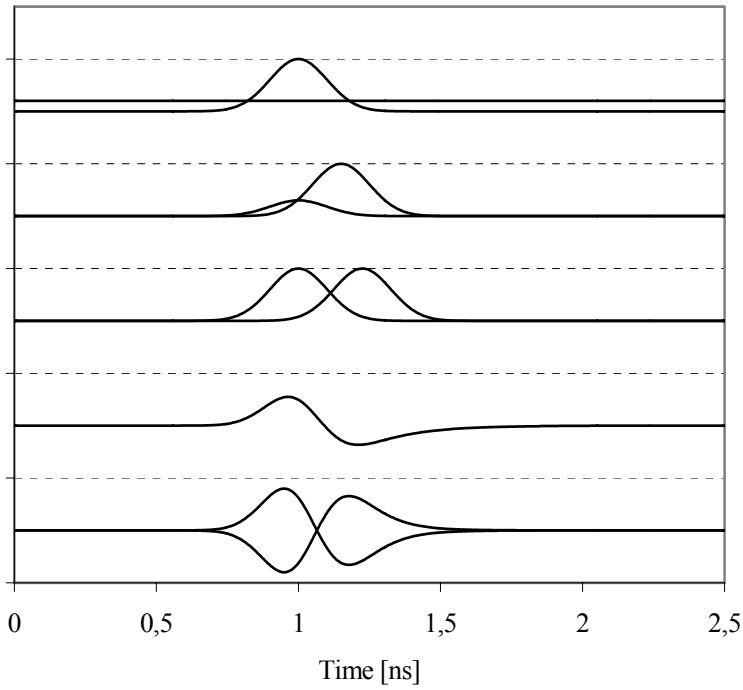

Fig. 11. In the leading edge discriminator the timing moment is the cross point of the input pulse and constant voltage (on the top). The second pulse from the top presents classical CFD and the third pulse from the top presents a CFD of ref. /Kostamovaara86/. When using the crossover timing, the timing moment is the crossing moment of zero voltage (second from the bottom). The pulse at the bottom represents a differential crossover timing.

In Fig. 12 a circuit diagram is presented for a leading-trailing- edge CFD, which is implemented with a fast ECL-comparator and ECL logic components. The circuit includes a noise comparator (top left in Fig. 12), which is used for separating the noise pulses and measurement pulses from each other. The offset voltage in the other input of the noise comparator is adjusted to be as small as possible, yet in such a way that the number of misses and false alarms is small enough, a normal value for the offset voltage being at least 10 times higher than the rms-value of the electronics noise. The delay of the divided input pulse is implemented with a 50 Ω coaxial cable. The output of the noise comparator is kept unchanged with the Latch Enable (LE)-input of the noise comparator and flip-flop n:o 1 until the timing pulse has propagated to the flip-flop n:o 2. The length of the output pulse is adjusted with the time constant of the RC-loop in the output of flip-flop n:o 2.

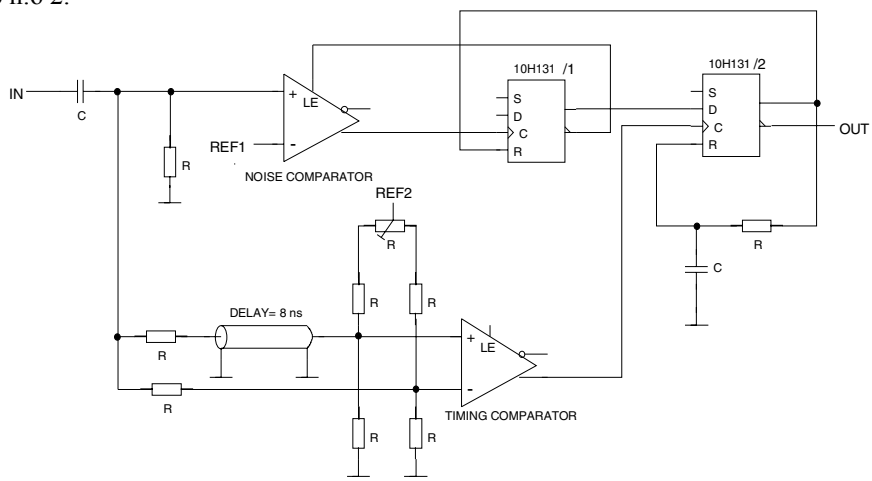

Fig. 12. A practical realization of a CFD.

3.6.2 Evaluation of the walk error

The walk error may arise from three different factors: firstly from the changes in the propagation delay of the comparator as a function of slew rate, overdrive and underdrive of the input pulses, secondly from the changes of the timing moment and thirdly from a potential crosstalk in the circuit board or inside the comparator circuit. The changes in the propagation delay of the comparator are due to the limited gain-bandwidth (GBW) product of the comparator. The higher the slew rate of the input pulses, the shorter the delay. If the amplitude of the input pulses is changed, but the slew rate is held constant by changing the rise time, the delay is constant, if the amplitude of the input pulses is so high that it is enough for a logic level change in the output of the comparator/Binkley88/. In Paper IV, Fig.5, the walk error of three comparator types has been compared. It was noticed that the comparator with highest GBW product gives the smallest walk error. The

timing moment may change due to the timing principle itself or due to the offset voltage between the two input nodes of the comparator. The offset voltage may cause an error, but it may also be used for decreasing the walk error arising from the limited GBW of the comparator, if properly adjusted. In principle the noise pulses can be separated from the measurement pulses with the timing comparator, if the offset voltage is adjusted high enough, but often the high offset voltage creates too high a walk error, and using a separate noise comparator becomes inevitable.

In Paper IV the walk error of the CFD has been evaluated by assuming that the comparator is a linear amplifier with one dominating pole /Arbel80/. Then the open loop gain of the amplifier presented in the s-plane is :

$$\frac{V_0(s)}{V_i(s)} = F(s) = \frac{e^{-s\tau_D} \cdot A(0)}{1 + sA(0)\tau_0} \tag{7}$$

where A(0) is the open loop gain in zero frequency and τ_0 is the time constant representing the corner frequency of unit gain. The constant part τ_D in the delay means that the comparator has a minimum propagation delay after which the input signal has propagated to the output. If it is assumed that the trailing and leading edges of the input signal are linear ramps, which have rise and fall times of t_r and t_f, respectively, the time t_{cross} , which is used for reaching a voltage level V_0 in the output, can be calculated by adding the formulas 3 and 4 presented in Paper IV together:

$$t_{cross} = \tau_D + \sqrt{\frac{2\tau_0 V_0}{SR}} + \frac{1 - \frac{V_{of}}{V_p}}{\frac{1}{t_r} + \frac{1}{t_f}}, \tag{8}$$

in which V_{of} is the offset voltage, V_p is the peak amplitude of the input voltage and SR is the combined slew rate of the leading and trailing edges of the input pulses in the timing point. The timing error can not be totally reduced, because the propagation delay of the comparator depends on the term $1//\sqrt{SR}$ and the term caused by the offset voltage has the form of 1/SR. Thus the total walk error is usually negative with small input amplitudes. The calculated and measured walk errors with different offset voltages for the comparator AD96687 are compared in Fig. 13, which shows that the calculations agree quite well with the measurements. In the calculations the rise and fall (0-100 %) times were 5.6 ns. The gain of the comparator was assumed to be 170 at the frequency of 100 MHz.

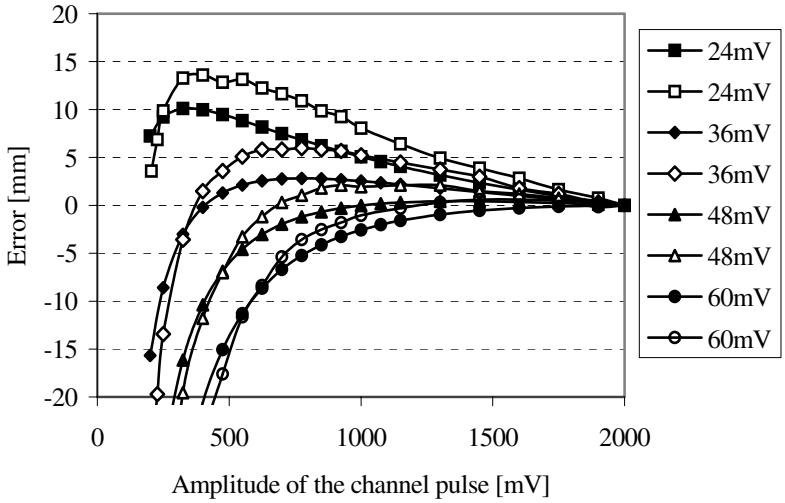

Fig. 13. The walk error of the constant fraction discriminator measured with the AD96687-comparator (open marks) and calculated for the AD96687 (closed marks) with different offset voltages.

The calculated walk error for comparator type SPT9689 has been presented in Fig. 14. The input pulses used in the calculations were Gaussian shaped pulses having bandwidths of 100 MHz and 1 GHz. It has been assumed that the gain of the comparator is 1000 at the bandwidth of 900 MHz. It can be seen (when compared to Fig. 13) that a fast comparator gives a smaller walk error than a slow comparator and that faster pulses give smaller walk error than slow pulses. In these calculations a walk error of +/- 1 mm is achieved with 1 GHz input pulses at least in a dynamic input pulse range of 1:10. Another fact noticed is that if a fast comparator and slow pulses are used, a small offset voltage is enough for correcting the walk error. If the pulses are fast, a larger offset voltage is needed, which can also be seen directly from equation 8.

In principle the walk error can be eliminated totally if the offset voltage is adjusted to constantly match with each input pulse amplitude. A changing offset amplitude has been used in /Loinaz95/. The large walk error of the leading edge discriminator was decreased with an additional circuit, the delay of which depends on the amplitude of the input signal.

However, equations 7 and 8 are not valid in a situation, in which the timing takes place in the leading edge of the input pulses and the overdrive is small and / or the slew rate is higher than the comparator is able to follow. Then the change of state in the comparator does not happen on the leading edge of the pulse and the state of the comparator is still changing, when the input pulse has transferred from the rising part to constant part. In this case the walk error is higher than shown by equations 7 and 8.

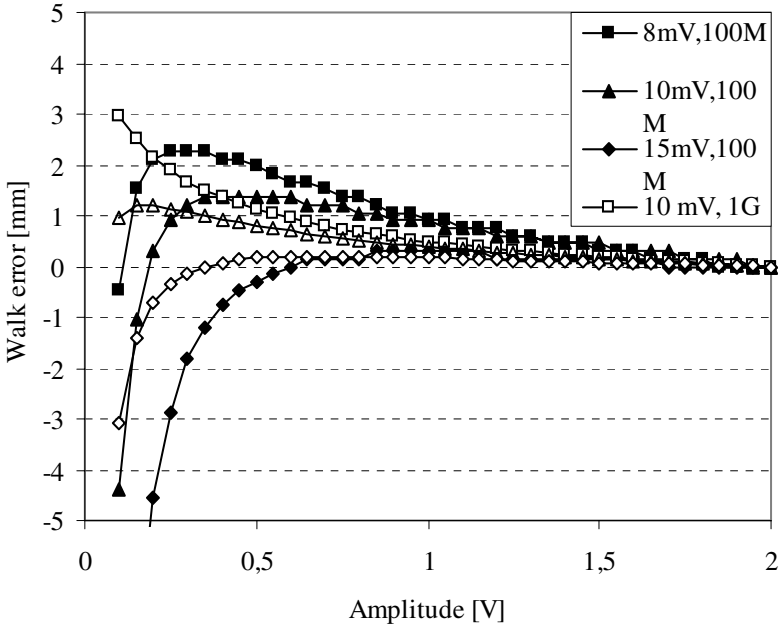

Fig. 14. The walk error for a leading-trailing-edge CFD with the comparator SPT9689 calculated for different offset voltages and using a 100 MHz Gaussian input pulses (closed marks, 100M) and 1 GHz Gaussian pulses (open marks, 1G).

3.6.3 Timing jitter

The noise level of the measurement pulse limits the best timing jitter achieved, which is expressed in practice as a single-shot precision. The root-mean-square (rms) value of the total noise is composed of the square root of the sum of all squared noises, if the noise sources are not correlated. The most important sources are electronics noise and the shot noise of the signal itself. In small signal levels the dominating noise source is the noise of electronics. Normally the shot noise of the optical background radiation is very small. If the signal is strong, the shot noise of the signal is dominating and the higher the level of the timing point in the measurement pulse, the worse the precision. On the other hand, if the input pulse is of Gaussian shape, the slew rate decreases and precision deteriorates, when the zero level of the pulse is approached, and an optimum value for the timing level can be found. The offset voltage between the input nodes of the comparator also has an impact on the timing point. The single-shot precision for the case of APD can be calculated using the following equation:

$$\Delta t = \sqrt{\frac{v_{n-rms}^2}{SR^2}} = \sqrt{\frac{v_{n-amp}^2 + 2 \cdot q \cdot V_{out} \cdot M \cdot F(M) \cdot B \cdot Z}{SR^2}} \quad (9)$$

in which $v_{n\text{-}rms}$ is the rms value of the total noise in the timing moment, $v_{n\text{-}amp}$ is the rms value of the electronics noise, V_{out} is the pulse voltage in the timing point, M = multiplication factor of the APD, F(M) = excess noise factor of the APD, B = signal bandwidth and Z = the transimpedance of the amplifier.

The timing point for best precision with Gaussian pulses varies according to the amplitude level, as shown Fig. 15. The precision achieved with different S/N-ratios and timing levels was calculated using leading edge timing and true Gaussian pulses having FWHM and rise time of 417 ps and 299 ps, respectively. The rise time and FWHM match signal bandwidth of 750 MHz, but it was approximated that the true measurement pulse is a mixture between a Gaussian pulse and a RC-time constant limited pulse and therefore slightly slower (than 1 GHz channel bandwidth) Gaussian pulses were used in the calculations. In a small S/N ratio (10) the precision decreases rather sharply, when the timing point is increased or decreased from 55% level (the constant level noise of the amplifier electronics dominates, so the highest slew rate gives the best precision). In a high S/N ratio (100) the 40 % point gives the best precision, but it does not decrease so strongly, when the timing point is changed (the signal noise dominates, so in lower timing points the signal noise is lower, even though slew rate is also lower and precision does not change). With S/N value of 30 the best timing point was at 45 % of the maximum amplitude. The noise current density referred to input, transimpedance, multiplication factor M and excess noise factor F(M) were 10pA/√Hz, 10kΩ, 100 and 2.2, respectively.

In Figure 10 in paper IV a level of 41 % was measured to give the best single-shot precision, when a 100 MHz receiver channel and leading-trailing edge timing discrimination were used. From the same figure it can be seen that when the S/N ratio is high, the optimum timing point can be found in lower level than with low S/N ratios. The difference in low S/N ratios with the calculations shown in Fig. 15 is due to the fact that the electronics noise and pulse shape were different - leading and trailing edges of the pulses measured in Paper IV were more linear than in the pulse used in the calculation shown in Fig. 15.

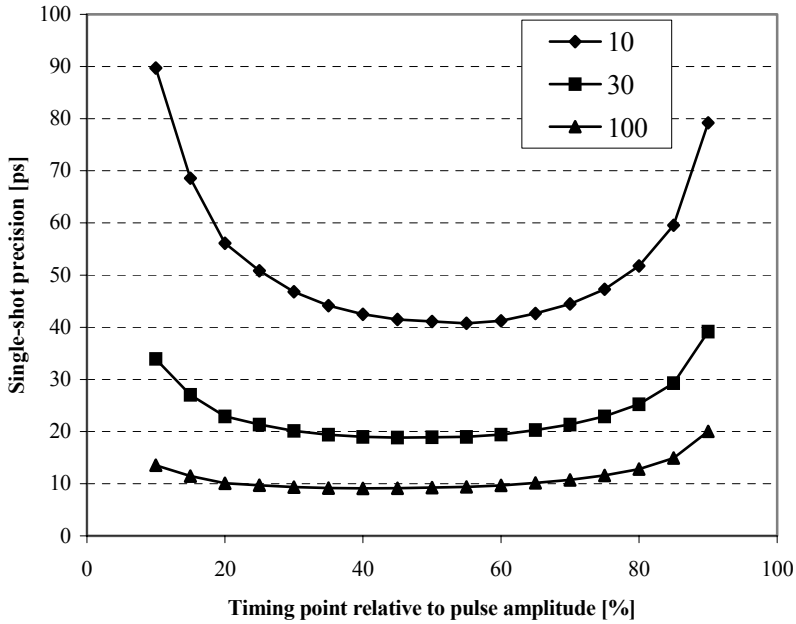

Fig. 15. The calculated single-shot precision for a leading edge timing with a 1GHz channel and 420 ps wide Gaussian shaped pulse as a function of relative timing point with three input pulse S / N –ratios.

The superiority of the 1 GHz receiver channel single-shot precision over 100 MHz channel precision can be seen in Fig. 16, in which the calculated single-shot precisions as a function of S/N-ratio for 100 MHz and 1 GHz channels equipped with leading-edge timing discriminators are presented. For the same reason as above 750 MHz and 75 MHz Gaussian pulses, which are slightly slower than the channel bandwidth, were used in the calculation. The parameters (I_n=6.6pA/√Hz, Z=140kΩ) of the 100 MHz channel are the same as presented in /Määttä95/ and the parameters of the 1 GHz channel are the same as presented above (I_n=10pA/√Hz, Z=10kΩ). An APD having parameters M=100 and F(M) = 2.2 (@M=100) was used in both channels. In both curves the peak amplitude range of the STOP pulse was 0.04 – 2 V and the peak amplitude of the START-pulse was 0.5 V in the 1 GHz channel and 1 V in the 100 MHz channel. The timing level was at 40 % of the maximum amplitude. The whole range of single-shot precision in this amplitude range was 43 to 810 ps and 3.4 to 35 ps with 100 MHz and 1 GHz channels, respectively. For example, if the goal is to reach an averaged precision of 1 mm (equates to ~6.6 ps) with S/N ratio of 50, 239 pulses are needed with the 100 MHz channel and 4 pulses with the 1 GHz channel, respectively. In the calculation it is assumed that the averaged precision is improved with $\sqrt{n}$ compared to single-shot precision, in which n is the number of averaged results.

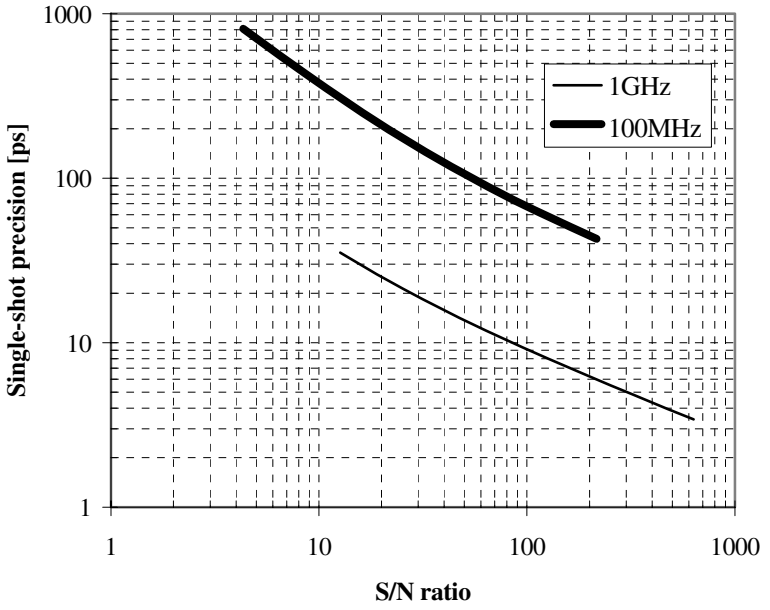

Fig. 16. The calculated single-shot precisions for 1GHz and 100MHz laser range finders with leading edge timing. The amplitude range of both curves in the figure is 0.04 V – 2 V.

The single-shot precisions of different timing methods for 1 GHz receiver channel are compared in Fig. 17. Three curves presented were simulated with PSPICE and one curve is based on calculated values using Eq. 9. The simulated alternatives are leading-trailing-edge timing at 40 % timing level, crossover timing (filtered with a single-pole 600 MHz high-pass RC-filter) and leading edge timing at 40 % timing level. For the latter also the calculated curve is presented. The precisions for leading-trailing-edge timing and crossover timing were better than the calculated and simulated precisions for the leading edge timing. The calculated and simulated results for the leading edge timing match well with each other. One explanation for the better precision of the leading-trailing-edge timing could be that the noise signals modulating the nondelayed and delayed pulses correlate at least to some extent with each other. In crossover timing the high-pass filtering decreases the total noise, which explains its good precision. The effect of the timing discriminator has not been taken into account in the simulation.

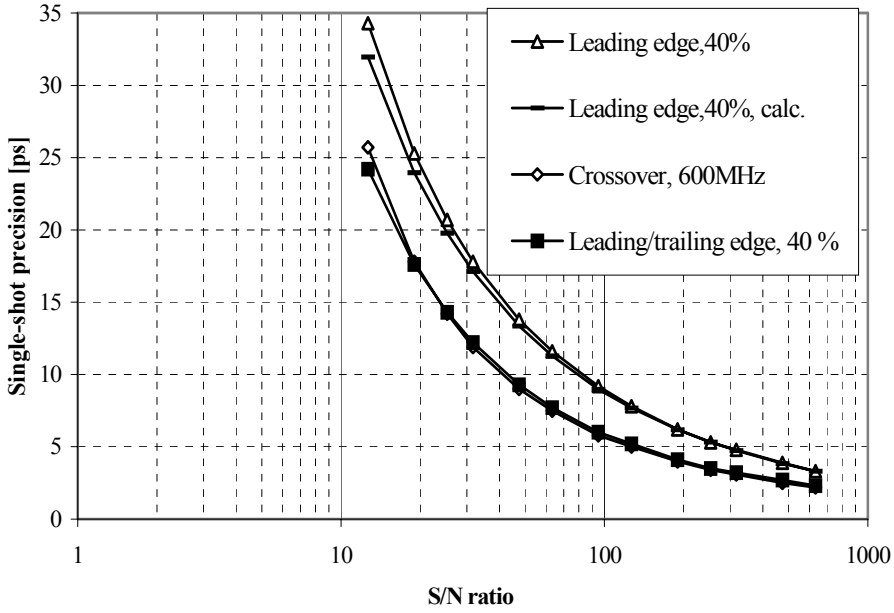

Fig. 17. The PSPICE-simulated single-shot precisions for the leading-trailing-edge timing at 40 % timing level, for the crossover timing with 600 MHz high-pass filtering and for the leading/trailing edge timing at 40 % timing level. The calculated single-shot precision for leading-edge timing and 40 % timing level is also shown. The input pulse was a 1 GHz Gaussian pulse.

In the simulation the input pulse was a 1 GHz Gaussian pulse (FWHM~314 ps) and the random shot noise generated with a random number generator was added to the measurement pulses. The random numbers in the table simulating shot noise modulated the amplitudes of the 1 ps wide pulses, which had a repetition frequency of 100 GHz. The 1 ps wide pulses with a 1 GHz Gaussian envelope were filtered with a passive 2-pole ~10 GHz Gaussian low-pass filter and were summed to the electronics noise. The rise time, fall time and FWHM of the pulses in the output of the low-pass filter were 266, 535 and 424 ps, respectively. The rms-voltage of the shot noise was adjusted to match the bandwidth of a 1 GHz transimpedance amplifier (Z = 10k, M = 100). The rms-voltage of the random noise that simulates electronics noise was adjusted to match a noise current density of 10 pA/√Hz reduced to the input of the 1 GHz channel. The original bandwidth of the random noise was 5 GHz, which was filtered with a single-pole low-pass RC-filter having a corner frequency of 2.5 GHz. In the calculated curve the shape of the measurement pulse was exactly the same as in the simulation after the 2-pole Gaussian filter.

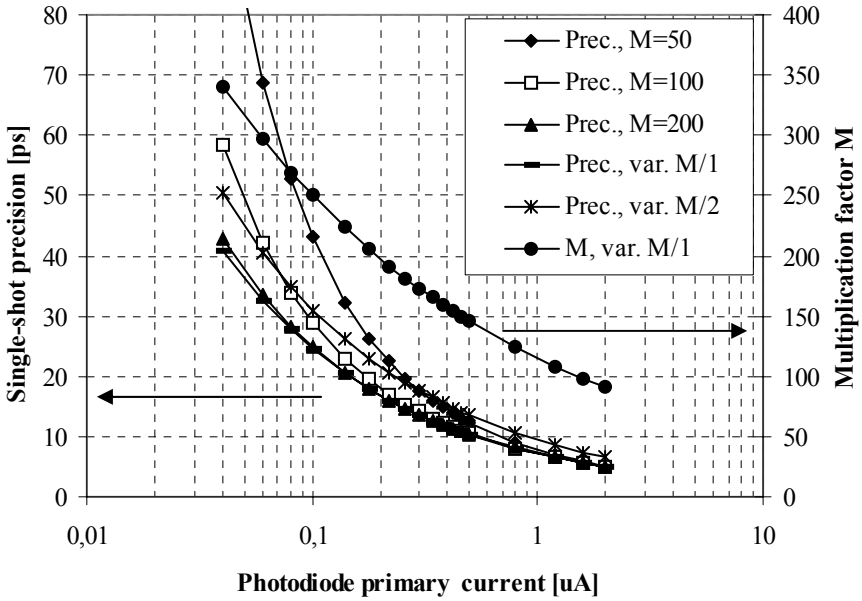

Fig. 18. The calculated single-shot precisions for 1 GHz channel and Gaussian pulses wih three constant values of APD multiplication factor M and with two varying values of M. The multiplication factor M calculated for optimum single-shot precision (curve M, var. M/1) is also presented in the figure.

Also the multiplication factor M affects the single-shot precision. The single-shot precisions for a 1 GHz channel as presented above with Gaussian pulses (FWHM = 420 ps) are presented in Fig. 18 with three constant values of M (50,100 and 200) and with two varying values of M as a function of photodiode primary current. One of the changing values (M/2 in the figure) was calculated according to the principle presented in chapter 3.5.2. so that the signal current noise and amplifier noise have equal rms-voltage values at each signal current level. The other one of the curves (M/1 in the figure) has been calculated so that the best achievable single-shot precision is searched at each point by changing the value of M. The best precision curve of the constant values of M is reached with M = 200 and the results are very close to the curve M/1, in which M is changed according to optimum precision. Also the values of M, which give the best single-shot precision at each primary current level, are shown in the figure (M, var. M/1).

3.6.4 The time measuring unit

Very accurate time measuring units for short time intervals are used in laser range finders, nuclear physics measurements and digital oscilloscopes /Park98/ and also in other

measuring equipment, such as cable length measurements, phase measurements and delay measurements of electronic components /HP97/. The time measuring unit may be the limiting factor for single-shot precision, if bandwidth, signal power and S/N-ratio are all high in the measurement. There are several methods to measure time, using digital, analog or combined methods, for example. The single-shot precision achieved varies in a wide range according to the method used. With all methods the single-shot precision can be improved by averaging in proportion to the square root of the number of the measurement results. However, with the digital methods it is required that the oscillators used in the transmitter and in the time measuring unit are independent of each other. Synchronization is usually avoided by adding random noise to the oscillator pulses of the transmitter.

In digital time measuring the idea is to calculate the number of clock pulses (for example in 100 MHz frequency) arriving during the time between the START- and STOP-pulses /Rankinen91/. The analog time measuring can be realized for example by discharging a capacitor with a constant current during the time between the two pulses and by measuring the voltage of the capacitor after the discharging cycle with an A/D-converter /Kilpelä90/. Another version of the analog time measuring is known as Nutt method, in which the capacitor is charged during the two measurement pulses and after charging it is discharged with a much smaller current, which extends the original time period so long that it can be measured digitally with a reasonable accuracy /Nutt68/. Digital measurement techniques enable good linearity even with long measurement times, while analogue methods enable high precision and the combination of both techniques enables both of the advantages to be achieved at the same time. The linearity of the analog method based on capacitor discharging is typically ~0.1% /Rankinen91/. The temperature stability of analogue measurement techniques is poor, for example 40 ps/°C 100 ns measurement time/Sasaki85/.

In a combined method the principle is to measure the time digitally, but the time period between the start pulse and the next digital clock pulse but one is measured analoguously with an interpolator. The same principle is also used for measuring the time position of a stop pulse. If the temperature drift of the interpolators is the same, they are excluded from the averaged result. In /Määttä98/ the interpolators are realized by discharging a capacitor with a constant current and by measuring the voltage change with an A/D-converter. The digital time measuring unit was realized with an ECL-ASIC-circuit and the interpolators were separate circuit boards. A small temperature drift (0.3 ps/°C), very high single-shot precision (10 ps) , and good linearity (+/- 20 ps in a measurement range of 0.02 – 1.3 μs), were achieved. Another example of a combined measurement realization is presented in /Räisänen-Ruotsalainen97/, in which the same CMOS-circuit contains a digital time measuring unit and interpolators based on the Nutt method. A single-shot precision of 30 ps, power consumption of 350 mW and a temperature drift of 0.8 ps/°C were achieved.

An analog time measuring method based on delay lines is for example a pulse-shrinking delay line, in which the input pulse (which extends the time between START- and STOP-pulses) shrinks during propagation in a special delay line, which has longer trailing edges than leading edges in the logic gates /Rahkonen93/. The advantage of a pulse shrinking delay line is small size of the die using a widely available CMOS-semiconductor process and the disadvantage is that only one STOP-pulse can propagate

at one time in the delay line. A single-shot precision of 500 ps has been achieved with the pulse-shrinking-delay line. Another choice for delay line methods is a Vernier-delay line (VDL) /HP97/, which enables a 30 ps single-shot precision to be achieved / Dudek2000/. In the VDL the START- and STOP-pulses propagate in separate delay lines, which are made of logic gates connected in series. The propagation speed of the START-pulse is faster, so the pulses coincide at some section of the delay lines, which is detected with separate logic flip flops connected to both delay lines. The delays of the logic gates can be adjusted by changing the internal threshold voltages or the bias currents of the output buffers, which have an impact on the rise and fall times /Sakamoto89/. In /Mäntyniemi2002/ a digital time measuring unit and delay line interpolators have been combined to one ASIC-chip realized with CMOS techniques. Using part of the delay lines as a reference has increased the accuracy of interpolators. Some of the delay lines are used for locking the delays of all lines with a Delay-Locked-Loop (DLL) to the frequency of a quartz-crystal oscillator. A very good temperature stability (0.2 ps/°C), high single-shot precision (28 ps) and good linearity (+/- 5 ps in a measurement range of 0.02 – 496 μs) have been achieved with small power consumption (50 mW). In /Szplet2000/ also the digital measurement principle and delay line interpolators have been combined to one chip, but it is realized with a programmable logic circuit (FPGA= Field-Programmable-Gate-Array), which consumes relatively high power (260 mW). Using calibration methods a single-shot precision of 70 ps has been achieved.

3.7 Optics

3.7.1 Influence of the target and medium to the measurement result

The attenuation of the atmosphere is mainly due to water vapor molecules and slightly also due to carbon dioxide molecules /Carmer96/, but the attenuation is very small in the distance range of some tens to some hundreds of metres in normal conditions. At these distances also the turbulences of the atmosphere have little impact on the measurement result when using multimode lasers /Byren93/. The turbulences are caused by temperature differences of the air and small particles in it which make the beam refract and widen. If the temperature is very hot, like inside iron converters, the measurement error due to turbulences may be some millimetres, when the temperature differences in the air in the optical path are some hundreds of degrees /Määttä93/.

The properties of the target surface affect strongly the reflection coefficient and the radiation pattern of the reflected light. Usually with passive targets (which do not include special reflective tapes or corner mirrors) the variation in the reflection coefficient is about 1:10 in perpendicular measurement angle /Kaisto83/. If also the changes in the measurement angle is taken into account, the variation is larger. In /Kilpelä85/ the amount of reflected light as a function of the measurement angle has been measured at 780 nm wavelength using nylon plastic, mild (black) steel, grinded aluminium and magnesium oxide powder (a Lambertian reflecting surface) as target surfaces. When the angle

changed between 0 and 45 degrees, the changes in the reflected signal power were 1:0.8, 1:3, 1:40 and 1:200 with magnesium oxide, nylon, mild steel and aluminium, respectively. In perpendicular measurement angle the largest difference was between aluminium and steel surfaces, about 1:20. All in all, if there are mirror like reflective surfaces and on the other hand, especially dark and unsmooth surfaces, the power variation may easily be 1:10 000, even if the differences in the measurement distance is not taken into account. The reflection coefficients of some common materials measured at 900 nm wavelength and perpendicular angle are compared in table 4 /Riegl2002/. The reflectivity of white paper is used as a reference surface having reflectivity of 100 %.

Table 5. The reflection coefficients of some materials on 900 nm wavelength /Riegl2002/.

Material	Reflectivity [%]
White paper	~100
Dimension lumber(pine,clean,dry)	94
Snow	80-90
Newspaper with print	60
Beach sand	~50
Concrete	24
Asphalt	17
Black rubber	2
Opaque white plastic	110 (max.)
Reflecting foil 3M2000X	1250 (max.)

3.7.2 Single-axis and double-axis optics

The alternatives for optics are single-axis and double-axis optics. In the single-axis optics one common lens is used for the transmitter and the receiver, whereas separate lenses are used in the double-axis optics. In the single-axis optics the transmitter and receiver beams are combined to the same optical axes using, for example, a prism or a semireflecting mirror, but in either case at least 50% is missed both in transmitted and received signal powers, so the difference to the double-axis optics is at least fourfold in a situation, where the lenses are focused to the target and the transmitter and receiver beams totally overlap each other (in the double-axis optics). However, the difference is smaller in practice, because in the double-axis optics the beams overlap totally only in a short distance range, whereas in other distances they overlap only partially, if the beams are not directed separately in each distance. For this reason the variation in the received power is usually larger with the double-axis optics than with the single-axis optics. The calculated power levels at the input of the photodiode using single-axis and double-axis optics were calculated using the formulas presented in /Wang91/ in the distance range of 1 to 30 m using focal lengths and diameters of 100 mm and 50 mm of the lenses, respectively. Both optics were focused in a 25 m distance (in order to receive enough power in long distances with the single-axis optics) and the beams overlap each other in 30 m distance in the double-axis optics. The diameter of the receiver fibre was 365 µm. According to the

calculation double-axis optics is better in the distance range of 5 to 30 m and the single-axis optics is better, if shorter than 5 m distances should also be measured. The total variation of power from minimum to maximum is smaller with the single-axis optics (~1:11) than with the double-axis optics (~1:30), so the single-axis optics is better, if no variable power attenuator is available and a wide measurement range is desired. The measurement error due to mode dispersion may also be higher with the double-axis optics, because the beam overlap is only partial in short distances and then only the high order modes in the multimode fibre are used /Nissilä95/. However, the dynamic variation of the optical power using the double-axis optics may be decreased slightly by cutting the edges of the lenses and bringing the transmitter and receiver axes closer to one another.

The efficiency of the optics can be increased by using lenses with a small enough distortion, by adding antireflection coating on the lenses, or by using a polarizing beam splitter in the single-axis optics. Because the fibres do not usually maintain the polarisation, the polarization effect can only be used with a laser without a fibre, which usually has at least a partially polarized light output /Melles2002/.

When the measurement beam hits simultaneously two targets located at different distances, the shape of the received light pulse distorts, giving a measurement result located somewhere between the distances of the targets. Usually the measurement result is a distance between the targets, depending on the power reflected back from each object. In /Adams93/ a method for analyzing and removing the unreliable measurement results caused by simultaneous reflections from several targets was presented.

3.7.3 Transmitter and receiver fibres

The type and sizing of the transmitter optics affects the size of the light spot on the target and the variation of the received signal power as a function of distance. In principle the measurement spots and the effect of the measurement distance on the signal power should be as small as possible. In order to have a small measurement spot, the divergence of the transmitter beam and the size of the active region of the laser should be small. The width of the active region of high power semiconductor lasers varies in the range of 100 to 400 µm and the height of the active region is ~2 µm. With multichip lasers the distances between the chips is adjusted so that the height and the width of the chip pile are about the same. The 1/e-width of the beam of one chip is ~+/- 6-7 ° in one direction and ~+/- 12-17° in the other. The flatness of the beam can be corrected by using a cylinder lens or an optical fibre between the laser and the transmitter lens. The laser power may be directed either directly or using a lens to the fibre. If a fibre and a lens is also used with the photodiode, the diameter of the fibre may be larger than the diameter of the photodiode, because the photodiode accepts incoming photons in rather wide angle. In this case the lens increases the NA (numerical aperture) of the light beam directed to the photodiode and a relatively small photodiode with small capacitance can be used.

Multimode fibres are preferred with high power lasers, because the diameter of the fibre and the laser should be about equal. With smaller lasers also graded index (GI)-fibres can be used, which helps to reduce the effect of multimode dispersion in the fibre.

The impulse response of several types of fibres can be approximated with a Gaussian low-pass filter. If the pulse emitting from the laser is also of Gaussian shape, the output pulse from a multimode fibre is again a Gaussian pulse, yet wider than the original /Hentschel89/. The shape of the electrical pulse after the amplifier channel in a laser range finder, in which multimode fibres are used both in the transmitter and in the receiver, is often close to Gaussian shape, which has an exponentially decaying trailing edge. The impulse response of a SI-fibre can be calculated by adding the Dirac-impulses of all modes (= angles) together in the output of the fibre. Each mode also has the material dispersion effect, which widens the impulses, but the impact is very small. In order to calculate the total response, the effective waveguide velocity of each mode should be calculated. The micro bendings mix the optical power between the modes and they also have their own impact on the impulse response. For these reasons, the impulse response, measured or calculated, is appropriate only in accurately defined conditions /Sharma81/. In /Senior92/ the largest delay difference between the different modes is approximated by the following formula:

$$\delta T_s = \frac{L(NA)^2}{2n_1 c} \qquad (5)$$

and the value for the rms pulse broadening has been approximated to be $\sigma_s = 0.288 * \delta T_s$, in which n_1=refraction index of the core, L=length of the fibre and c=speed of light. For example for a 1 m long HCS (hard clad silica)- fibre (core diameter 365 µm, NA = 0.22) the largest delay difference can be calculated to be 55 ps and the widening of the pulse to be 16 ps, which is not of importance until in bandwidths of a few gigahertz. However, the widening of the pulse is directly related to the length of the fibre, so the maximum total length of the fibre type described above, using a bandwidth of 1-2 GHz, is about 10 metres. The widening of the pulse may be smaller than described above because of the modes propagating in the cladding. As the bending of the fibre has a strong impact on the cladding modes, they should be avoided. The proportional fraction of the cladding modes can be reduced by designing the optics so that no light is guided outside the core /Nissilä95/.

The fibres also have a temperature drift, but with short distances (1-2 m) its effect remains quite small. In /Nissilä95/ the temperature drift of a HCS-fibre with a core and length of 200 µm and 1 m, respectively, has been measured to be 1 ps in a temperature range of –20 °C - +60 °C. The temperature drift may become a problem when the time between the START and STOP pulses may have to be increased because the time measuring unit does not allow short times to be used /Kaisto93/.

3.7.4 Optical attenuators

As compared to the electrical attenuators, the optical attenuators have usually a smaller walk error, but they are slower. The optical attenuator may also significantly increase the

price and size of the optics. As noted in practice in /Kilpelä90/, mechanically adjustable optical attenuators are not very well suited for fast changes in the optical power, as with 3D-laser range finders. The optical attenuator types used in laser range finders are an adjustable neutral density filter /Kaisto93/, covering part of the receiver beam with a plastic film /Kilpelä90/, liquid crystal (LC) attenuator /Karppinen92/ and a wavelength selective filter /Aikio99/. The electrical power needed in mechanically adjustable and LC attenuators varies from tens of milliwatts to some watts. The wavelength selective filter is not very practical, when semiconductor lasers are used, because narrowing the wavelength range may severely affect the shape of the optical pulse.

Adjustable neutral density (ND) filters are available commercially as round and rectangular /Newport2003/. The attenuation is realized with a thin aluminium film packed inside a glass plate, and the thickness of the aluminium film changes as a function of position in the glass plate. The ND filter may be attached, for example, between a fibre and a lens either on the transmitter or receiver side. In /Kaisto93/ a ND filter was used as an attenuator and a dynamic optical power range of 1:1000 was achieved without a noticeable error in the distance measuring result. The advantage of a ND filter is that it does not change significantly the mode distribution launched into the fibre. The disadvantage is the high price of commercially available adjustable ND filters, which is probably due to the accuracy of the adjustable attenuation and to low amount of production.

A more simple method as compared to the ND filter is to cover part of the light launched into the fibre with some obstacle, for example a metal plate or a plastic film. A disadvantage of this method is that the mode distribution changes. In /Kilpelä90/ a black round photographic film disc was used as an attenuator. In the outer edge of the disc 1-3 opaque spirals were created, the width of which changed as a function of the rotating angle. Three spirals were used for minimizing the effect on the mode distribution. When only one spiral was used, the mode distribution changed, according to the measurements, quite noticeably, whereas by using short fibres the effect on the distance measurement result was less than +/- 1 mm in a power range of 1:60. A step motor was used for rotating the discs, and the maximum time used for changing the attenuation between the minimum and the maximum was 150 ms.

The operating principle of the LC film is based on the longitudinal LC cells, the orientation of which is changed with an electric field (Fig. 19). When the electric field is high, the cells have the same orientation and the film operates as an almost opaque polarizing film. When the electric field is absent, the cells have random orientation that makes the incoming light scatter strongly, and the attenuation is high. The electric load of the LC film is practically only capacitive, needed to be charged and discharged with continuous AC voltage. An optical attenuator realized with LC film was presented in /Karppinen92/ and its effect on the measurement result of the laser range finder was presented in Paper V. In both references the same kind of attenuator modules were used, where 1-2 dark NCAP (Nematic Curvilinear Aligned Phase) films were attached between two collimating lenses and fibres having a core diameter of 400 μm. The LC film used was available commercially, but only as large sheets, which needed to be cut for suitable size. The developed optical LC attenuator was pulsed with a 2 kHz square wave voltage, the peak amplitude of which was changed in the range of 0 to 100 V in order to vary the transmittance. The whole dynamic optical power range of the lens attenuator was 1:26 at

a wavelength of 903 nm, and the measured walk error of the laser range finder in a 1:30 optical power range was +/- 1 mm (thus also including some walk error from the laser range finder itself), when the LC optical attenuator was adjusted for eliminating the optical power variation as much as possible. The speed of a LC filter depends strongly on the temperature, slowing down at low temperatures. In room temperature the time needed for changing the attenuation between the minimum and the maximum was 5 ms /Karppinen92/. Also contrast depends on the temperature, decreasing at low temperatures, as shown in Paper V, Fig. 4). The LC film is nowadays also commercially available /Anteryon2002 /, which is actually sold as an optical switch, but it can also be used as an attenuator. The diameter of the open aperture is 1 inch and the response time between the minimum and maximum attenuations is 2 ms at room temperature. The Anteryon film was also measured in a 100 MHz laser range finder attached between the receiver lens and the fibre, and the maximum attenuation was measured to be 1:57 at the wavelength of 903 nm.

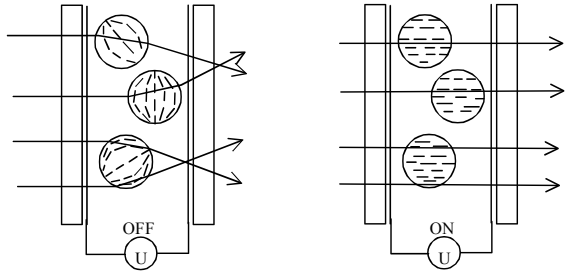

Fig. 19. Light passing through a LC film without external voltage (maximum attenuation) and with external voltage (minimum attenuation).

4 An example of the realization of a wide bandwidth laser range finder

4.1 General structure, optics, TDC and interface card

A high bandwidth laser range finder was constructed and tested in laboratory environment for verifying the performance and comparing it to other, earlier developed laser range finders. As described in chapter 3.1, the basic structure consisted of a laser pulser, two identical receiver channels with integrated amplifiers and timing discriminators, a TDC, optics, an interface and power card, and a PC for collecting the measurement results.

A single-axis optics was chosen for the laser range finder for two reasons, high linearity and wide measurement range. An optical attenuator was not used, because the walk error of the prototype laser range finder was evaluated to be small enough and also for the reason that the single-axis optics, when properly adjusted, has such a small dynamic range of the optical power variation that an optical attenuator is not needed. The structure of the optics designed is presented in Fig. 20. The focal length and diameter of the achromatic lens used in the optics were 100 mm and 50 mm, respectively. The type of the beam splitter was a semireflecting mirror based on a metal film. Step index multimode fibres with a core diameter of 365 μm and NA of 0.22 were used both in the transmitter and in the receivers. The unwanted laser pulse originating from the semireflecting mirror was directed to a “black box”, which consisted of a mirror and a 180 mm long tube with nonreflecting material located at the end of the tube. Using these methods the peak amplitude of the unwanted pulse in the STOP-channel was ~10 mV, which was lower than the triggering level of the noise comparator, ~20 mV. Also by limiting the measurement time scale of the TDC it was possible to eliminate the unwanted pulse from the measurement results.

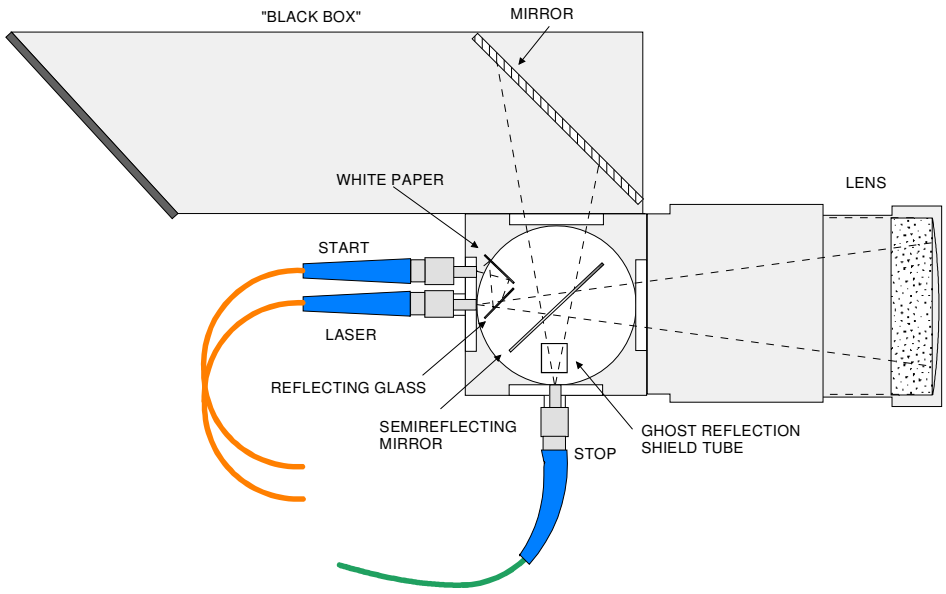

Fig. 20. The structure of the single-axis optics designed for the high bandwidth laser range finder.

The type of the TDC used is presented thoroughly in /Määttä98/. The TDC is constructed as a single E1-card unit and it consists of the digital counter, which counts the clock cycles of a 100 MHz oscillator, and analogue time interpolators (TACs), which enable to measure more accurately the 10 ns time periods between the clock pulses. The digital counter is manufactured as an ECL-ASIC circuit with a Plessey gate array process. The TACs are realized with discrete components and they are based on capacitor discharging. The total measurement range of the TDC is 0 to 2.55 µs. The periodic nonlinearity and single-shot precision have earlier been measured to be +/- 20 ps (in a period of 40 ns) and 10-11 ps, respectively. The output voltage values from the interpolators are measured with a 10-bit A/D converter located in the card and they are transferred with the interface card to a PC.

The interface card acts as a logic level buffer for collecting the results with a second interface card connected to the ISA bus of the PC. The interface card also includes DC/DC converters and filters, which convert and stabilize the 12 V input voltage to +/- 5V and +/-12 V voltages for the TDC.

4.2 The transmitter

The transmitter includes a single avalanche transistor as a switch and a LD-65 type SH-laser heated with a constant bias current. The laser operates (when heated) in a Q-switching mode at 1-10 kHz pulsing frequencies. Higher frequencies were also tested, the only problem being excess heating, which necessitates additional cooling. The transmitter

was constructed especially for this prototype laser radar. Special attention was paid to minimizing all lead inductances in the high current loop. The laser was equipped with a low inductance case, and the avalanche transistor used was a commercially available surface mounted model (FMMT417). The measured FWHM and peak power of the light pulse were 35 ps and 86 W without the fibre (but with the fibre connection lens) and 74 ps and 44 W with a 1 m long fibre, respectively. More than 100 W peak powers were measured from the laser without the lens. The light pulses were measured with a 20 GHz oscilloscope equipped with a 25 GHz PIN photodiode. The optimal laser pulse length for the 1 GHz receiver would be 300 - 400 ps, but the laser pulse cannot be lengthened significantly, when the Q-switching mode is used. Special attention was paid to preventing electromagnetic interference (EMI) from leaking out of the metal transmitter case and the supply voltage cables from acting as radiating antennas. The transmitter is a very powerful source of EMI because of high current slew rates. The aluminium metal case was manufactured with thick walls and the holes were as small as possible. Twisted pairs and metal screen shielded cables were used for power supply input. Pi-type panel mount filters were used for connecting the supply voltages into the case.

4.3 Amplifier channels and timing discriminators

The amplifier channel includes a commercially available silicon APD chip (Silicon Sensor AD230-I) and an ASIC amplifier chip glued on a printed circuit board plated with a gold layer (Fig. 21). The amplifier chip includes a gain adjustment block, a transimpedance preamplifier, a postamplifier and a timing discriminator and it is manufactured in a MAXIM GST-2 –bipolar process (f_t = 27 GHz). The signal proceeds from the photodiode to the output of the timing discriminator all the way differentially in order to minimize the influence of the external and internal noise sources. The bandwidth of the amplifier was measured (with an electrical input signal) to be 40 MHz - 2.5 GHz without the timing discriminator. The differential transimpedance is 11 kΩ. The APD has a capacitance of 1.5 pF, sensitivity of 33 A/W (λ~900 nm) and bandwidth of 2 GHz (at a gain of 100) specified in the datasheets. The structure of the amplifier channel is presented in Paper VI and in more detail in /Pennala98/.

The gain adjustment element is based on a Gilbert cell and it has a 55 dB dynamic range, which is limited in the low signals by the noise of the cell and in high signals by the bias current of the transistors. In practice the adjustment range is 20-40 dB (depending on how large a walk error is acceptable) and outside of that range the walk error of the cell is too high for mm-level accuracy.

The differential input pulses to the timing discriminator are filtered with a single-pole high-pass CR filter, which has a corner frequency of 600 MHz. This selection was estimated to maximize the single-shot precision. The walk error of the comparator is minimized by adding a suitable offset voltage between the positive and negative input nodes.

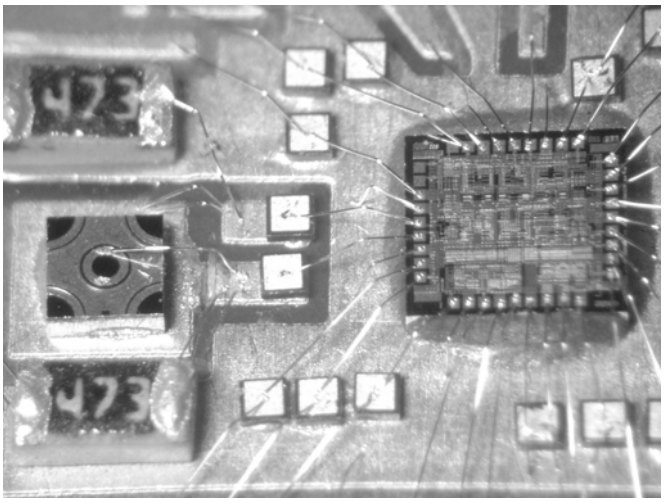

Fig. 21. Photo of the APD chip (left), amplifier chip (right), capacitors and bias resistors attached on a printed circuit board.

4.4 Measurement results

The performance of the prototype distance meter was evaluated by measuring a number of parameters, such as bandwidth, noise, total gain and linearity of the amplifier, and single-shot precision and walk error of the distance meter.

In Fig. 22 the output pulse of the laser transmitter and the pulse response of the amplifier channel are presented. Both pulses are measured with a 20 GHz oscilloscope. The laser output pulse is measured with a 25 GHz reference photodiode. The amplitudes of the pulses are not comparable with one another. According to the pulse response the upper cut-off frequency of the channel can be estimated to be ~1 GHz (t_r ~260 ps, t_f ~370 ps). An APD gain of 200 was used in the measurements. From Fig. 22 it can be seen that the pulse continues as a ”tail” of several nanoseconds after the short peak. The tail can be removed by optical wavelength filtering. In the measurements presented here, however, the light pulse has not been filtered, but when tested, filtering was not found to have any measurable effect on the performance.

The rms-noise of the channel output was measured to be 3.9 – 9.9 mV. Thus the minimum measurable pulse amplitude is ~ 39 mV in order to keep the S/N-ratio 1/10 or more. The noise is at its smallest in minimum attenuation and increases, when the attenuation is increased due to the excess noise created by the Gilbert attenuator cell.

The sensitivity of the total channel was measured to be 100 kV/W for a short pulse shown in Fig. 22, which gives a sensitivity of 8-9 A/W for the APD with an internal gain of 200 (for short pulses). The sensitivity is limited by the limited speed of the APD. However, the sensitivity is clearly better than the typical MSM sensitivity of 0.2-0.3 A/W, for example.

The walk error and single-shot precision of the channel in an S/N-ratio range of 9.5 - 843 are presented in Fig. 23. The distance was constant and the optical input power was varied with a neutral density filter. In Fig. 23 the power level is defined so that the smallest amplitude is limited by noise (differential output voltage amplitude of the channel was 36 mV). The walk error above the S/N value of 94 is caused by the Gilbert cell and below that by the timing discriminator. The walk error remains below +/- 1 mm in the whole range and also the precision is on the same level, 2 mm (~14 ps) at its best, remaining below 5 mm (~34 ps) in the whole measurement range. The precision of the TDC, which is ~10-11 ps at its best, is included in the measurements. The measured values agree well with the simulated values for crossover timing shown in Fig. 17 for small signal amplitudes, where amplifier noise dominates. For large amplitudes there is slight difference in the simulated and measured values due to the fact that in the measurement the APD gain was 200 and in the simulation it was 100. The rise times of the pulse in the simulation and in the real channel are practically the same.

The effect of varying APD voltage was also tested and the results were quite similar as before. When the APD-voltage was varied resulting in 1:3 change in signal amplitude, the walk error was ~10 ps. Outside that region the walk error was measured to rise steeply. So, varying the APD voltage could be used in a limited range of optical power variation for cancelling walk error, but when used in a high bandwidth laser range finder, the walk error caused by the APD voltage changes is easily higher than the walk error caused by the comparator in the timing discriminator.

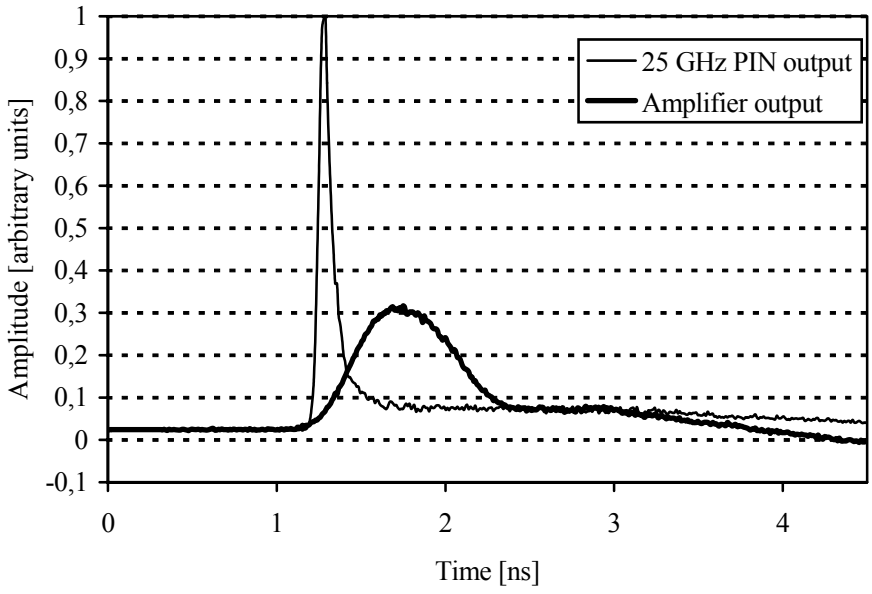

Fig. 22. The light pulse of a laser transmitter measured with 25 GHz reference photodiode and the pulse response of the amplifier channel, both measured with a 20 GHz oscilloscope.

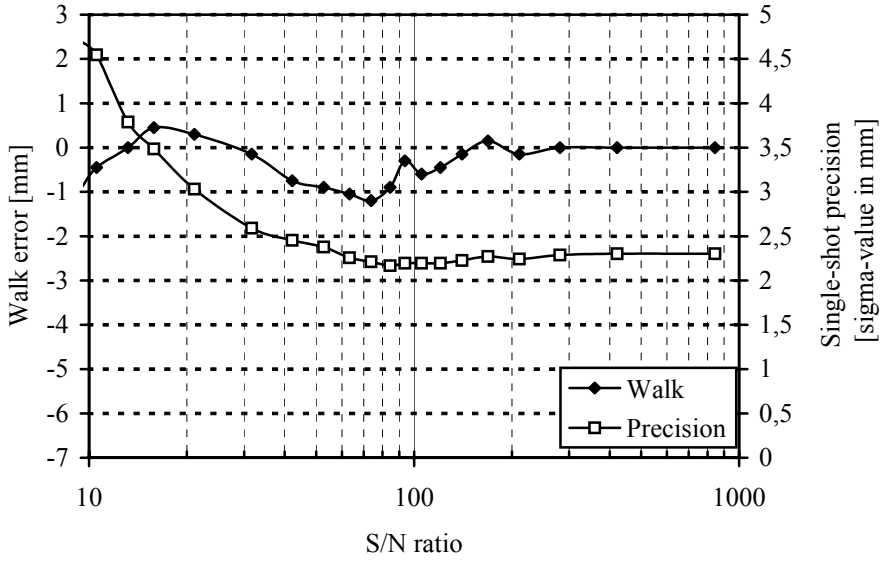

Fig. 23. The walk error and precision of the receiver channel

The linearity error and single-shot precision of the whole distance meter in a distance range of 0.5 m – 34.5 m is presented in Fig. 24. The target was a piece of white printing paper. The nonlinearities of the TDC and the calibrated measurement track were eliminated from the measurement result. A single-axis optics was used in the measurement and it was focused to the maximum distance, 34.5 m. The range of variation of the optical power in the whole distance range was 1:18. The Gilbert cell attenuator was in minimum attenuation in the distance range of 12.5 m – 34.5 m. The total error was less than +/- 2 mm and the precision (σ-value) was better than 34 ps (~5 mm) in all distances. In the longest 34.5 m distance the S/N-ratio was approx. 1:10, the lowest possible value. The cyclic peaks appearing in the precision curve were due to the properties of the TDC.

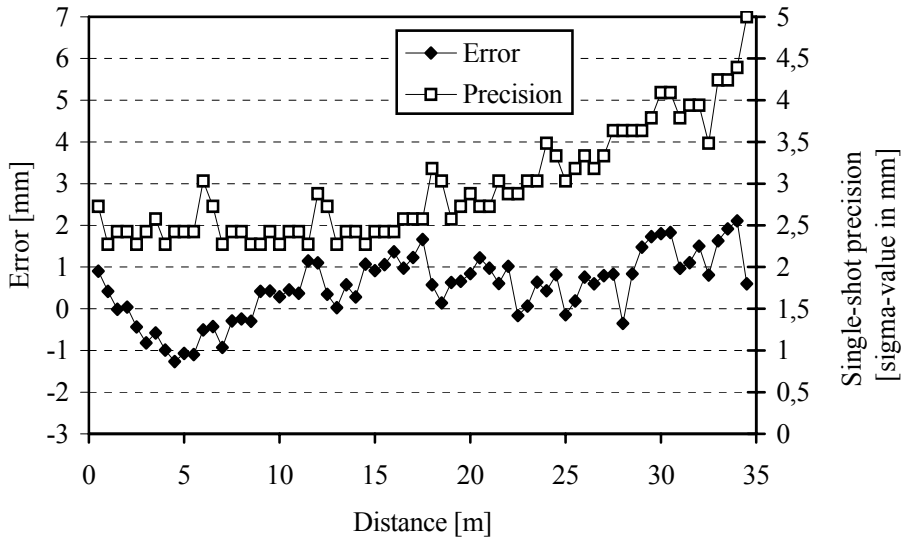

Fig. 24. The measurement error and precision of the distance meter in range of 0.5 to 34.5 m

The single-shot precision value of 14 ps (at S/N-value of 100) achieved with the 1 GHz channel and 74 ps laser pulse is clearly better than the 42 ps and 70 ps precision values achieved earlier as best with the 130 MHz /Palojärvi2002/ and 100 MHz /Määttä93/ channels, respectively, at S/N value of 100. The best walk error achieved with lower bandwidth channels has been on the same level as with the 1 GHz channel, but the walk error is small in a wider input amplitude range using the 1 GHz channel.

The linearity error using a 4 m long receiver fibre with single-axis and double-axis optics can clearly be seen in Fig. 25. The same measurement is also presented with shorter fibres in Paper VIII. With shorter fibres the linearity error was measured to be quite small using either single-axis or double-axis optics. The reason for the linearity error with double-axis optics is that the intersection of the areas of the transmitter and receiver beams in the target plane changes as a function of distance. If only part of the fibre area is illuminated, the larger the incoming angle to the fiber is, the larger is the delay of the fibre. In both optics the transmitter beams were focused to 12 m distance and the receiver optics were focused to infinity. In the double-axis optics the transmitter and receiver axes crossed each other at 6.5 m distance.

The best precision achieved, ~14 ps, is limited clearly by the single-shot precision value of the TDC, ~10 ps. So the TDC should be changed in order to reach 1 mm level single-shot precision with the present laser range finder realization. The APD used limits the bandwidth, and so increasing the bandwidth of the amplifiers probably would not improve the precision significantly, if the present APD were used. It seems that the APD

and TDC are the limiting components, because faster APDs and better TDCs are not commercially available.

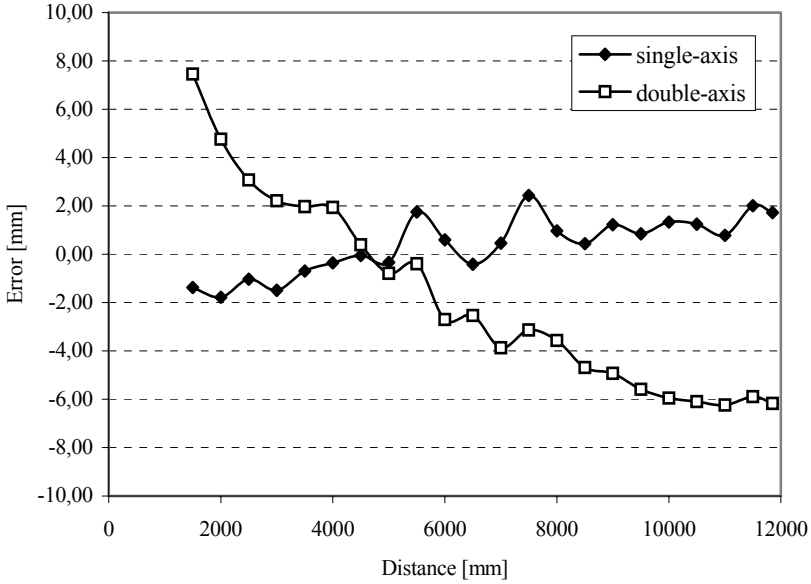

Fig. 25. The linearity of the laser radar measured with single and double-axis optics and 4 m long receiver fibres.

5 Summary

The idea of pulsed TOF laser rangefinding is to send a short laser pulse to the target and to measure the elapsed time between the sent and received pulses. The signal is received with a photodiode, amplified in the transimpedance amplifier and changed to logic state pulses in the timing discriminator. The elapsed time is measured with a time measuring unit. This technique has been used since 1960s for a number of applications, such as measuring the position, shape or speed of rather large objects, for example houses, caves, silos, aeroplanes, ships or trains. In these applications a signal bandwidth of ~100 MHz and pulse length of 5-10 ns have been suitable. In applications like fast 3D scanning, structure analysis using embedded fibre gratings or optical time tomography for paper or pulp analysis very fast and accurate distance measurement is needed. In order to reach high single-shot precision the noise should be low and the slew rate of the signal should be high, which can be attained by increasing the signal power or bandwidth. For distinguishing two targets in 3D measurement and in a fibre with fibre gratings not only high bandwidth but also short pulses are needed. Small walk error (measurement error due to variation of the received signal power) should also be small in many applications, such as 3D scanning. In this thesis the goal was to improve the performance of pulsed TOF laser range finders for old and new applications. In order to reach better single-shot precision and walk error, some parts of the TOF laser radar like the laser pulser, timing discriminator and optical attenuator were examined and developed. The most important factor in improving the single-shot precision is to increase the signal bandwidth of the laser range finder, and for this reason a high bandwidth (~1 GHz) laser range finder utilizing short (~100 ps) laser pulses was developed and tested.

The main components of the laser pulser are a semiconductor laser and an avalanche transistor, which is used as a current switch for the laser. Several transistor types were tested as an avalanche transistor and it was noticed that large differences exist in the maximum available current and also in the switching delay, which depends on the trigger voltage. The latter is important, when the avalanche transistors are parallelled. In the test the maximum peak current measured with a 1 Ω resistive load and transistors ZTX415 and 2N5192 varied in the range of 55 to 75 A, while the rise time of the pulse varied in the range of 2.6 to 3.7 ns. Increasing the amplitude and decreasing rise time of the current pulse are limited strongly by the lead inductances, which can be minimized by using

surface mount components. By decreasing the serial loop inductances even further a peak current of 130 A with a rise time of 2.6 ns was achieved with a surface mount transistor FMMT417. It was also noticed that the maximum optical peak power of the laser pulsed with a single avalanche transistor could be increased significantly, in this case 26%, by adding a parallel capacitor with the laser. The maximum current can also be increased, for example, by using several transistors connected as a Marx-bank type circuit, but the circuit becomes rather complex and often the reliability decreases due to nonsynchronous triggering of the transistors even though the trigger delays of the transistors are measured carefully to match with each other.

The origin of the walk error of the timing discriminator was examined. It was noticed that the walk error in the laser range finder is mainly due to the limited bandwidth of the comparator in the timing discriminator and the changing slew rate of the input pulse. The higher is the bandwidth of the comparator and the higher is the slew rate of the input pulse, the smaller is the propagation delay of the comparator. The offset voltage between the input nodes of the comparator is used for decreasing the walk error, but it cannot eliminate it totally. By using a very fast comparator, fast measurement pulses and avoiding crosstalk inside the comparator and in the printed circuit board it is possible to minimize the walk error. For example, by using a fast comparator, SPT9689, but relatively slow pulses, a rise time of 4.5 ns, a walk error of +/- 1 mm was achieved in an amplitude range of 1:10.

The operation of several timing discriminator types was analyzed and the timing precision achievable with 100 MHz and 1 GHz laser range finders was evaluated with calculations and PSPICE simulations. The simulations showed that both the leading-trailing-edge CFD and crossover timing discriminator provide equally good single-shot precision in practice and they both give a better precision than the leading edge discriminator.

A liquid crystal (LC) optical attenuator was proved to suit well for minimizing the input signal power variation in a TOF laser range finder. Two types of LC attenuators were tested, firstly a dark NCAP film, which was available in large sheets and secondly a round (diameter 1 inch) film, which was originally manufactured for an optical shutter. An attenuator module utilizing two dark LC films and two collimating lenses was installed between two multimode fibres in the input of the receiver. The maximum optical contrast of the optical power achieved was 1:26. A dynamic range of 1:57 was achieved with the round optical LC film, when attached between the receiver lens and the fibre. In all tests the wavelength was 903 nm. The walk error using the LC attenuators remained on the level of +/- 1 mm in all measurements. However, the drawbacks of LC attenuators are that an operating voltage of some tens of volts is needed and that the contrast decreases at low temperatures. Thus, electrical attenuators like the Gilbert cell are more practical, if the optical power is not too high for the photodiode, because optimally they provide as good a walk error as the LC attenuator.

Very short optical pulses were achieved with a semiconductor laser by utilizing an internal Q-switching phenomenon in a commercially available SH-laser type (LD-65). The FWHM and peak power of the optical laser pulses from the output of 1 m long multimode SI-fibre were 74 ps and 44 W, respectively, including all optical coupling losses and mode dispersion in the fibre. In order to reach the Q-switching mode the laser must be heated to a temperature of some tens of degrees Celsius above room temperature,

the actual temperature depending on the laser item. Also a very high slew rate of the current is needed for the laser. The current pulse for the Q-switched laser was realized by using a single avalanche transistor as a switch and by minimizing all inductances in the high current loop.

A high bandwidth prototype laser range finder was constructed using two ~2.5 GHz integrated ASIC receiver channels and commercially available silicon avalanche photodiodes (APDs). The internal Q-switching mode of the laser LD-65 was used in the laser pulser. The integrated receiver channel included a Gilbert cell attenuator, transimpedance and postamplifiers, as well as a timing discriminator based on differential crossover timing. The structure of the receiver channel was totally differential from the input to the output in order to minimize the influence of external and internal noise sources. The measured upper –3 dB corner frequency of the receiver channel including the photodiode was ~1 GHz, when the multiplication factor M = 200 was used in the APD. The total error of the laser range finder was less than +/- 2 mm and the single-shot precision was better than 34 ps (5 mm) in the distance range of 0.5 – 34.5 m, when measured to white printing paper. The single-shot precision varied in the range of 14 – 34 ps (2-5 mm) in the S/N-ratio range of 9.5 to 843. The measured single-shot precision agrees well with the simulated results for the crossover timing.

The performance achieved with single-axis and double-axis optics was compared in the 1 GHz laser range finder. Mode dispersion in step-index multimode fibres was noticed to cause quite large measurement errors, when double-axis optics and 4 m long receiver fibre were used. The reason is that in the double-axis optics the areas in the target seen by the transmitter and receiver overlap with each other only partially in all distances except in one distance, where the optical axes are aligned to cross each other, and mode dispersion in the multimode fibre causes extra delay. When the single-axis optics and a 4 m long fiber was used, no measurement error was noticed originating from mode dispersion. With 1 and 1.5 m long fibres no significant difference was found between the measurement results achieved with single-axis and double-axis optics. The single-axis optics also provides two other benefits as compared to double-axis optics: the variation of the received optical power is smaller and the usable measurement range is wider, especially at short distances. The disadvantage of the single-axis optics is power loss in the semi-reflecting mirror, which makes the double-axis optics a better choice with long distances and / or poorly reflecting targets.

As a conclusion, a 1 GHz laser range finder combined with a silicon avalanche photodiode seems to give a clearly better single-shot precision compared to pulsed laser range finders published earlier and which typically are using laser pulses with lengths in the range of 5-10 ns. The best achieved single-shot precision of ~2 mm (with S/N-ratio of 100) is good enough to have only a single-shot used as a distance measurement result, for example, in fast scanning 3D laser range finders, thus enabling fast creation of target images. The best single-shot precision achieved earlier with 100-130 MHz laser range finders was 6-10 mm with S/N-ratio of 100. The optical power achieved using internal Q-switching mode in a commercially available SH-laser is at least on the same level or higher (50-100 W) than the nominal peak powers achieved with DH-lasers operating in a normal laser operation mode, in which gain switching oscillation has decayed. In order to achieve even better single-shot precision with the present high bandwidth laser range finder, an even higher laser power should be used and the optic loss should be minimized.

The APD limits the bandwidth of the receiver and the TDC limits the best achievable single-shot resolution, so these are the components that should also be improved, if even higher bandwidths were to be used.

References

Adams93 Adams, M.D. (1993), 1993. Proceedings of 1993 IEEE International Conference on Robotics and Automation, Page(s): 8 -13 vol.2.

Ahola86: Ahola R., Myllylä R. (1984) A Time-of-Flight Laser Sensor for To and Fro Motions, International Conference on Industrial Electronics, Control and Instrumentation, Tokyo, Japan, Oct. 1984, pp. 812-818.

Aikio99 Aikio J., Karioja P. (1999) Wavelength Tuning of a Laser Diode by using a Micromechanical Fabry-Perot Interferometer, IEEE Photonics Technology Letters, Vol. 11, No. 10, pp. 1220 – 1222.

Ammon70 Ammon G., Russell S. (1970) A Laser Tracking and Ranging System. Applied Optics, Vol. 9., No. 10., pp. 2256-2259.

Anandarajah2000 Anandarajah P., Kaszubowska A., Barry L.P. (2000) High Frequency Pulse Generation Using a Gain-Switched Commercial Semiconductor Laser with Strong External Injection. High Frequency Postgraduate Student Colloquim 2000, pp. 121-126.

Anteryon2002 Data sheet (2002): LCP 250, fast scattering liquid crystal polymer shutter, www.anteryon.com

Araki94 Araka T., Yokoyama S., Suzuki N. (1994) Simple optical distance meter using an intermode-beat modulation of a He-Ne laser and an electrical-heterodyne technique. Review of Scientific Instruments, Vol. 65(6), pp. 1883-1888.

Araki96 Optical Distance Meter Using a Pulsed Laser Diode and Fast Avalanche Photo Diode for Measurements of Molten Steel Levels (1996) Jouranl of Dynamic Systems, Measurement, and Control, Vol. 118, pp. 800-803.

Arbel80 Arie F. Arbel, "Analog Signal Processing and Instrumentation", pp.172-176, Cambridge University Press (1980).

Arumov93 Arumov G.P., Altshuler G.B., Heikkinen V., Khramov V.J., Kostamovaara J., Lehto M, Myllylä R., Määttä K., Nekhaenko V.A., Turin A.V., Verkasalo R. (1993) A laser range finder and reflectivity meter for the MARS-96 international project.

Baker90 Baker R.J., Pocha M.D. (1990) Nanosecond switching using power MOSFETs. Review of Scientific Instruments 61(8), August 1990, pp. 2211-2213.

Baker91 Baker R.J. (1991) High voltage pulse generation using current mode second breakdown on a bipolar junction transistor. Review of Scientific Instruments 62 (4), April 1991, pp. 1031-1036.

Barrow93 Barrow, D.A.; Marsh, J.H.; Portnoi, E.L (1993) Field distribution measurements in Q-switched semiconductor lasers . IEE Colloquium on Measurements on Optical Devices, , 19 Nov 1992, pp. 8/1 -8/4.

Bender67 Bender P.L. (1967) Laser Measurements of Long Distances. Proceedings of the IEEE, VOl. 55(6), pp. 1039-1045.

Benzel85 Benzel D.M., Pocha M.D. (1985) 1000V, 300-ps pulse-generation circuit using silicon avalanche devices. Review of Scientific Instruments, 56(7), July 1985, pp. 1456-1458.

Bertolini68 G. Bertolini, "Pulse shape and time resolution", In: Bertolini, G. & Coche, A. (eds.), Semiconductor detectors, pp. 243-276, North-Holland Publishing Co., Amsterdam, 1968.

Besl88 Besl P.J. (1988) Active Optical Range Imaging Sensors. Machine Vision and Applications, Vol. 1., (1988) pp. 127-152.

Bhattacharya97 Bhattacharya P. (1997) Semiconductor Optoelectronic Devices, Prentice-Hall Inc., 613 pages.

Bien81 Bien F., Camac M., Caulfield H.J., Ezekiel S. (1981) Absolute distance measurements by variable wavelength interferometry. Applied Optics, Vol. 20(3), pp.400-403.

Binkley88 David M. Binkley, Michael E. Casey, "Performance of fast monolithic ECL comparators in constant-fraction discriminators and other timing circuits", IEEE Transactions on Nuclear Science, Vol. 35, No. 1, pp.226-230, February 1988.

Bluestone A., Zhong S., Andronica R., Soller I., Ramirez N.,

Boehmke98 Boehmke S.K., Bares J., Mutschler E., Lay N.K. (1998) A High Speed 3D Radar Scanner for Automation. Proceedings of the 1998 IEEE International Conference on Robotics & Automation, pp. 2777-2782.

Boers75 Boers P.M., Vlaardingerbroek M.T. (1975) Dynamic Behaviour of Semiconductor Lasers, Electronics Letters, Vol. 11, No. 10, pp. 206-208.

Bosch95 Bosch T., Lecure M. (1995) Selected Papers on Laser Distance Measurements, SPIE Milestone Series, vol. 115, pp. xi – xiii.

Bosch96 Bosch T., Servagent N., Chellali R. (1996) A Scanning Range Finder using the Self-Mixing Effect inside a Laser Diode for 3-D Vision, IEEE Technology Conference on Instrumentation and Measurement, Jne 1996, pp. 226-231.

Bostanjoglo87 Bostanjoglo O., Tornow W. (1987) Increasing the lifetime of avalanche transistors by cryogenic cooling. Semiconductor Science and Technology No. 2, 1987, pp. 175-176.

Bowers89 Bowers J.E., Morton P.A., Mar A, Corzine A.W. (1989) IEEE Journal of Quantum Electronics, Vol. 25, No. ., pp. 1426-1439.

Braun97 Braun B., Kärtner F.X., Zhang G., Moser M., Keller U. (1997) 56-ps passively Q-switched diode-pumped microchip laser. Optics Letters. Vol. 22, No. 6, pp. 381-383.

Bufton89 Bufton J.L. (1989) Laser Altimetry Measurements from Aircraft and Spacecraft. Proceedings of the IEEE, Vo. 77, No. 3, March 1989.

Byren93 Byren R.W. (1993) Laser Rangefinders. Infrared & Electro-Optical Systems Handbook, Vol. 6, Chapter 2.

Carmer96 Carmer D.C., Peterson L.M. (1996) Laser Radar in Robotics. Proceedings of the IEEE, Vol. 84, No. 2, Feb. 1996, pp. 299-320.

Carmer96 Carmer D.C., Peterson L.M. (1996) Laser Radar in Robotics. Proceedings of the IEEE, Vol. 84, No. 2, Feb. 1996, pp. 299-320.

Caverly87Caverly R..H., Hiller G. (1987) Distortion in p-I-n Diode Control Circuits, IEEE Transactions on Microwave Theory and Technology, Vol. MTT-35, No. 5, May 1987, pp. 11-20.

Chang90 Chang G.K., Hong W.P., Gimlett J.L., Bhat, R., Nguen C.K., Sasaki, G., Young J.C. (1990) A 3 GHz Transimpedance OEIC Receiver for 1.3 – 1.55 um Fibre-Optic Systems. IEEE Photonics Tecnology Letters, Vo. 2., No. 3, March 1990, pp. 197-199.

Chang92 Chang G.-K., Liu T.P., Gimlett J.L., Shorokmann H., Iqbal M.Z., Hayes J.R., Wang K.C. (1992) A Direct-Current Coupled, All-Differential Optical Receiver for High-Bit-Rate Sonet Systems. IEEE Photonics Technology Letters, Vol. 4., No. 4., April 1992, pp. 384-386.

Cheng88 Cheng C-L, Chang R.P.H., Tell B., Parker S. M. Z., Ota Y., Vella-Coleiro G.P., Miller R.C., Zilko J. L. , Kasper B. L., Brown-Goebeler K. F., Mattera V. D. (1988) Monolithically Integrated Receiver Front End: $In_{0.53}Ga_{0.47}As$ p-i-n Amplifier. IEEE Transactions on Electron devices, Vol. 35, No. 9, Sept. 1988, pp. 1439-1444.

Cheo89 Cheo, P.K., editor (1989) Handbook of Solid-State Lasers, Marcel Dekker, Inc., New York 1989, p. 3.

Czylwik89 Czylwik A. (1989) A Theoretical Analysis of the Transient Intensity Noise of Semiconductor Lasers. IEEE Journal of Quantum Electronics. Vol. 25, No. 1, pp. 49-46.

Czylwik90 Czylwik A., Eberle W. (1990) Transient Intensity Noise of Semiconductor Lasers: Experiments and Comparison with Theory. IEEE Journal of Quantum Electronics, Vol. 26., No. 2, pp. 225 – 230.

Davidson88 Davidson F.M. (1988) Gaussian Approximation Versus Nearly Exact Performance Analysis of Optical Communication Systems with PPM Signaling and APD Receivers. IEEE Transactions on Communications, Vo. 36, No. 11, pp. 1185-1192.

Davidson88 Davidson F.M. Xiaoli S. (1988) Gaussian Approximation Versus Nearly Exact Performance Analysis of Optical Communication Systems with PPM Signaling and APD Receivers. IEEE Transaction on Communications, Vol. 36, No. 11, pp. 1185-1192.

Delfyett92 Delfyett P.J., Florez L.T., Stoffel N., Gmitter T., Andreadakis C., Silberg Y. Heritage J.P. (1992) High-Power Ultrafast Laser Diodes. IEEE Journal of Quantum Electronics, Vol. 28, No. 10, pp. 2203-2219.

Dixon97 Dixon G.J. (1997) Time-resolved spectroscopy defines biological molecules. Laser Focus World, Oct. 1997, pp. 115-122.

Dragoman99 Dragoman D., Dragoman M. (1999) Advanced Optoelectronic Devices, Springer-Verlag, 424 p.

Dudek2000 Dudek P., Szczepanski S., Hatfield J.V. (2000) A High-Resolution CMOS Time-to-Digital Converter Utilizing a Vernier Delay Line. IEEE Transactions on Solid-State Circuits, Vol. 35, pp. 240-247.

Duncan93 Duncan B.D., Mark M. B., McManamon P.F. (1993) Performance Analysis of a Hetrodyne Lidar Sytmen incorporating a Multimode Optical Waveguide Receiver. Aerospace and Electronics Conference vol.2 , . NAECON 1993., Proceedings of the IEEE 1993 National , pp. 1133 –1141.

EG&G95 (1995) Short Form Catalog, Emitters and Detectors, EG&G Optoelectronics Co., Canada (http://opto.perkinelmer.com/).

Fisher92 Fisher P. (1992) Improving on police radar. IEEE Spectrum July 1992, pp. 38-43.

Focia96 Focia R.J., Schamiloglu E., Fleddermann C.B. (1996) Simple techniques for the generation of high peak power pulses with nanosecond rise times. Review of Scientic Instruments 67 (7), July 1996, 2626-2629.

Focia97 Focia R.J., Schamiloglu E., Fleddermann C.B., Agee F.J., Gaudet J. (1997) Silicon Diodes in Avalanche Pulse-Sharpening Applications. IEEE Transactions on Plasma Science, Vol. 25, No. 2., April 1997.

Forrester81 Forrester P.A., Hulme J.A. (1981) Laser Rangefiders. Optical and Quantum Electronics, Vol. 13, pp. 259-293.

Garside83 Garside B.K., Park R.E. (1983) Ultrashort pulses from semiconductor diode lasers. Optics and Laser Technology, April 1983, pp. 91-94.

Gedcke68 Gedcke D.A., McDonald W.J. (1968), Design of the constant fraction of pulse height trigger for optimum time resolution , Nuclear Instruments and Methods **5**8, 253, 1968, pp. 82–84.

Gilbert68 Gilbert B. (1968) A precise four-quadrant multiplier with subnanosecond response. IEEE Journal of

Goldstein67 Goldstein B.S., Dalrymple G.F. (1967) Gallium Arsenide Injection Laer Radar. Proceedings of the IEEE, Vol. 55 (2), pp. 181-188.

Goyal95 Goyal R. (1995) High-Frequency Analog Integrated Circuit Design. John Wiley & Sons, Inc.

Gramsch94 Gramsch E., Szalowski M., Zhang S., Madden M. (1994) Fast, High Density Avalanche Photodiode Array. IEEE Transactions on Nuclear Science, Vol. 41, No. 4, pp. 762-766.

Grekhov83 Grekhov I.V., Efanov V.M., Kardo-Sysoev A.F., Shenderei S.V. (1979) Formation of nanosecond high-voltage drops across semiconductor diodes with voltage recovery by a drift mechanism. So. Tech. Phys. Lett. 9(4) April 1983, pp. 188-189.

Grimes92 Grimes M.D., Owen T.E. (1992) A High-Repetition rate, Solid-State, Marx-Bank Pulse Generator for Geophysical Instrumentation. Twentieth Power Modulator Symposium, June 23-25 1992, pp. 181-184.

Guyer82 Guyer R.C., Stenton Wm C. (1982) Optical alignment retention in the AN/GVS-5 hand held laser rangefinder. SPIE Vo. 330 Optical Systems Engineering II, pp. 117-121.

Halmos93 Halmos M. J., Wang J.H.S. (1993) Laser radar systems and applications. In: Optical Tecnologies for Aerospace Sensing. Pearson, J. E. (ed.) Bellingham, Washington, SPIE Vol. CR47, pp. 308-338.

Hansen69 Hansen J.P. (1969) Profiling with a GaAs Laser Diode Radar. Proceedings of the IEEE, May 1969, pp. 854-855.

Hentschel89 Hentschel C. (1989) Fibre Optics Handbook, Hewlett Packard Company, 3. Edition, pp. 85-87.

Herden73 Herden W., Metz S (1973) A Fast Current Drive Circuit for Injection Lasers. IEEE Journal of Solid-State Circuits,June 1973, pp. 247-248.

Honkanen99 Honkanen K., Hakkarainen N., Määttä K., Kilpelä A., Kuivalainen P. (1999) High-Speed Metal-Semiconductor-Metal Photodetectors Fabricated on SOI-Substrates. Physica Scripta, Vol. T79, pp. 127-130.

Hovanessian88 Hovanessian S.A. (1988) Introduction to Sensor Systems. Artech House, p.2.

HP97 Hewlett Packard (1997): Application Note 200-3, Fundamentals of Time Interval Measurements

Huber99 Huber A., Huber D., Morf T., Jäckel H., Bergamashi C., Hurm V., Ludwig M., Schlechtweg M. (1999) Monolithic high transimpedance gain (3.3 kΩ), 40 Gbit/s InP-HBT photoreceiver with differential outputs, Electronics Letters Vol. 35, No. 11, pp. 897-898.

Hulme81 Hulme K.F., Collins B.S., Constant G.D., Pinson J.T. (1981) A CO2 laser rangefinder using heterodyne detection and chirp pulse compression. Optical and Quantum Electronics, Vol. 13, pp. 35-45.

IEEE96 Radatz J., chair (1996) The IEEE standard dictionary of electrical and electronics terms / Standards Coordinationg Committee 10, terms and definitions.

Isomet2001 Isomet Corporation (2001) Modulators, datasheet, http://www.isomet.com/

Jang93 Jang S.-L., Wu J.-Y. 81993) Low-frequency current and intensity noise in AlGaAs Laser Diodes. Solid-State Electronics., Vol. 36, No.2, pp. 189-196.

Jarvis83a Jarvis R.A. (1983) A Perspective on Range Finding Techniques for Computer Vision. IEEE Transactions on Pattern Analysis and Machine Intelligence, Vol. PAMI-5(2), March 1983, pp. 122-139.

Jarvis83b Jarvis R.A. (1983) A Laser time-of-Flight Range Scanner for Robotic Vision. IEEE Transactions on Pattern Analysis and Machinen Intelligence, Vol. PAMI-5, No. 5, Sept. 1983, pp. 505-512.

Johns97 Johns, D.A., Martin K. (1997) Analog Integrated Circuit Design. John Wiley & Sons, Inc.

Jungerman90 Jungerman R.L., Johnsen C., McQuate D.J., Salomaa K., Zurakowski M.P., Bray R.C., Conrad G., Cropper D. Hernday P. (1990) High-Speed Optical Modulator for Application in Instrumentation. Journal of Lightwave Technology, Vol. 8, No. 9, pp. 1363-1370.

Kaisto83 Kaisto I., Kostamovaara J., Manninen M., Myllylä R. (1983) Optical range finder for 1.5-10 m distances. Applied Optics, Vol. 22(20), pp. 3528-3264.

Kaisto93 Kaisto I., Kostamovaara J., Manninen M., Myllylä R. (1993), Laser radar based measuring systems for large scale assembly applications, SPIE Proceedings Vol. 2088 Laser Dimensional Metrology: Recent Advances for Industrial Application, pp. 121-131.

Kardo-Sysoev95 Kardo-Sysoev A.F., Efanov V.M., Chasnikov I.G. (1995) Fast power switches from picosecond to nanosecond time scale and their application to pulsed power. Pulsed Power Conference, 1995. Digest of Technical Papers, Vol. 1, pp. 342-347.

Karppinen92 Karppinen A., Kopola H., Myllylä R. (1992) Fibre Optic Attenuator, Journal of Electronic Imaging, Vol. 1., pp. 104-110.

Karppinen95 Karppinen, A., Kilpelä, A., Karras, M., Tornberg, J., Myllylä, R.. Papermaking furnish properties estimated by time-resolved spectroscopy. Journal of Pulp and Paper Science., vol. 21 (1995) 5, pp. 151- 154.

Kawashima95 Kawashima S., Watanabe K., Kobayashi K. (1995) Proceedings of the Intelligent Vehicles '95 Symposium, pp. 299-303.

Keller96 Keller U., Weingarten K.J., Kärtner F.X., Kopf D., Braun B., Jung I.D., Fluck R., Hönninger C., Matuschek N., der Au J.A. (1996) Semiconductor Saturable Absorber Mirrors

(SESAM's) for Femtosecond to Nanosecond Pulse Generation in Solid-State Lasers, IEEE Journal of Quantum Electronics, vol. 2., No. 3, pp. 435-453.

Kester90 Kester W. (1990) High Speed Design Seminar, Analog Devices Inc.

Kilpelä 85 Kilpelä A." ", Diploma Thesis, University of Oulu, 1985.

Kilpeläa89a Kilpelä, A., Ahola, R., Myllylä, R. (1989)A TOF laser range finder for a 3D vision system, URSI radiotieteen päivät, Tampere, Finland.

Kilpeläa89b Kilpelä A., Ahola R., Kostamovaara J., Myllylä R. (1989) An Avalanche VMOS Driver for pulsing Semiconductor Laser Diodes, Proceedings of the International Conference on Lasers '89, pp. 1010-1015.

Kilpelä90 Kilpelä A. Laseretäisyysmittari pyyhkäisevään 3D-anturiin (1990), Licenciate Thesis, Univ. of Oulu, 81 p.

Kim2001 Kim H. H., Chandrasekhar S. Burrus A. Jr. Bauman J. (2001) A Si BiCMOS Transimpedanse Amplifier for 10-Gb/s SONET Receiver. IEEE Journal of Solid-State Circuits, Vol. 36, No. 5, pp. 769-776.

Klepsvik94 Klepsvik, J.O., Bjarnar, M., Brosstad, P.O., Braend, D.A., Westrum, H. (1994) Proceedings of Oceans Engineering for Today's Technology and Tomorrow's Preservation.Vol. 2 , pp. II/700 -II/705.

Koechner68 Koechner W. (1968) Optical Ranging System Employing a High power Injection Laser Diode. IEEE Transactions on Aerospace and Electronic Systems, Vol. AES-4(1), pp. 81-91.

Kompa84 Kompa G. Optical short-range radar for level control measurement (1996) IEEE Procedings, Vol. 131, No. 3., pp. 159-164

Koskinen89 Koskinen M, Ahola R, Kostamovaara J & Myllylä R (1989) Automatic gain control electronics for fast pulsed time-of-flight laser rangefinding. Proc. ISA, ISA Calgary'89 Symposium, Galgary, Canada: 295-303.

Koskinen92 Koskinen M., Kostamovaara J., Myllylä R. (1992) Comparison of the continuous and pulsed time-of-flight laser rangefinding techniques, Optics, Illumination and Image Sensing for Machinen Vision VI, SPIE Vol. 1614, pp. 296-305.

Koskinen92 Koskinen M., Kostamovaara J., Myllylä R. (1992) Comparison of the continuous wave and pulsed time-of-flight laser rangefinding techniques. Optics, Illumination and Image Sensing for Machine Vision VI, Proc. SPIE Vol. 1614, pp. 296-305.

Kostamovaara86 Kostamovaara J. (1986) Techniques and Devices for Positron Lifetime Measurement and Time-of-Flight Laser Rangefinding. Doctoral Thesis, University of Oulu, 69 pages.

Kostamovaara86 Kostamovaara, J., Myllylä, R. (1986) Time-to-digital converter with an analog interpolation circuit. Review of Scientific Instruments 57(11), November 1986, pp. 2880-2885.

Kostamovaara90 Kostamovaara J., Määttä K., Myllylä R. (1990) A laser radar for measuring of liquid level heights. SPIE Vol. 1230 International Conference on Optoelectronic Science and Engineering '90 / 297

Koumans96 Koumans G.M.P., van Roijen R. (1996) Theory for Passive Mode-Locking in Semiconductor Laser Structures Including the Effects of Self-Phase Modulation, Dispersion and Pulse Collisions. IEEE Journal of Quantum Electronics, Vol. 32, No. 3., March 1996, pp. 478-492.

Krishnamurthy2000 Krishnamurthy V., Hargis M.C., Melloch M.R. (2000) A 4 –GHz Large-Area (160000μm2) MSM-PD pn ITG-GaAs. IEEE Photonics Technology Letters, Vol. 12, No. 1, pp. 71-73.

Krotkov94 Krotkov E., Hoffman R. (1994) Terrain Mapping for a Walking Planetary Rover. IEEE Transactions on Robotics and Automation, Vol. 10., No. 6, pp. 728-739.

Lamela96 Lamela H., Garcia E. (1996) A Low Power Laser Rangefinder for autonomous Robot. Proceedings of the 22nd International Conference on Applications Industrial Electronics, Control, and Instrumentation, Vol. 1 ,pp. 161 –167.

Lange89 Lange M., Detlefsen J. (1988) 94 GHz 3D-imaging radar for sensorbased locomotion. .Microwave Symposium Digest, 1989., IEEE MTT-S International 1989 vol.3, pp.1091 -1094

Laser2000 Laser Diode Incorporated (2000) High Power Pulsed Laser Diodes, data sheet, (http://www.laserdiode.com/).

Lasermetrics99 Lasermetrics / Fast Pulse Technology Inc., (1999) Datasheet: 1040 Series Pockels cell electro-optic light modulators, 27. Sept. 1999, pp. 1-4, http://www.lasermetrics.com/

Leskovar76 Leskovar B., Lo C.C. (1976) Photon counting system for subnanosecond fluorescence lifetime measurements, Review of Scientific Instruments, Vol. 47, No. 9, pp. 1113 – 1121.

Lewis77 Lewis R.A., Johnston A.R. (1977) A scanning laser rangefinder for a robotic vehicle. 5th International Conference on Artificial Intelligence, pp. 762-768.

Liou90 Liou J.J., Yuan J.S. (1990) An Avalanche Mulplication Model for Bipolar Transistors. Solid-State Electronics, Vol. 33, No. 1, pp. 35-38.

Liu93 M.Y. Liu, S.Y. Chou, S. Alexandrou, C.C. Wang (1993) 110 GHz Si MSM Photodetectors, IEEE Transactions on Electron Devices, Vol. 40, pp. 2145-2146.

Liu97 Liu H., Hornia O., Chen Y.C., Zhou S.H. (1997) Single –Frequency Q-Switched Cr-Nd:YAG Laser Operating at 946-nm Wavelength. IEEE Journal of Selected Topics in Quantum Electronics, Vol. 3., No. 1., Februaru 1997.

Loinaz95 Loinaz M. J., Wooley B. A. (1995) A CMOS Multichannel IC for Pulse Timing Measurements with 1 mV Sensitivity. IEEE Journal of Solid State Circuits, Vol. 30, No. 12, Dec. 1995.

Lyöri97 Lyöri V., Määttä K., Nissilä S. Kopola H., Englund M. (1997) A high precicion fresnel-OTDR for distribured fibre-optic sensor network applications. 12th Intrnational Conference on Optical Fibre Sensors, Oct 28-31, 1997, USA, pp. 520-523.

Määttä90 Määttä K, Kostamovaara J., Myllylä R.On the measurement of hot surfaces by pulsed time -of-Flight laser radar techniques. SPIE Proc. Int. Congr. Optical Science and Engineering, The Hague, The Netherlands, Mar. 12. – 15. 1990, Vol. 1265, pp. 179-191.

Määttä93 Määttä K, Kostamovaara J., Myllylä R. (1993) Profiling of hot surfaces by pulsed time-of-flight laser range finder techniques. Applied Optics, Vol. 32, No. 27, 20. Sept. 1993, pp. 5334-5347.

Määttä95 Määttä K. (1995) Pulsed time-of-flight laser rangefinding techniques and devices for hot surface profiling and other industrial applications. Doctoral Thesis, Acta Univ Oul. C81, 75 p.

Määttä98 Määttä K., Kostamovaara J. (1998) A High-Precision Time-to-Digital Converter for Pulsed Time-of-Flight Laser Radar Applications. IEEE Transactions on Instrumentation and Measurement, Vol. 47, No. 2., pp. 521-536.

MacDonald99 MacDonald R.P., Tarr N.G., Syrett B.A., Boothroyd S.A., Chrostowski J. (1999) MSM Phtodetector Fabricated on Polycrystalline Silicon. IEEE Photonics Tecnology Letters, Vol. 11, No. 1, pp. 108-110.

Mäkynen94 Mäkynen A.J., Kostamovaara J.T., Myllylä R.A. (1994) Tracking Laser Radar for 3-D Shape Measurements of Large Industrial Objects Based on Time-of-Flight Laser Rangefinding and Position-Sensitive Detection Techniques. IEEE Transactions on Instrumentation and Measurement, Vol. 43, No. 1, pp. 40-49.

Mäkynen94 Makynen, A.J.; Kostamovaara, J.T.; Myllyla, R.A. (1994) Tracking laser radar for 3-D shape measurements of large industrial objects based on time-of-flight laser rangefinding and position-sensitive detection techniques. IEEE Transactions on Instrumentation and Measurement, Vol. 43, Issue 1, Feb. 1994, pp. 40 – 49.

Mamon78 Mamon G., Youmans D.G., Sztankay Z.G., Mongan C.E. Pulsed GaAs laser terrain profiler. Applied Oprics, Vol. 17, No.6., pp. 868-877.

Manninen92 Manninen M., Jaatinen J. (1992), Productive method and System to Control Dimensional Uncertainties at Final Assembly Stages in Ship Production, Journal of Ship Production, Vol. 8., No. 4, Nov. 1992, pp. 244-249.

Mäntyniemi2002 Mäntyniemi A., Rahkonen T., Kostamovaara J. (2002) An Integrated 9-channel Time Digitizer with 30 ps Resolution, Proceedings of ISCC 2002

Melcer91 Melcer, L.G., Karin, J.R., Nagarajan R., Bowers J.E. (1991) Picosecond Dynamics of Optical Gain Switching in Vertical Cavity Surface Emitting Lasers, IEEE Journal of Quantum Electronics, Vol. 27. No. 6, pp. 1417-1425.

Melles2002 http://www.mellesgriot.com/

Meyer86 Meyer R.G., Blauschild R.A. (1986) A Wide-Band low-Noise Monolithic Transimpedance Amplifier. IEEE Journal of Solid-State Circuits, Vol. SC-21, No. 4, pp. 530-533.

Meyer94 Mayer, R.G., Mack W.D. (1994) A Wideband Low-Noise Variable-Gain BiCMOS Transimpedance Amplifier. IEEE Journal of Solid-State Circuits, Vol. 29, No. 6, pp. 701-706.

Mizushima67 Mizushima Y., Okamoto Y. (1967) Prperties of Avalanche Injection and Its Applications to Fast Pulse Generation and Switching. IEEE Transactions on Electron Devices, Vol. ED-14, No. 3, March 1967, pp. 146-157.

Morikuni92 Morikuni J.J., Kang, S.-M. (1992) An Analysis of Inductive Peaking in Photoreceiver Design, Journal of Lightwave Technology, Vol. 10, No. 10, pp. 1426-1437.

Moring89 Moring, I., Heikkinen, T., Myllylä, R., Kilpelä ,A. (1989) Acquisition of three-dimensional image data by a scanning laser range finder. Optical Engineering, Vol. 28(8), pp. 897 – 902.

Morkel92 Morkel P.R., Jedrzejewski E.R., Taylor, E.R., Payne D.N. (1992) Short-Pulse, High-Power Q-Switched Fibre Laser. IEEE Photonics Technology Letters, Vol. 4, No. 6, 1992.

Muoi84 Muoi T. V. (1984) Jouranl of Lightwave Technology, Vol. LT-2, No.3, June 1984, pp. 243-267.

Myllylä78: Myllylä R. (1978), A Modern Positron Lifetime Spectrometer, Nuclear Instruments and Methods 148, pp. 267-271.

Nampoothiri98 Nampoothiri A.V.V., Kundu T., Singh B.P. (1998) Single pulse selection from a cw mode-locked laser. Review of Scientific Instruments, Vol. 69, No. 3, pp. 1240-1242.

Neuhäuser95 Meuhäuser M., Möller M., Rein H.-M., Wernz H. (1995) Low-Noise, High-Transimpedance Si-Bipolar AGC Amplifier for 10 Gb/s Optical-Fibre Links. IEEE Photonics Technology Letters, Vol. 7., No.5, pp. 549-551.

Neuhold99 Neuhold S.M., Benedickter H.R., Schmatz M.L. (1999)A 300 V mercury switch pulse generator with 70 psec risetime for investigation of UHF PD signal transmission in GIS , 1999. Eleventh International Symposium on High Voltage Engineering (Conf. Publ. No. 467) Volume: 5 , 1999 , Page(s): 78 -81 vol.5

Newport2003 http://www.newport.com/

Nissilä95 Nissilä S. (1995) On the use of optical fibres in industrial applications, Doctoral Thesis, Univ. of Oulu, 73 pages.

Nunes77 Nunes F.D., Batel N.B., Ripper J.E. (1977) A Theory on Long Time Delays and Internal Q Switching in GaAs Junction Lasers. IEEE Journal of Quantum Electronics, Vol. QE-13, No. 8., pp. 675-681.

Nutt68 Nutt R. (1968) Digital Time Intervalometer. Review of Scientific Instruments, vol. 39, no. 9, pp.1342-1345.

Ohya94 Ohya A., Shoji E.,Yuta S. Intelligent Robots and Systems '94. 'Advanced Robotic Systems and the Real World', IROS '94. Proceedings of the IEEE/RSJ/GI International Conference on,Vol. 3, pp.1759 –1763.

Optinav2002 http://www.optinav.com/, Accuracy of Range Determination from Blur Circle Diameter (product broschure attachment).

Ota92 Ota Y., Swartz R.G., Archer V.D. (1992) DC-1 Gb/s Burst-Mode Compatible Receiver for Optical Bus Applications. Journal of Lightwave Technology, Vol. 10., No. 2, Feb. 1992, pp. 244-248.

Palojärvi97 Palojärvi P., Ruotsalainen T., Kostamovaara J. (1997) A Variable Gain Transimpedance Amplifier with a Timing Discriminator for a Time-of-Flight Laser Radar. Proceedings of ESSCIRC'97 Conference, Southampton, UK, Seotember 16-18 1997, pp. 384-387.

Palojärvi2001 Palojärvi P., Mäntyniemi A, Kostamovaara J. (2001) A Multi-Channel Pulsed Time-of-Flight Laser Radar Chip, Proceedings of Odimap III3rd TopicalMeeting on Optoelectronucs Distance Measurement and Applications, September 20-22 2001, Pavia, Italy, pp. 112-117.

Palojärvi2002 Palojärvi P., Määttä K., Kostamovaara J. (2002) Pulsed Time-of-Flight Laser Radar Module With Millimeter-Level Accuracy Using Full Custom Receiver and TDC ASICs, IEEE Transactions on Instrumentation and Measurement 51(5), pp. 1102-1108.

Park98 Park K., Park J.(1998) 20 ps Resolution Time-toDigital Converter for Digital Storage Oscilloscopes, Nuclear Science Symposium, 1998, Volume 2, pp. 876 –881.

Payne73 Payne J.M. (1973) An Optical Distance Measuring Instrument. Review of Scientific Instruments, Vol. 44(3), pp. 304-306.

Payne92 Payne J.M., Parker D., Bradley R.F: (1992) Rangefinder with multiple range capability. Review of Scientific Instruments, Vol. 63(6), pp. 3311-3316.

Pennala98 Pennala R., Ruotsalainen T., Palojärvi P., Kostamovaara J. (1998) A 4 GHz differential transimpedance amplifier channel for a pulsed time-of-flight laser radar, Proceedings of IEEE International Symposium on Circuits and Systems, Monterey, CA, 31 May-3 June 1998, pp. 1:229-232.

Peremans93 Peremans H., Audenaert K., Van Campenhout J.M. (1993) A High-Resolution Sensor Based on Tri-aural Perception. IEEE Transactions on Robotics and Automation, Vol. 9. , No. 1, February 1993.

Plucinski99 Plucinski P., Männistö R., Myllylä R.A., Tornberg J. (1999) Paper parameter estimation using time-resolved spectroscopy. Third International Symposium on Optiacs in Engineering Jan. 19-21, 1999, Kajaani, Finland.

Poon72 Poon H.C., Meckwood J.C. (1972) Modeling of Avalanche Effect in Integral Charge Control Model. IEEE Transactions on Electron Devices, Vol. ED-19, No. 1., Jan. 1972, pp. 90-97.

Portnoi97 Portnoi E.L., Venus G.B., Khazan A.A., Gadijiev I.M., Shmacev A. Yu., Frahm J., Kuhl D. (1997) Superhigh-Power Picosecond Optical Pulses from Q-Switched Diode Laser. IEEE Journal of Selected Topics in Quantum Electronics, Vol. 3., No. 2., April 1997, pp. 256-260.

Poultney77 Poultney S.K. (1977) Single photon detection and timing in the lunar laser ranging experiment. IEEE Transactions on Nuclear Science, Vol. 19, pp. 12-17.

Querzola79 Querzola B. (1979) Hign accuracy distance measurement by two-wavelength pulsed laser suorces. Applied Optics, Vol. 18(17), pp. 3035-3047.

Rahkonen93 Rahkonen T., Kostamovaara J. (1993) The use of stabilized CMOS deley line for the digitization of short time intervals, IEEE Journal of Solid State Circuits, vol. 28, pp. 887-894.

Räisänen-Ruotsalainen97 Räisänen-Ruotsalainen, E., Rahkonen, T., Kostamovaara, J. (1997) A Time Digitizer with Interpolation Based on Time-to-Voltage Conversion. Proceedings of the Midwest Symposium on Circuits and Systems, Sacramento, CA, USA, August 3-6 1997, Vol. 1, pp. 197-200.

Ramar2001 Ramar Corporation, Series 500 20 GHz Intensity Modulator, datalehti, http://www.ramar.com/

Rankinen91 Rankinen, R.; Maatta, K.; Kostamovaara, J. (1991) Time-to-digital conversion with 10 ps single-shot resolution. Proceedings of 6th Mediterranean Electrotechnical Conference vol.1, pp. 319 – 322, 22-24 May 1991.

RCA88 RCA ElectroOptics, Inc. (1988) Silicon Avalanche Photodiodes, Data Sheet.

Rehak83 Rehak P. (1983) Detection and signal processing in high-energy physics. In. Bologna G & Vincelli M. (ed.) Data acquisition in high energy physics. North-Holland, Amsterdam, Netherlands.

Riegl2001 Riegl USA Inc. (2001) Application sheets. (http://www.rieglusa.com/)

Riegl2002 http://www.riegl.com/

Riesz93 Riesz F. (1993) Normalized Expression of the Frequency Response of p-I-n Avalanche Photo Diodes. Solid-State Electronics, Vol. 36, No. 2, pp. 293-294.

Riggs85 Riggs A. J., Sampson R.E., Tomko L.M. (1985) Application of 3D-vision and high speed image processing to robot control. IMS Proceedings Oct. 1985, pp. 291-299.

Ripper74 Ripper J.E., Rossi J.A. (1974) Delays and Q Switching in Semiconductor Lasers-Still an Open Question. IEEE Journal of Quantum Electronics, Vol. QE-10, No. 4., pp. 435-441.

Rogers91 Rogers D.L. (1991) Integrated Optical Receivers using MSM Detectors. Journal of Lightwave Technology, Vol. 9, No. 12, pp. 1635-1638.

Ruotsalainen94 Ruotsalainen, T., Kostamovaara, J. (1994) A 50-MHz CMOS Amplifier Channel for a Laser Radar. Analog Integrated Circuits and Signal Processing 5, pp. 257-264.

Ruotsalainen97 Ruotsalainen T, Palojärvi P & Kostamovaara J (1997) A BiCMOS Differential Amplifier and Timing Discriminator for the Receiver of a Laser Radar. Journal of Analog Integrated Circuits and Signal Processing, Kluwer Academic Publishers, 13(3): 341-352.

Ruotsalainen99 Ruotsalainen T. Integrated Receiver Channle Circuits and Structures for a Pulsed Time-of-Flight Laser Radar. Acta Univ Oul C 136.

Sah57 Sah C.-T., Noyce R.N., Shockley W. (1957) Carrier Generation and Recombination inP-N Junctions and P-N Junction Characteristics. Proceedings of the IRE, Sept. 1957, pp. 1228-1243.

Sakamoto89 Sakamoto, K.; McDonald, J.; Swapp, M.; Weir, B. (1989), Proceedings of the 1989 Bipolar Circuits and Technology Meeting, pp. 295 –297

Salathe77 Salathe R., Bolleter W., Gilgen H. (1977) Long range injection laser radar. Applied Optics, Vol. 16(10), pp. 2621-2623.

Sasaki85 Sasaki O., Taniguchi T., Ohska T.K. (1985) A High Resolution TDC in TKO BOX System. IEEE Transactions on Nuclear Science, Vol. 35, No. 1, pp. 342-345.

Schmitz2000 Schmitz C.H. , Graber H.L., Luo H., Arif I. , Hira J., Pei Y., Barbour S., and Barbour R.L. (2000) Instrumentation and calibration protocol for imaging dynamic features in dense-scattering media by optical tomography, APPLIED OPTICS y Vol. 39, No. 34, pp. 6466-6486.

Schöll84 Schöll E., Bimberg D., Schumacher H., Landsberg P.T. (1984) Kinetics of Picosecond Pulse Generation on Semiconductor Lasers with Bimolecular Recombination at High Current Injection. IEEE Journal of Quantum Electronnics, Vol. QE-20, No. 4., April 1984.

Schow99 Schow C.L., Schaub J.D., Li R., Qi J., Campbell J.C. (1999) A Monolithically Integrated 1-Gb/s Silicon Photoreceiver. IEEE Photonics Tecnology Letters, Vol. 11, No.1, pp. 120-121.

Sekine92 Sekine M., Senoo T., Morita I., Endo H. (1992) Design Method for an Automotive Laser Radar System and Future Prospects for Laser Radar, Intelligent Vehicles '92 Symposium., pp. 120 –125.

Senior92 Senior J.M. 81992) Optical Fibre Communications, Principles and Practice, Second Edition, Prentice Hall Ltd.

Sharma81 Sharma A.B., Halme S.J., Butusov M.M. (1981) Optical Fibre Systems and Their Components. Springer-Verlag, 1981.

Slater76 Slater L.E., Huggett G.R. (1976) A Multiwavelength Distance-Measuring Instrument for Geophysical Experiments. Journal of Geophysical Research. Vol 81(35), pp. 6299-6306.

Smith&Personick73 Smith R.G., Personick S.D. (1979) Receiver Design for Optical Fibre Communication Systems. In Topics in Applied Physics, Vol. 39: Semiconductor Devices for Optical Communication, Ed. Kressel H. Springer-Verlag 1979.

Smith80 Smith D.E. (1980) Electronic Distance Measurement for Industrial and Scientific Applications. Hewlwtt-Packard Journal, June 1980, pp. 3-11.

Sogawa91 Sogawa T, Arakawa Y. (1991) Picosecond dynamics in gain-switched uncoupled and coupled quantum well lasers. Applied Physics Letters, Vol. 58, No. 19, pp.2064-2066.

Solid-State Circuits, 3(4): 365-373.

Steele76 Steele W.W. (1976) Presision Aircraft Tracking System . Range Instrum., Weapons Syst. and Relat. tech., no. 219, 1976, pp. 13-1 – 13-6.

Strand85 Strand T.C. (1985) Optical three-dimensional sensing for machine vision. Optical Engineering, Vol. 24 (1), Feb. 1985, pp. 33-40.

Streetman80 Streetman B.G. (1980) Solid State Electronic Devices. Prentice-Hall, Englewood Cliffs, NJ, pp. 269-270.

Sze85 Sze S.M. (1985) Semiconductor Devices, Physics and Technology. John Wiley & Sons, Inc..

Szplet2000 Szplet R., Kalisz J., Szymanowski R. (2000) Interpolating Time Counter with 100 ps Resolution on a Single FPGA Device, IEEE transactions on instrumentation and measurement, vol. 49, no. 4, pp. 879-883.

Tamari97 Tamari Y. (1997) Custom silicon photodiodes offer design flexibility. Laser Focus World, January 1997, pp. 123-126.

Taylor78 Taylor M.J., Davies P.H., Brown D.W., Woods W.F., Bell I.D., Kennedy C.J. (1978) Pulsed CO2 TEA laser rangefinder. Applied Optics, Vol 17(6), pp. 885-889.

Teshigawara89 Teshigawara M.,Shiaata F., Teramoto H. (1989) High Resolution (0.2 mm) and fast response (2 ms) range finder for industrial use in air. Ultrasonics Symposium 1989 vol.1., pp. 639 –642.

Tewksbury93 Tewksbury S.K., Hornal L.A., Nariman H.E., McGinnis S.P. (1993) Co-Integration of Optoelectronics and Submicrometer CMOS. IEEE Transactions on Components, Hybrids, Nad Manufacturing Technology, Vol. 16, No.7, pp. 674-685.

Thedrez93 Thedrez B.J., Saddow S.E., Yuan Q.L., Wood C., Wilson C., Lee C.H. (1993) Experimental and Theoretical Investigation of Large Output Power Q-Switched AlGaAs Semiconductor Lasers. IEEE Photonics Technology Letters, Vol. 5, No. 1, pp. 19-22.

Tilleman96 Tilleman M. M., Krishnaswami K. K., (1996) Design of fibre optic relayed laser radar. Opt. Eng. Vol. 35(11), pp. 3279-3284.

Unagami2002 Unagami T. (2002) Novel Phenomenon of Avalanche Breakdown Saturation With Negative Resistance in a Bipolar Transistor. IEEE Transactions on Electron Devices, Vol. 49, No. 1, Jan. 2002, pp. 120-124.

Vainshtein94 Vainshtein S., Kilpelä A., Kostamovaara J., Myllylä R., Starobinets S.,Zhyliaev J. (1994) Multistreamer regime of GaAs thyristor switching. IEEE Trans. of Electron Devices, ED-41, No. 8, Aug. 1994, pp. 1444-1450.

Vainshtein97 Vainshtein S., Kostamovaara J., Kilpelä A., Määttä K. (1997) A novel compact 35 A/150 ps current pulse generator for a new generation of the laser radars. Proceedings of the 40th Midwest Symposium on Circuits and Systems, Vol. 1, pp. 148 –151.

Vali66 Vali V, Krogstadt R.S., Moss R.W., Engel R. (1966) Measurement of strain rate as the Kern River using a laser interferometer. Trans. Am. Geophys. Union, vol. 47, June 1966, p. 424.

Vanisri92 Vanisri T., Gonzalez-Wiren F., Toumazou C. (1992) Low-Noise Optimisation of Current-Mode, Common-Gate Transimpedance Optical Preamplifiers. IEE Colloquim of Linear Analogue Circuits and Systems, pp. 10/1-10/6.

Vanisri95 Vanisri T., Toumazou C. (1995) Integrated High Frequency Low-Noise Current-Mode optical Transimpedance Preamplifiers: Theory and Practice. IEEE Journal of Solid-State Circuits, Vol. 30, No. 6, June 1995, pp. 677-685.

Vaughan96 Vaughan J.M., Steinvall K.O., Werner C., Flamant P.H. (1996) Coherent Laser Radar in Europe. Proceedings of the IEEE, Vol. 84, No. 2, Feb. 1996., pp. 205-226.

Wang91 Wang J., Määttä K., Kostamovaara J. (1991) Signal power Estimation in Short Range Laser Radars, Proc. LIA International Sumposium on Optical Sensing and Measurement Symposium (ICALEO ´91), San Jose, California, USA, 73:16-26.

Watanabe92 Watanabe S., Yoneyama M. (1992) An Ultrasonic Visual Sensor fot Three-Dimensional Object Recognition Using Neural Networks. IEEE Transactions on Robotics and Automation, Vol. 8., No. 2, April 1992, pp. 240 – 249.

Wehner87 Wehner D.R. (1987) High Resolution Radar. Norwood, Mass. Artech House cop. 1987 .

White93 White I.H., Williams K.A., Burns D., Sibbett W., Vasilev P.P., Fice M.J. (1993) Picosecond Pulse Generation in Multisection Diode Lasers by Gain-switching and Q-switching. IEE Colloquium on Ultra-Short Optical Pulses, pp. 5/1 -5/4.

Wilson96 Wilson, B.; Drew, J.D. (1996) New current-mode transimpedance amplifier configuration for gain-independent bandwidth **.** Wideband Circuits, Modelling and Techniques, IEE Colloquium , pp. 9/1 -9/5.

Yamawaki97 Yamawaki T., Kokubo M., Irie K., Matsui H., Hori K., Endou T., Hagisawa H., Furuya T., Shimizu Y., Katagishi M., Hildersley J.R. (1997) A 2.7-V GSM RF Transceiver IC, IEEE Journal of Solid State Circuits, VoL. 32, No. 12, pp.2089-2096.

Yano90 Yano H., Aga K., Kamei H., Sasaki G., Hayashi H. (1990) Low-Noise Current Optoelectronic Integrated Receiver with Internal Equalizer for Gigabit-per-Second Long-Wavelength Optical Communications. Journal of Lightwave Technology, Vol. 8, No.9, pp. 1328-1333.

Yariv97 Yariv A. (1997) Optical Electronics on Modern Communications, Oxford University Press

Zahid97 Zahid M., Smith J.S., Lucas J. (1997) High-frequency phase measurement for optical rangefinding system, IEE Proc. Sci. Meas. Technol., Vol. 144, No. 3, May 1997, pp. 141-148

Ziemer76 Ziemer R.E., Tranter W.H. (1976) Principles of Communications – Systems, Modulation and Noise (Chapter 4), Houghton Mifflin Company, USA, 513 pages.